CASTNET

2016

Annual Report

EPA United States Environmental Protection Agency

Clean Air Status and Trends Network
(CASTNET)

2016 Annual Report

Prepared by:
Wood Environment & Infrastructure Solutions, Inc.

Prepared for:
U.S. Environmental Protection Agency
Office of Air and Radiation
Clean Air Markets Division
Washington, DC

EPA Contract No. EP-W-16-015

August 2018

Table of Contents

Executive Summary ii

Chapter 1 ***CASTNET Update*** 1
- Introduction 1
- Related Air Quality Networks 2
- Locations of Monitoring Sites 3
- Measurements Recorded at CASTNET Sites 4
- Quality Assurance Program 4
- Estimating Dry, Wet, and Total Deposition 5

Chapter 2 ***Ozone Concentrations*** 6
- 2015 NAAQS for Ozone 7
- Eight-hour Ozone Concentrations 8
- Uinta Basin, Utah Ozone Concentrations 10

Chapter 3 ***Nitrogen Pollutant Concentrations*** 16
- Total Nitrate Concentrations 16
- Particulate Ammonium Concentrations 18

Chapter 4 ***Update on the Ammonia Monitoring Network*** 21

Chapter 5 ***Sulfur Pollutant Concentrations*** 23
- Sulfur Dioxide Concentrations 23
- Particulate Sulfate Concentrations 25

Chapter 6 **Continuous *Trace-level Gas Concentrations*** 27
- Continuous Trace-level NO_y and Ozone 31
- Continuous Trace-level NO_y and Filter Pack Total Nitrate Concentrations 32

Chapter 7 ***Effects of Wildfires on Air Quality*** 35

Chapter 8 ***Atmospheric Deposition of Nitrogen*** 41

Chapter 9 ***Monitoring on Whiteface Mountain during 2015 and 2016*** 47

Chapter 10 ***Atmospheric Deposition of Sulfur, Base Cations, and Chloride*** 56
- Sulfur Deposition 56
- Deposition of Base Cations and Chloride 56

Chapter 11 ***Critical Loads for Open and Closed Canopy Herbaceous Ecosystems*** 60

References 64

Appendix A **Locational and Operational Characteristics of CASTNET Sites**

Appendix B **Acronyms and Abbreviations**

Executive Summary

The EPA Clean Air Status and Trends Network (CASTNET) measures concentrations of atmospheric pollutants across the United States. The primary objectives of the network are to determine compliance with ozone National Ambient Air Quality Standards and to provide data to evaluate the effectiveness of national and regional air pollution control programs. CASTNET data are also used to provide input to the National Atmospheric Deposition Program's Total Deposition Hybrid Method for calculating total deposition and evaluating regional air quality models. This report presents maps of 2016 ozone levels, nitrogen and sulfur pollutant concentrations, and deposition fluxes and examines trends in air quality over the 27-year period from 1990 through 2016. In 2016, CASTNET measured rural, regionally representative concentrations of nitrogen and sulfur species at 95 monitoring stations at 93 locations and ozone levels at 81 locations.

Key Results and Highlights through 2016

The median fourth highest daily maximum 8-hour average (DM8A) ozone (O_3) concentration for 2016 at the eastern CASTNET reference sites (see Appendix A for designated reference sites) was 64 parts per billion (ppb). This is a slight increase from the 2015 median of 63.5 ppb. At the western CASTNET reference sites, the median was 66 ppb. Three-year averages of fourth highest DM8A O_3 concentrations exceeded the 2015 8-hour National Ambient Air Quality Standard (NAAQS) of 0.070 parts per million (ppm) or, equivalently, 70 ppb, at three California CASTNET sites and one site in New Jersey during the most recent 3 year period (2014–2016). During 2016, 10 eastern, 4 California sites, and Dinosaur National Monument (DIN431), UT measured fourth highest DM8A O_3 concentrations greater than 70 ppb. Three-year averages of fourth highest DM8A O_3 concentrations have been reduced by 24 percent at the eastern reference sites since 1990–1992 and by 10 percent at the western reference sites since 1996–1998. Figure E-1 and Table E-1 summarize the long-term changes in measured concentrations.

Regional O_3 concentrations are influenced by nitrogen oxides (NO_x) emissions. Federal, state, and local NO_x control programs have resulted in substantive reductions in emissions. For example, NO_x emissions declined by 86 percent over the 27 year period, 1990 through 2016, at regulated electric generating units (EGUs) in the East.

Three-year mean annual concentrations of total nitrate (NO_3^-), which is comprised of nitric acid plus particulate NO_3^-, declined 48 percent at the eastern reference sites over the 27-year period. Three-year

Figure E-1 Trends in O_3, Total NO_3^-, and SO_2 at Eastern Reference Sites

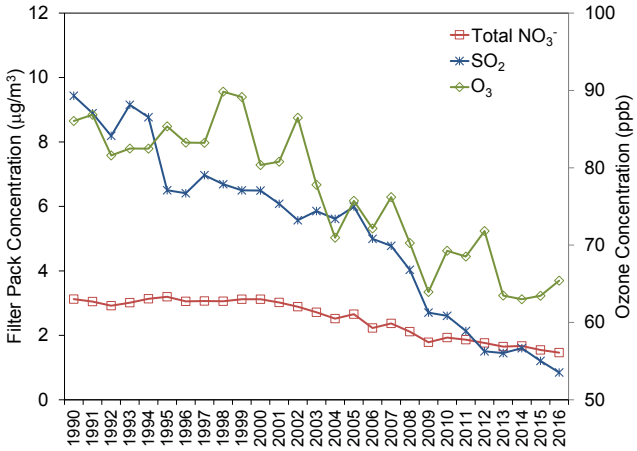

mean annual total NO_3^- levels measured at the western reference sites dropped by 34 percent over the 21-year period.

Mean annual sulfur dioxide (SO_2) concentrations measured at the eastern reference sites have declined significantly over the 27-year period, 1990 through 2016. Three-year mean annual SO_2 levels at eastern sites decreased 86 percent. SO_2 concentrations measured at the western reference sites declined by 46 percent over the 20 years from 1996 through 2016.

The percent reduction in SO_2 concentrations at the eastern reference sites is consistent with the reduction in regulated eastern EGU SO_2 emissions (94 percent).

Table E-1 Trends in Aggregated Western and Eastern O_3, Total NO_3^-, and SO_2 Pollutant Concentrations

Pollutant	Western Reference Sites		Eastern Reference Sites		Percent Changed	
	1996–1998	2014–2016	1990–1992	2014–2016	West	East
O_3 (ppb)	74	66	85	64	-10	-24
Total NO_3^- (µg/m^3)	1.0	0.7	3.0	1.6	-34	-48
SO_2 (µg/m^3)	0.6	0.3	8.8	1.2	-46	-86

The original intent of CASTNET was to measure pollutant concentrations to estimate trends in sulfur and nitrogen pollutants. Currently, the focus also includes demonstrating compliance of rural, regional O_3 concentrations with the NAAQS. The network also features measurements of trace-level gases and speciated nitrogen pollutants. Additionally, CASTNET supports the National Atmospheric Deposition Program's Ammonia Monitoring Network with operation of ammonia samplers at 69 CASTNET sites. This report provides information on CASTNET pollutant measurements, estimated deposition fluxes, and other topics that can be addressed using CASTNET data, such as wintertime ozone concentrations in the Uinta Basin, Utah, effects of wildfires on air quality in Wyoming and Arizona, and pollutant concentrations measured on Whiteface Mountain, New York.

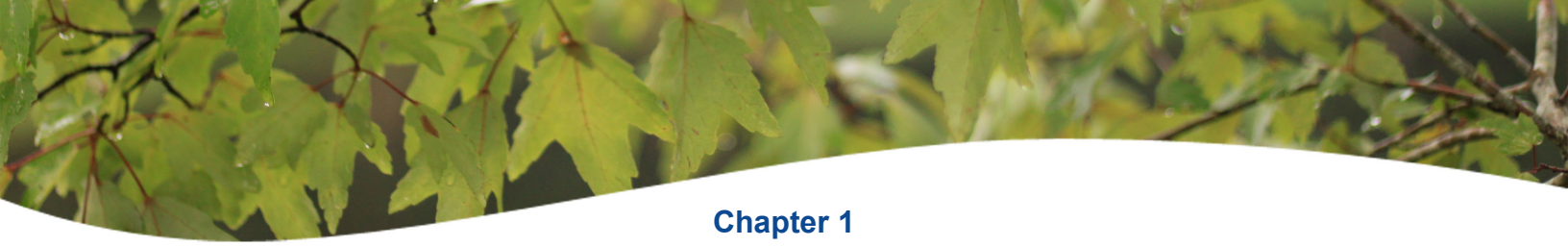

Chapter 1

CASTNET Update

The Clean Air Status and Trends Network (CASTNET) is a nationwide air quality monitoring network that began operating in 1991. The network provides measurements of air pollutant concentrations in rural areas across the United States over the long term to determine compliance with ozone National Ambient Air Quality Standards and to evaluate the effectiveness of national and regional emission control programs. CASTNET data are used to provide input to regional air quality models. CASTNET is managed and operated by the U.S. Environmental Protection Agency in cooperation with the National Park Service and other federal, state, tribal, and local partners. In 2016, the network operated 95 monitoring stations throughout the contiguous United States, Alaska, and Canada. CASTNET data show a 27-year decline in ozone concentrations and in nitrogen and sulfur pollutant levels and deposition rates.

Introduction

The Clean Air Status and Trends Network (CASTNET) operated 95 monitoring stations throughout the contiguous United States, Alaska, and Canada in 2016. All 95 sites included filter pack systems to sample weekly concentrations of acid gases and aerosols. Eighty-one sites included continuous ozone (O_3) analyzers. The U.S. Environmental Protection Agency (EPA) and the National Park Service (NPS) are the primary sponsors of CASTNET. NPS began its participation in 1994 and operated 25 sites during 2016. The Bureau of Land Management-Wyoming State Office (BLM) operated five sites in Wyoming.

CASTNET depends on contributions from many organizations (EPA, 2015a) including Native American tribes, state and federal government agencies, and universities. These participants sponsor individual CASTNET sites and provide in-kind services that support the overall performance of the network. For example, partners operate and repair site instruments, change weekly filter packs, and perform general site maintenance. Many partners provide the land for the CASTNET site. Others, such as universities, provide their expertise in air quality monitoring, which is invaluable for improving CASTNET monitoring capabilities and ensuring that CASTNET collects data that are valued by the scientific research community.

In 2016, ozone monitoring was added to the Nez Perce Tribe's site in Idaho (NPT006), and the site was converted from off grid to normal power. The seasonal small footprint site at the summit of Whiteface Mountain, NY (WFM007) was operated by the New York State Department of Environmental Conservation (NYSDEC) during the summer of 2016. The site at Coweeta, NC (COW005) was shut down in August 2016 after completion of a special study that utilized solar and wind energy as sources of power for the small footprint site.

The U.S. Congress established the Acid Rain Program (ARP) in 1990 to reduce emissions of sulfur dioxide (SO_2) and nitrogen oxides (NO_x) from electric generating units (EGUs). Congress also directed EPA to establish CASTNET to assess the effectiveness of the ARP by providing consistent, long-term measurements for determining relationships between changes in emissions and changes in air quality, atmospheric deposition, and ecological effects. Figure 1-1 shows the locations of the CASTNET monitoring sites that were operational during 2016.

Related Air Quality Networks

CASTNET monitors air quality and deposition in cooperation with other national and international networks. EPA uses data from CASTNET and the other long-term national networks to assess the effectiveness of emission control programs. These networks include the National Atmospheric Deposition Program (NADP) (http://nadp.slh.wisc.edu/) and its affiliated networks:

- National Trends Network (NTN)
- Ammonia Monitoring Network (AMoN)
- Mercury Deposition Network (MDN)
- Atmospheric Mercury Network (AMNet).

Other cooperating networks include:

- Canadian Air and Precipitation Monitoring Network (CAPMoN)
  (https://www.canada.ca/en/environment-climate-change/services/air-pollution/monitoring-networks-data/canadian-air-precipitation.html)
- EPA's National Core Monitoring (NCore)
  (https://www3.epa.gov/ttnamti1/ncore.html)
- BLM's Wyoming Air Resources Monitoring System (WARMS)
  (https://www.blmwarms.net/)
- Interagency Monitoring of Protected Visual Environments (IMPROVE)
  (http://vista.cira.colostate.edu/IMPROVE/)

Locations of Monitoring Sites

A map of CASTNET monitoring sites is given in Figure 1-1. Ninety-five monitoring sites were operated at 93 distinct locations. To estimate precision across the network, co-located sites were operated at Mackville, KY (MCK131/231) and Rocky Mountain National Park, CO (ROM406/206) during 2016. The ROM406/206 pair ensures consistency between EPA (ROM206) and NPS (ROM406). Of the two Rocky Mountain monitoring sites, ROM406 is specified as the regulatory monitoring site for O_3. The location of each site and information on start date, latitude, longitude, elevation, identification of the nearby NADP site, land use, terrain type, operating agency, and if the site is a reference site used for trends are given in Appendix A.

Figure 1-1 CASTNET Sites Operational during 2016

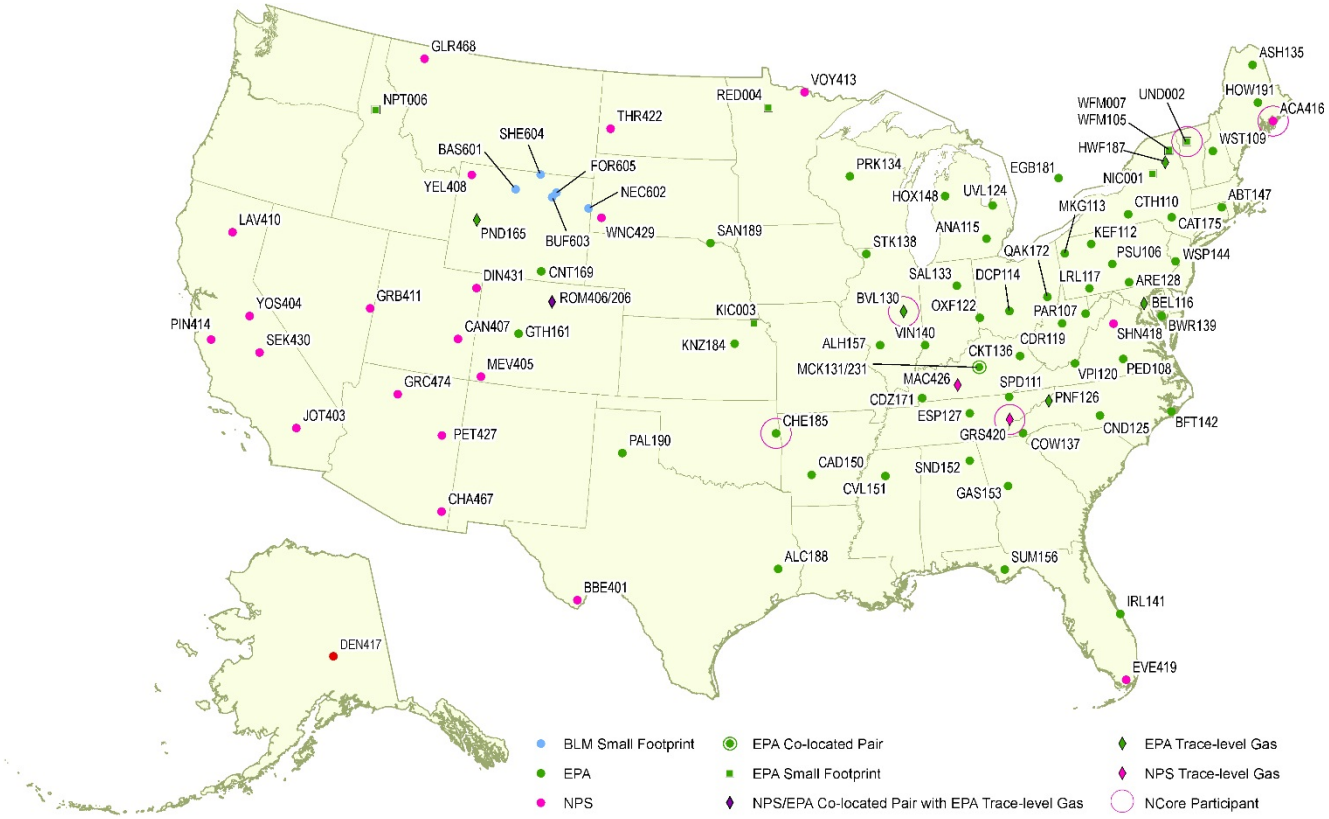

Measurements Recorded at CASTNET Sites

All CASTNET sites measure weekly ambient concentrations of acidic pollutants, base cations, and chloride (Cl^-) using a 3-stage filter pack with a controlled flow rate (Wood, 2015). Gaseous pollutant concentrations include nitric acid (HNO_3) and SO_2. Particulate concentrations include nitrate (NO_3^-), ammonium (NH_4^+), sulfate (SO_4^{2-}), magnesium (Mg^{2+}), calcium (Ca^{2+}), potassium (K^+), sodium (Na^+), and Cl^-. The filter pack is exchanged each Tuesday and shipped to the analytical chemistry laboratory for analysis. Ambient temperature is measured at 9 meters (m) at all sites in part to enable conversion of concentrations to local conditions.

Most CASTNET sites also include a temperature-controlled shelter and continuous O_3 monitoring system. O_3 concentrations were measured at 81 sites. The O_3 inlet and filter pack are located atop a 10-m tower. Some CASTNET sites also measure trace-level SO_2, carbon monoxide (CO), and nitrogen oxide/total reactive oxides of nitrogen (NO/NO_y). In 2016, meteorological parameters were measured at 6 EPA-, 25 NPS-, and 5 BLM-sponsored CASTNET sites. Measured meteorological parameters include 2-m temperature, wind speed and direction, standard deviation of the wind direction, solar radiation, relative humidity, precipitation, and surface wetness (at select sites).

Quality Assurance Program

The CASTNET quality assurance (QA) program was established to ensure that all reported data are of known and documented quality in order to meet CASTNET objectives. The QA program also ensures intra-network consistency and comparability and the delivery of data that are reproducible and comparable with data from other monitoring networks. The 2016 QA program elements are documented in the CASTNET Quality Assurance Project Plan (QAPP; Wood, 2015). The QAPP includes standards and policies for all components of project operation, from site selection through final data reporting, with appendices that provide standard operating procedures for CASTNET operations.

Data quality indicators (DQI) such as precision, accuracy, and completeness are used to assess CASTNET measurements and supporting activities. Routine assessment and analysis help guarantee the production of high-quality data and information to meet project objectives. Measurements taken during 2016 and historical data collected over the period 1990 through 2015 were analyzed relative to DQI and their associated metrics. Results from these analyses are available in quarterly and annual QA reports posted on the EPA CASTNET website: https://www.epa.gov/castnet/.

The Wood CASTNET laboratory regularly participates in interlaboratory comparison studies and proficiency testing (PT) programs such as the Environment Canada (ECAN) PT Program for Inorganic Environmental Substances (http://www.ec.gc.ca/inre-nwri/default.asp?lang=En&n=7A20877C-1). The ECAN PT program conforms to the requirements of the American Association for Laboratory Accreditation (A2LA). The program meets the International Organization for Standardization

(ISO)/International Electrotechnical Commission (IEC) 17043:2010 conformity assessment – general requirements for proficiency testing with scope of accreditation 2867.01. The results reported are evaluated for systematic bias and precision. Systematic bias is assessed using the Youden (1969) non-parametric analysis, while precision is calculated using algorithm A from the ISO standard 13528 (ISO, 2005). CASTNET laboratory results from the PT studies are summarized in the QA quarterly and annual reports posted to the EPA CASTNET website: https://www.epa.gov/castnet/.

Estimating Dry, Wet, and Total Deposition

Total deposition was assessed using the NADP's Total Deposition Hybrid Method (EPA, 2015d; Schwede and Lear, 2014), which is a hybrid approach that combines data from established ambient monitoring networks and chemical transport models. To estimate dry deposition, ambient measurement data from CASTNET and other networks were merged with dry deposition rates and flux output from the Community Multiscale Air Quality (CMAQ) modeling system. Wet deposition estimates were derived from precipitation chemistry measurements and precipitation amounts from the Parameter-elevation Regressions on Independent Slopes Model (PRISM). Dry and wet deposition fluxes were added to obtain the estimates of total deposition that are discussed in Chapters 8 and 10.

This report summarizes CASTNET monitoring and the resulting concentration and deposition data collected over the 27-year period from 1990 through 2016. The report covers such topics such as wintertime air quality in the Uinta Basin in Utah, trace-level gas concentrations measured at eight CASTNET sites, effects of wildfires on air quality, and air quality on Whiteface Mountain in New York. Additional information, previous annual reports, descriptions of CASTNET operations, other CASTNET documents, and the CASTNET database can be found on the EPA CASTNET website: https://www.epa.gov/castnet/.

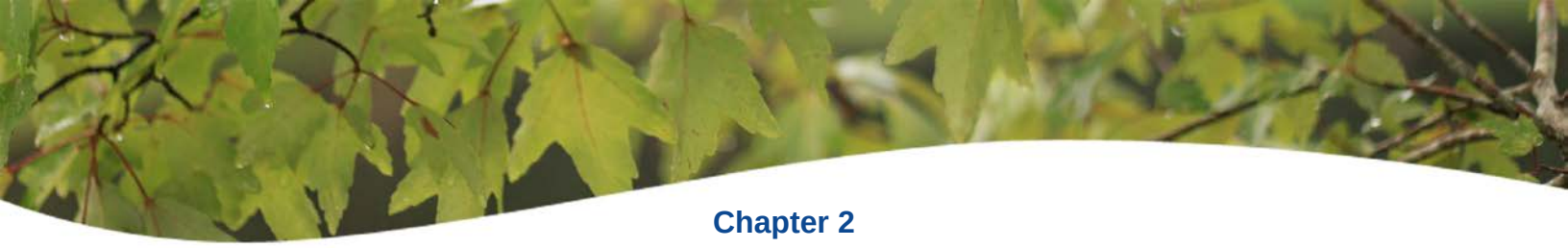

Chapter 2

Ozone Concentrations

CASTNET is the principal network for monitoring rural, ground-level ozone concentrations in the United States. The network produces ozone data for evaluation of compliance with the National Ambient Air Quality Standards (NAAQS; EPA, 2015) plus information on geographic patterns in regional ozone levels. CASTNET ozone data are of the highest quality as demonstrated by the results from the CASTNET QA program and its rigorous QA/quality control procedures. Ozone data measured at 78 of 81 CASTNET sites from 2014 through 2016 were evaluated with respect to the NAAQS and used to calculate design values under Title 40 Code of Federal Regulations Part 50 Appendix U (EPA, 2015b). Maps of 3-year averages of fourth highest daily maximum 8-hour average (DM8A) ozone concentrations for 2014 through 2016 and fourth highest DM8A ozone concentrations for 2016 are presented. Trends in fourth highest DM8A ozone concentrations for eastern and western reference sites are shown. For the 2014 through 2016 period, three California sites and one eastern site measured concentrations greater than the 0.070 ppm NAAQS.

Hourly average concentrations were measured at 81 CASTNET sites in 2016. These data are archived in the CASTNET database and delivered routinely to the EPA Air Quality System (AQS) database. Data from these sites, with the exception of Howland, ME (HOW191) and the co-located sites at MCK231, KY and ROM206, CO, which are designated as non-regulatory, are used to calculate fourth highest DM8A O_3 concentrations when three years of Title 40 Code of Federal Regulations (CFR) Part 58-compliant data become available. CASTNET measurements provide information for evaluating rural O_3 concentrations in the context of the O_3 NAAQS and in terms of presenting information on trends and geographic patterns in regional O_3.

A design value describes the air quality status of a given area with respect to the concentration values required by the NAAQS. Design values change as each new 3-year period of monitored ozone concentrations becomes available (e.g., 2014–2016). Design values are used to classify nonattainment areas, assess progress towards meeting the NAAQS, and develop control strategies to achieve the NAAQS. For example, to achieve the 2015 ozone NAAQS, 3-year averages of fourth highest DM8A ozone concentrations cannot exceed 0.070 parts per million (ppm). Designated criteria pollutant nonattainment areas are provided on the EPA website: https://www.epa.gov/green-book.

The information presented in this chapter includes maps of and trends in the annual fourth highest DM8A O_3 concentrations measured at CASTNET sites. Ozone data from Dinosaur National Monument (NM) in Utah (DIN431) and from measurements in the Uinta Basin in the northeast corner of Utah are also discussed. Additional maps of O_3 concentrations from the NPS Air Atlas can be viewed at https://nature.nps.gov/air/maps/airatlas/ and https://nature.nps.gov/air/data/products/parks/.

Measurements from 34 eastern and 16 western reference sites (see Appendix A) were analyzed to determine trends in O_3 concentrations. These sites were also used to show trends in ambient nitrogen and sulfur concentrations (chapters 3 and 5). The eastern reference sites have been reporting CASTNET measurements since at least 1990 and the western reference sites since at least 1996.

2015 National Ambient Air Quality Standards for Ozone

	Primary Standard		Secondary Standard	
	Level	Averaging Time	Level	Averaging Time
Ozone[1]	0.070 ppm[1]	8-hour[2]	0.070 ppm[1]	8-hour[2]

Note: [1] The NAAQS was revised from 0.075 ppm to 0.070 ppm on October 15, 2015.

[2] To attain this standard, the 3-year average of the fourth highest DM8A O_3 concentrations measured at each monitor within a specified area must not exceed 0.070 ppm or 70 parts per billion (ppb) in practice (effective December 28, 2015). Ozone concentrations are commonly presented in units of ppb.

The primary O_3 NAAQS is designed to protect public health. The secondary standard is designed to protect public welfare and the environment. Both O_3 NAAQS are set at a level of 0.070 ppm averaged over eight hours for the annual fourth highest value.

To assess compliance with the primary and secondary standards, EPA uses measured O_3 pollutant concentrations, an 8-hour averaging time, and the fourth highest daily maximum averaged across three consecutive years. The secondary standard is equivalent, based on the W126 index (Lefohn and Runeckles, 1987), to a level of protection of 17 ppm-hour or lower averaged over three years (EPA, 2008). The W126 index is a weighted index designed to reflect the cumulative exposures that can damage plants and trees during the consecutive three months in the growing season when daytime O_3 concentrations are the highest, and plant growth and production are most affected.

The EPA and other federal, tribal, state, and local agencies measure O_3 concentrations on an hourly basis through national and local monitoring programs. Wood followed EPA procedures (2015b) to estimate O_3 design values and 2016 fourth highest DM8A O_3 concentrations at CASTNET sites. Measurements potentially affected by exceptional events were not removed when calculating these estimates. “Exceptional events are unusual or naturally occurring events that can affect air quality but are not reasonably controllable using techniques that state, tribal, or local air agencies may implement in order to attain and maintain the NAAQS” (EPA, 2016). The Exceptional Events Rule was updated on October 3, 2016 (https://www.epa.gov/air-quality-analysis/exceptional-events-rule-and-guidance), and provides the requirements for excluding air quality data from regulatory decisions if the data are affected by events outside an agency’s control, such as a wildfires or stratospheric intrusion.

CASTNET O_3 data were used to gauge compliance with the NAAQS at EPA-, NPS- and BLM-sponsored sites that were 40 CFR Part 58 compliant for the years 2014 through 2016.

Eight-hour Ozone Concentrations

All CASTNET sites, with the exception of HOW191, ME; MCK231, KY; and ROM206, CO, are regulatory and may be used for NAAQS compliance. HOW191 does not meet regulatory siting criteria. MCK231 and ROM206 are co-located sites used solely for QA purposes and are designated as "NAAQS excluded." Three-year averages of the fourth highest DM8A O_3 concentrations for 2014 through 2016 are presented in Figure 2-1. Ozone concentrations were not included on the map if the 3-year average was not available because of incomplete data; these sites are shown as dots with no value. Three California CASTNET sites and one eastern site measured fourth highest DM8A O_3 concentrations above the 2015 NAAQS. The highest 3-year design value of 89 parts per billion (ppb) was sampled at the Sequoia and Kings Canyon National Parks, CA (SEK430) site. The highest 3-year eastern concentration (73 ppb) was measured at Washington Crossing, NJ (WSP144). Table 2-1 lists sites with 2014–2016 O_3 design values greater than 70 ppb.

Figure 2-1 Three-year Averages of Fourth Highest DM8A O_3 Concentrations for 2014–2016

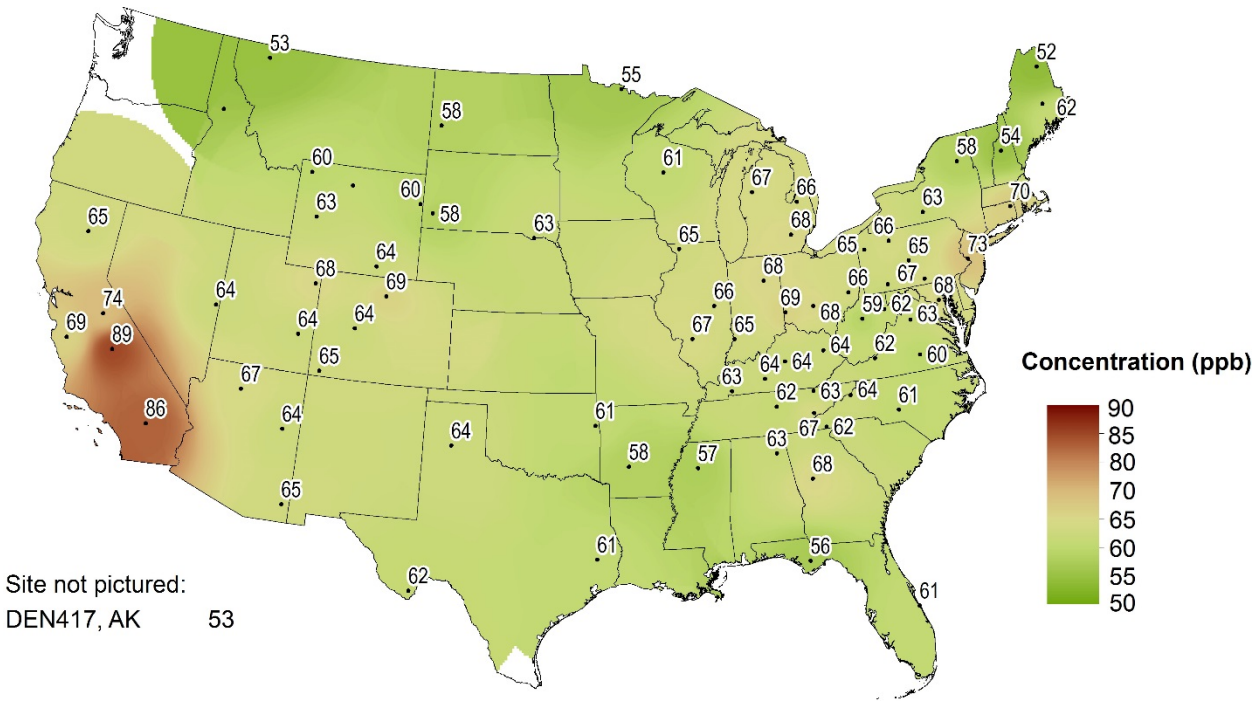

Table 2-1 Sites with Design Values for 2014–2016 greater than 70 ppb

Site ID	State	Sponsor	3-year Average
SEK430	California	NPS	89
JOT403	California	NPS	86
YOS404	California	NPS	74
WSP144	New Jersey	EPA	73

Figure 2-2 shows 2016 fourth highest DM8A O_3 concentrations that met percent completeness criteria. During 2016, 10 eastern, 4 California sites, and 1 site in Utah measured fourth highest DM8A O_3 concentrations greater than 70 ppb.

Figure 2-2 Fourth Highest DM8A O_3 Concentrations for 2016

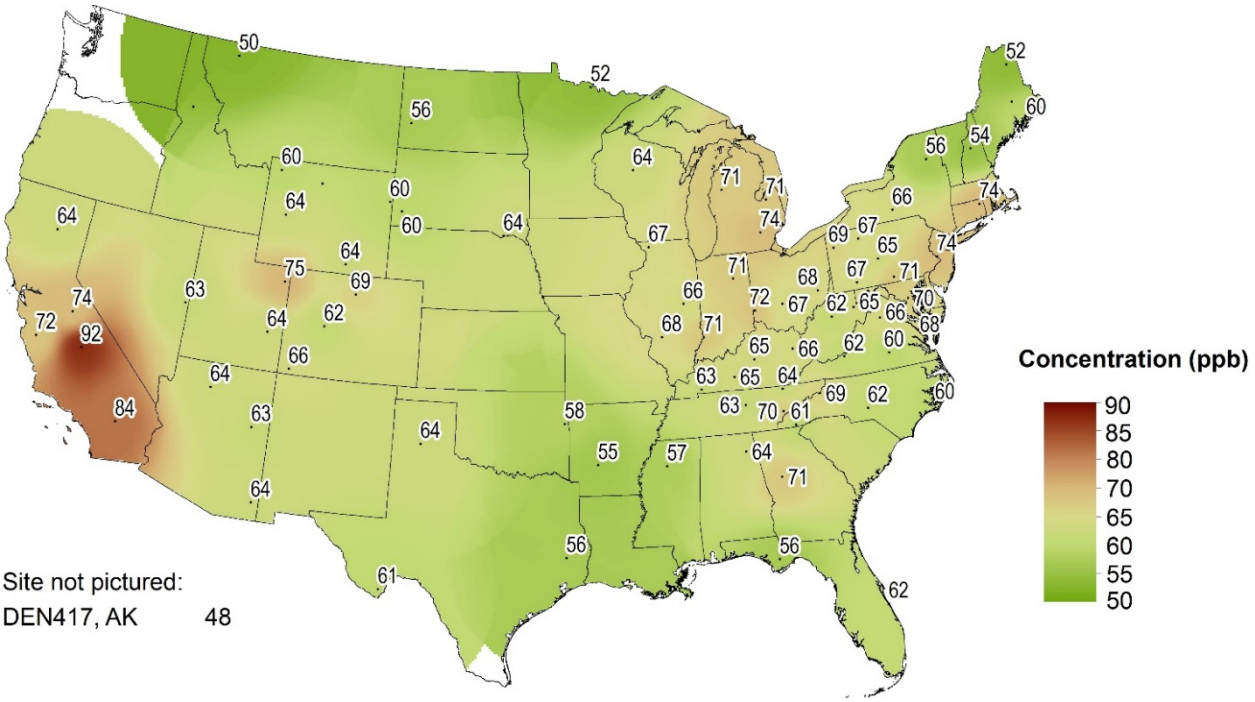

Figure 2-3 provides box plots depicting trends in 1-year mean, median, and annual distributions of fourth highest DM8A O_3 concentrations from the eastern reference sites (right side) for 1990 through 2016 and for the western reference sites (left side) for 1996 through 2016. The reference sites were selected for their long-term data record and consistent performance. The eastern O_3 data show an overall decline since 2002. The 2016 median data point, 64 ppb, was higher than the 2015 value of 63.5 ppb.

The western O_3 data show an increase in fourth highest DM8A O_3 concentrations from a 2009 minimum through 2012, followed by a decline through 2016. The 2016 median of the fourth highest

DM8A O_3 concentrations for the western reference sites was 66 ppb, the lowest value for the western reference sites.

Figure 2-3 Trends in Fourth Highest DM8A O_3 Concentrations

Western Reference Sites

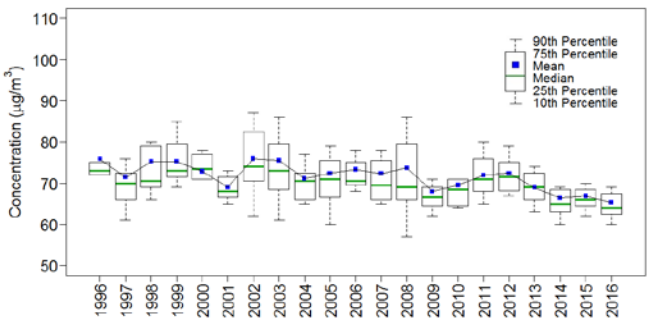

Eastern Reference Sites

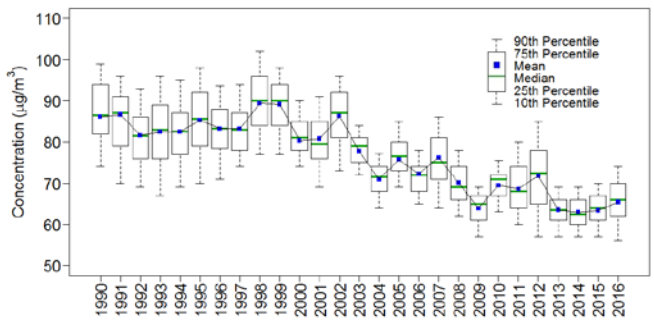

Uinta Basin, Utah Ozone Concentrations

A network of O_3 monitors throughout the Uinta Basin has measured elevated DM8A O_3 levels. In fact, the Uinta Basin is one of only two places in the United States that measures wintertime O_3 concentrations in excess of the NAAQS. Wyoming's Upper Green River Basin is the other (CASTNET 2010 Annual Report; Wood, 2012).

The Uinta Basin is an enclosed basin that lies in the northeast corner of Utah and is part of a larger area known as the Colorado Plateau. The Basin is bounded on the north by the Uinta Mountain range, on the south by the Book and Roan Cliffs, on the west by the Wasatch Range, and on the east by elevated terrain separating it from the Piceance Basin in Colorado. The Green River runs through the Basin from northeast to southwest, exiting through the Book Cliffs via Desolation Canyon. The floor of the Basin is at approximately 1,463 meters above sea level with significant local surrounding topography with elevations of tens to hundreds of meters.

Wintertime air quality in the Uinta Basin deteriorates when strong inversion events persist over several days (Lyman *et al*., 2016). These multi-day inversions occur with stagnant, high-pressure weather conditions and sufficient snow cover to reflect incoming sunlight, which keeps the ground from absorbing sunlight and warming. Snow also provides energy for the chemical reactions that form O_3 by increasing the amount of available solar radiation. Ozone forms in the atmosphere from reactions involving NO_x and volatile organic compounds (VOC). Inversion conditions trap these pollutants near ground level and increase their concentrations and their subsequent ability to generate O_3. Numerous exceedances of the NAAQS have occurred during winters with adequate snow cover and sustained high-pressure conditions, and no wintertime exceedances have ever been observed without snow cover. During lengthy inversion conditions, high O_3 concentrations first form in the low-elevation center of the Basin. The O_3 concentrations increase daily while expanding towards the

Basin's edges. The highest O_3 concentrations occur primarily in areas at lowest elevation. Longer inversion episodes and episodes that occur late in the winter season tend to lead to higher O_3 levels.

Figure 2-4 depicts DM8A O_3 concentrations measured throughout the Basin on February 12, 2016. Color shading shows the magnitude of the O_3 concentration (Lyman *et al*., 2016). Ozone monitoring locations are also shown. The site labeled Dinosaur N.M. is the DIN431 CASTNET site. Table 2-2 lists 8-hour average O_3 concentrations measured in the Uinta Basin during the winter of 2015–2016. The highest DM8A O_3 concentration exceeded 100 ppb.

Figure 2-4 DM8A O_3 Concentrations Measured throughout Uinta Basin on February 12, 2016

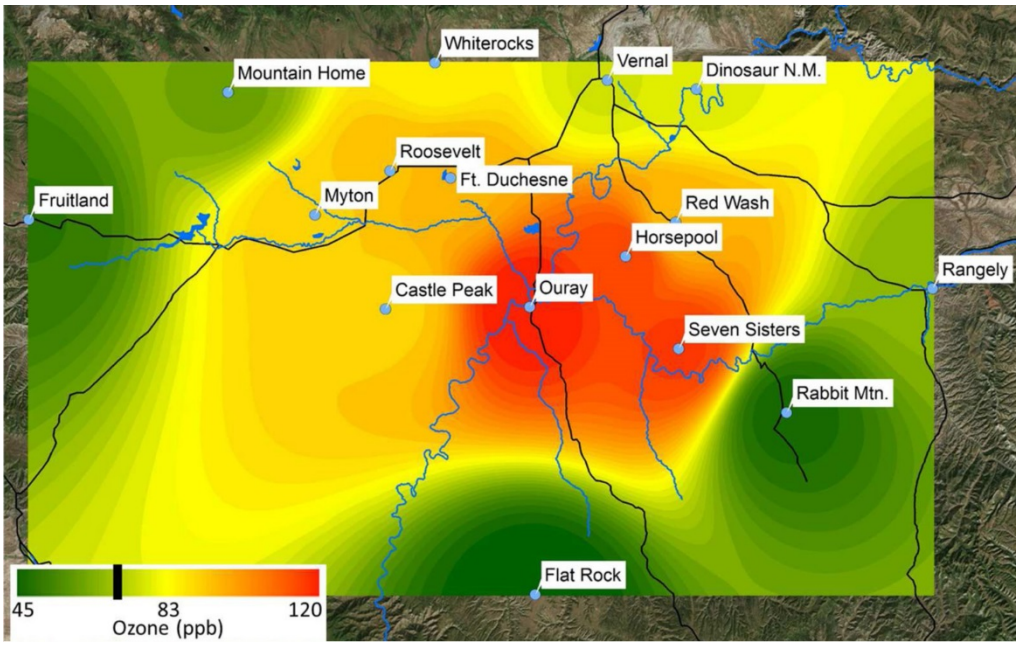

Source:Lyman *et al*., 2016
Esri, DigitalGlobe, i-cubed, USDA, USGS, AEX, Getmapping, Aerogrid, IGN, IGP, swisstopo, and the GIS User Community

Note: Vertical black bar = 70 ppb

Air quality monitoring in the Basin began in 2006 when the Utah Department of Air Quality (UDAQ) installed monitors in Vernal to measure fine particulate matter ($PM_{2.5}$), O_3, and NO_x. EPA added two monitoring sites in 2009, and the network further expanded to the number of sites shown in Figure 2-4 and Table 2-2. The NPS added the DIN431 CASTNET site in November 2013 (Appendix A). The site is located in the northeast corner of the Basin east of Vernal (Figure 2-4) at an elevation of 1,463 meters. Ozone concentrations measured at DIN431 were generally lower than those measured near the center of the Basin.

Table 2-2 8-hour Average O_3 Concentrations Measured in the Uinta Basin during Winter 2015–2016

Location	Site Elevation (Meters)	Mean (ppb)	Maximum (ppb)	Minimum (ppb)	Fourth Highest DM8A (ppb)	Number of Exceedances
Dinosaur NM	1463	37.0	83.6	9.5	75.3	5
Ouray	1464	37.7	120.6	8.8	96.8	11
Fort Duchesne	1559	31.9	96.8	6.8	90.4	9
Horsepool	1569	44.1	115.8	16.4	93.6	11
Roosevelt	1587	35.2	96.0	10.8	84.8	10
Castle Peak	1605	39.0	99.8	16.3	84.0	8
Vernal	1606	34.7	78.4	10.3	73.6	5
Myton	1610	38.7	95.1	16.6	85.5	8
Seven Sisters	1618	39.3	117.5	11.0	100.9	9
Rangely	1648	36.9	67.4	19.8	59.8	0
Red Wash	1689	39.9	96.0	18.6	83.5	7
Rabbit Mountain	1879	32.9	52.9	11.8	48.2	0
Whiterocks	1893	43.4	86.1	25.3	81.3	7
Fruitland	2021	36.4	62.4	9.3	53.1	0
Mountain Home	2234	46.7	72.4	32.6	64.3	1
Flat Rock	2274	44.2	58.2	30.0	54.6	0

Source:Lyman *et al*., 2016

Figure 2-5 presents a time series of DM8A O_3 concentrations measured at DIN431 from its inception through mid-2017. Several DM8A O_3 concentrations exceeded 70 ppb. Most of the high concentrations were observed during first quarter. However, several high values were measured during summer months. Some investigators (Ute Indian Tribe, 2016) have concluded that stratospheric O_3 intrusions and wildfires contribute to elevated spring and summer O_3 levels. No concentrations greater than 70 ppb were sampled during the first quarter of 2015 because of a lack of snow cover (Neeman *et al*., 2015).

Figure 2-5 Time Series of DM8A O_3 Concentrations Measured at DIN431 from November 2013 through July 2017

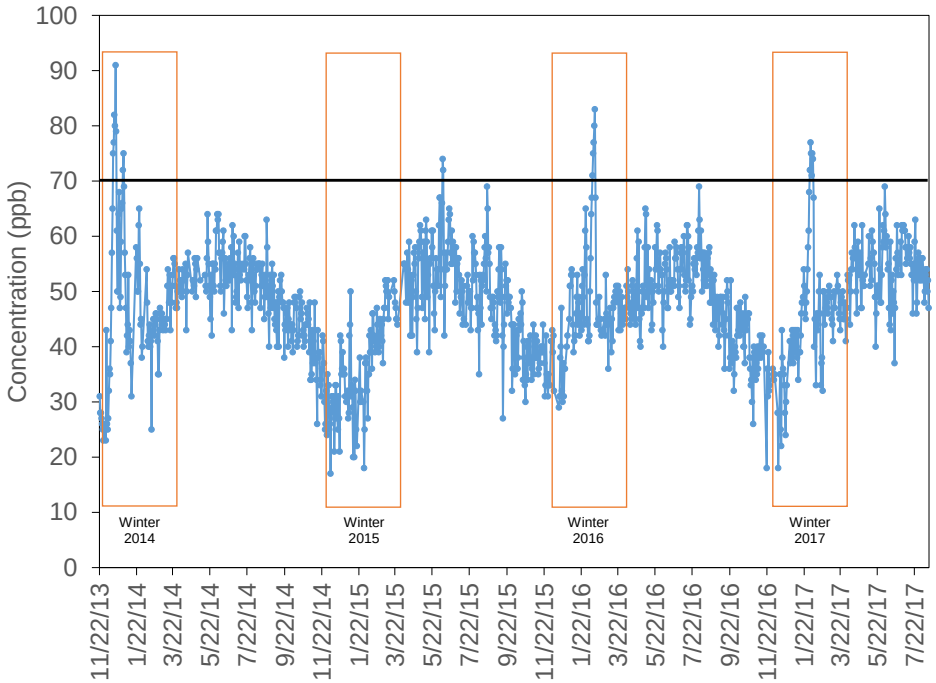

Dinosaur National Monument (DIN431), North (full site)

Table 2-3 summarizes the 10 highest DM8A O_3 concentrations annually at DIN431 over the four years 2014 through 2017.

Table 2-3 Ten Highest DM8A O_3 Concentrations at DIN431 for 2014 through 2017

Date	DM8A (ppb)	Rank
2014		
1/1/14	69	1
1/26/14	65	2
5/18/14	64	3
6/3/14	64	3
6/5/14	64	3
6/4/14	63	6
8/23/14	63	6
1/25/14	62	8
6/28/14	62	8
6/1/14	61	10
6/2/14	61	10
6/13/14	61	10
2015		
6/8/15	74	1
6/9/15	72	2
8/20/15	69	3
6/3/15	67	4
6/4/15	67	4
6/7/15	66	6
6/19/15	65	7
8/21/15	65	7
6/20/15	64	9
5/12/15	63	10
6/18/15	63	10

Date	DM8A (ppb)	Rank
2016		
2/13/16	83	1
2/12/16	80	2
2/11/16	77	3
2/10/16	75	4
2/9/16	71	5
8/2/16	69	6
2/8/16	67	7
2/14/16	67	7
1/29/16	65	9
5/6/16	65	9
2017		
2/1/17	77	1
2/2/17	75	2
2/4/17	75	2
2/5/17	74	4
1/31/17	72	5
2/3/17	71	6
6/3/17	69	7
1/30/17	68	8
2/6/17	67	9
9/7/17	66	10
3-year Averages		
Date	DM8A (ppb)	
2014–2016	68	
2015–2017	72	

Data from DIN431 also provides information on SO_2 and total NO_3^- concentrations in micrograms per cubic meter (µg/m^3) of air over the period November 2014 through July 2017. Figure 2-6 presents weekly average concentrations. Sulfur dioxide concentrations were low throughout the period while total NO_3^- concentrations showed occasional spikes that were 5 to 10 times higher than average. Two periods with high DM8A O_3 concentrations (Table 2-3) were observed during weeks with high total NO_3^- concentrations.

Figure 2-6 Weekly Average Concentrations of SO_2 and Total NO_3^- at DIN431

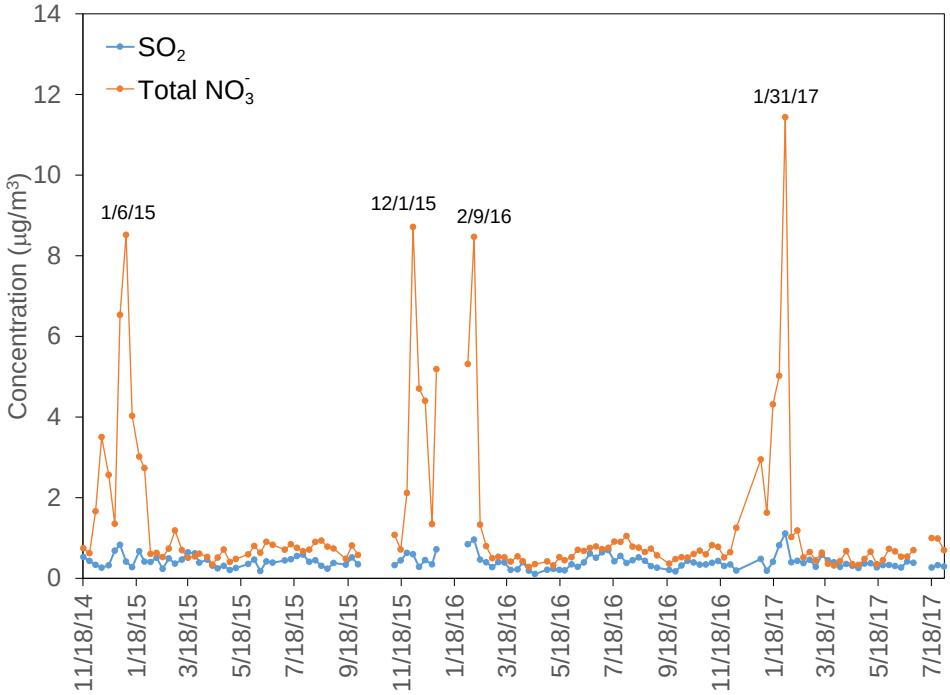

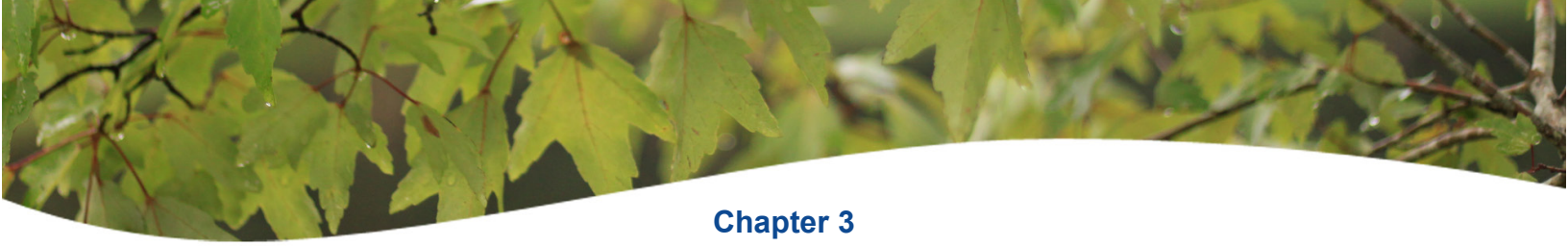

Chapter 3

Nitrogen Pollutant Concentrations

During 2016, weekly average concentrations of nitric acid, particulate nitrate, and particulate ammonium were measured using 3-stage filter packs at 95 CASTNET monitoring stations. Maps of 2016 annual mean total nitrate (nitric acid plus nitrate) and ammonium concentrations show the geographic distribution of the two pollutants measured. Box plots provide trends in annual mean total nitrate and ammonium concentrations aggregated over 34 eastern and 16 western reference sites. The nitrogen pollutants measured at the 34 eastern reference sites declined over the 27-year period from 1990 through 2016. Annual mean concentrations of total nitrate were reduced by 48 percent from 1990 through 2016. Ammonium concentrations declined by 63 percent. Total nitrate and ammonium concentrations measured at the 16 western reference sites were reduced by 34 percent and 31 percent, respectively, over the 21-year period 1996 through 2016.

Annual mean concentrations of total NO_3^- (HNO_3 + NO_3^-) and NH_4^+ for 2016 are presented in two maps in this chapter. Additional maps of 2016 quarterly mean concentrations are provided in CASTNET quarterly data reports (Wood, 2016a; 2016b; 2017a; 2017b). Trends in annual mean concentrations over the 27-year period, 1990 through 2016, were calculated from measurements from the 34 CASTNET eastern reference sites and for the 21-year period, 1996 through 2016, from data measured at the 16 CASTNET western reference sites. See Appendix A for the designated reference sites.

Total Nitrate Concentrations

Mean total NO_3^- concentrations measured in 2016 are presented in the map in Figure 3-1. To illustrate trends, Figure 3-2 provides box plots of total NO_3^- levels for the eastern and western reference sites through 2016. Each box presents the mean and median concentrations and the 10th, 25th, 75th, and 90th percentiles for that year. The data shown on the right side of the figure were aggregated from the 34 eastern reference sites. The data show no trend in mean concentrations until 2000 when total NO_3^- levels began to decline in response to NO_x emission controls. Total NO_3^- levels measured at the eastern reference sites were reduced by 53 percent from a mean value of 3.1 µg/m^3 in 2000 to a mean value of 1.5 µg/m^3 in 2016. Over the history of the network, 3-year mean levels declined from 3.0 µg/m^3 for 1990–1992 to 1.6 µg/m^3 for 2014–2016, producing a 48 percent reduction in total NO_3^-.

The left side of Figure 3-2 shows data aggregated from the 16 western sites. Total NO_3^- levels declined from 1.1 µg/m^3 to 0.6 µg/m^3 from 2000 through 2016, a 43 percent reduction. The 3-year mean total NO_3^- concentration for 2014–2016 was 34 percent lower than the corresponding 1996–1998 level. The 3-year mean concentration was 1.0 µg/m^3 for 1996–1998 and 0.7 µg/m^3 for 2014–2016.

Figure 3-1 Annual Mean Total NO_3^- Concentrations for 2016

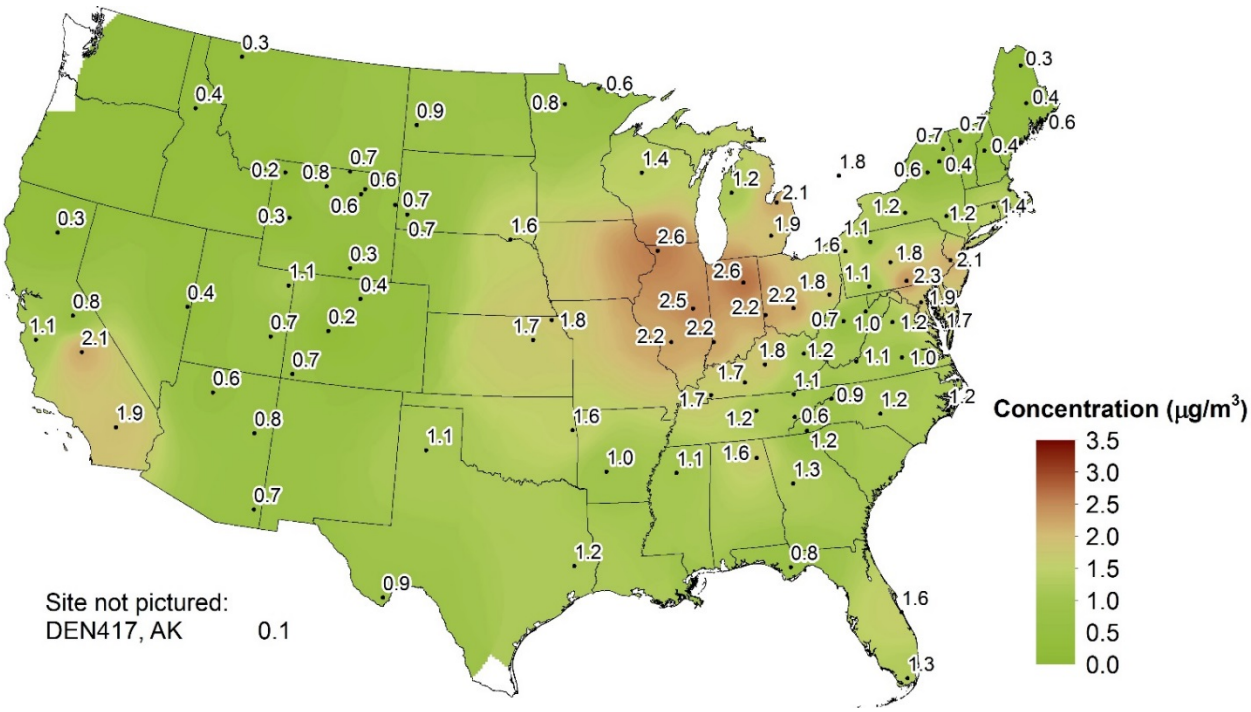

Figure 3-2 Trends in Annual Mean Total NO_3^- Concentrations

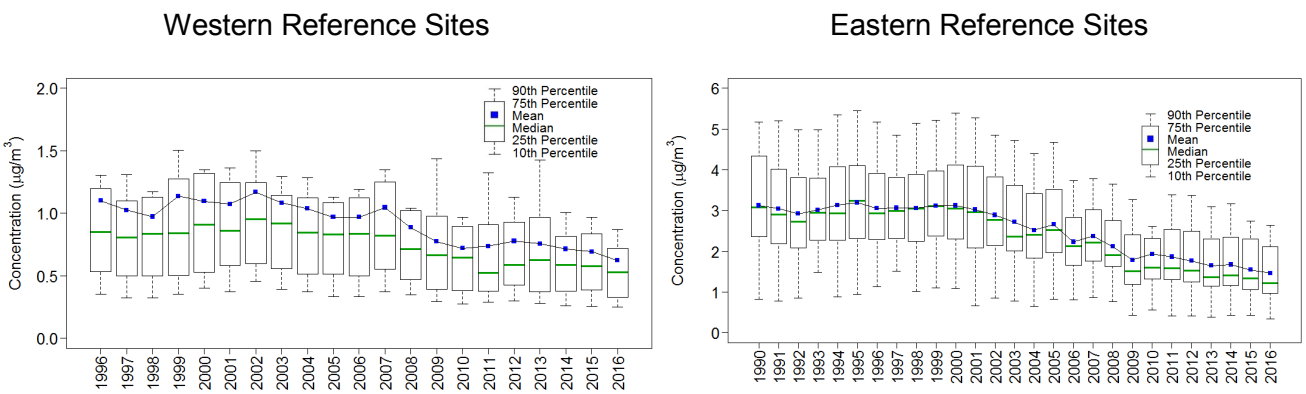

Figure 3-3 illustrates the trend in NO_x emissions from regulated EGUs operating in the eastern United States from 1990 through 2016. The 27-year decline in aggregated EGU emissions was 86 percent.

Figure 3-3 Trend in Annual Composite NO_x Emissions from Regulated EGUs Operating in the Eastern United States

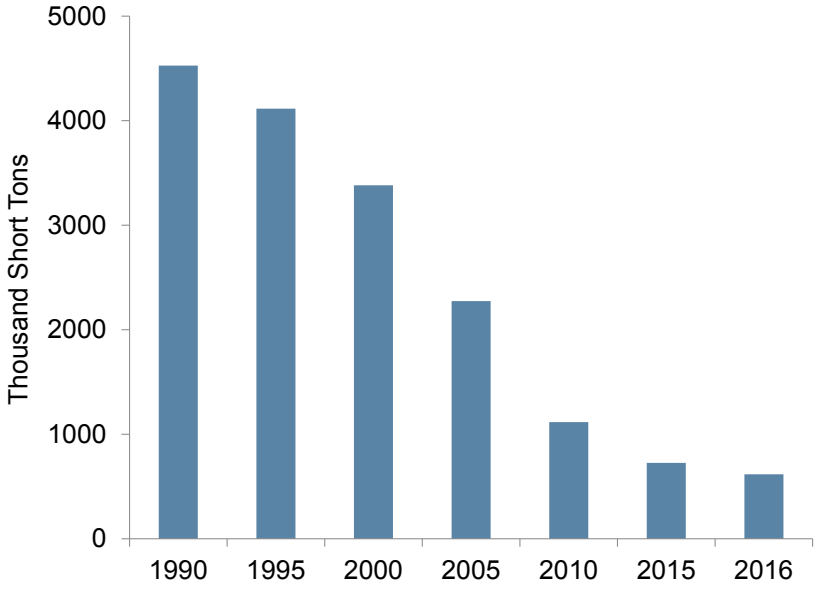

Source: EPA (2017)

Particulate Ammonium Concentrations

A map of 2016 mean particulate NH_4^+ concentrations is provided in Figure 3-4. Figure 3-5 shows box plots of NH_4^+ concentrations. The trend diagram for the eastern sites (right side) shows a reduction in mean NH_4^+ levels from 1990–1992 to 2014–2016. The 1990–1992 mean concentration was 1.8 µg/m^3, and the 2014–2016 value was 0.7 µg/m^3, a 63 percent decline. Similar to total NO_3^-, the eastern NH_4^+ concentrations began to decline in 2000 and have been reduced from 1.6 µg/m^3 in 2000 to 0.5 µg/m^3 in 2016. The western reference sites show a decline from 0.3 µg/m^3 in 1996–1998 to 0.2 µg/m^3 in 2014–2016, a 31 percent reduction.

QA PROGRAM SUMMARY

Quality Assurance Program Results

Precision of Filter Pack Measurements

Historical (1990 through 2015) mean absolute relative percent difference (MARPD) data for all 11 co-located site pairs operated over the history of the network are provided in the bar chart in Figure 3-a. The 2016 data for the current co-located sites at MCK131/231 and ROM406/206 are also provided. The precision criterion is a MARPD of 20 percent. Historical and 2016 measurements met the criterion for each analyte. The MARPD for SO_2 at ROM406/206 was unusually high because of the imprecision of lower concentrations measured during the first two quarters.

Figure 3-a Historical and 2016 Precision Results for Atmospheric Concentrations and Laboratory Replicate Samples

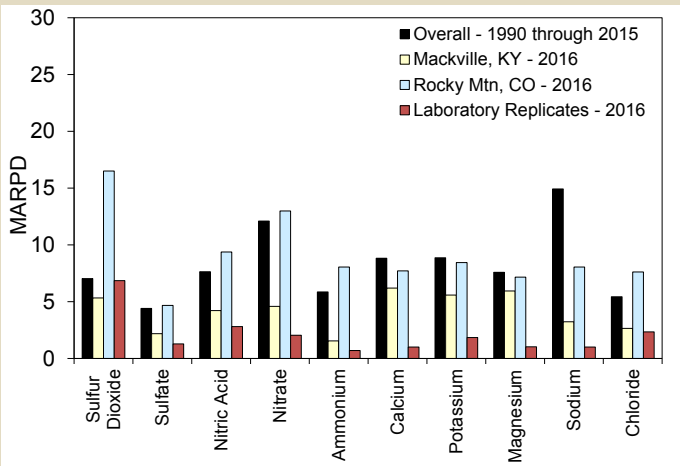

The 2016 analytical precision results for 10 analytes are also presented in Figure 3-a. The results were based on analysis of 5 percent of the samples that were randomly selected for replication in each batch. The results of in-run replicate analyses were compared with the original concentration results. The laboratory precision data met the 20 percent measurement criterion.

Data Completeness

Completeness is defined as the percentage of valid data points obtained from a measurement system relative to total possible data points. The CASTNET measurement criterion for completeness requires a minimum completeness of 90 percent for every parameter for each quarter. The historical results and the results for 2016 are given in Figure 3-b. Historical results for trace-level gas measurements represent data from 2013–2015. The completeness criterion was met for atmospheric (filter pack) and O_3 concentrations, filter pack flow, and meteorological measurements. Completeness of trace-level gas measurements (Chapter 6) met the completeness requirements of 40 CFR Part 50 (EPA, 2015c).

Figure 3-b Historical and 2016 Percent Completeness of Measurements (black bars are 1990–2015 for long-term data and 2013–2015 for trace-level gas data)

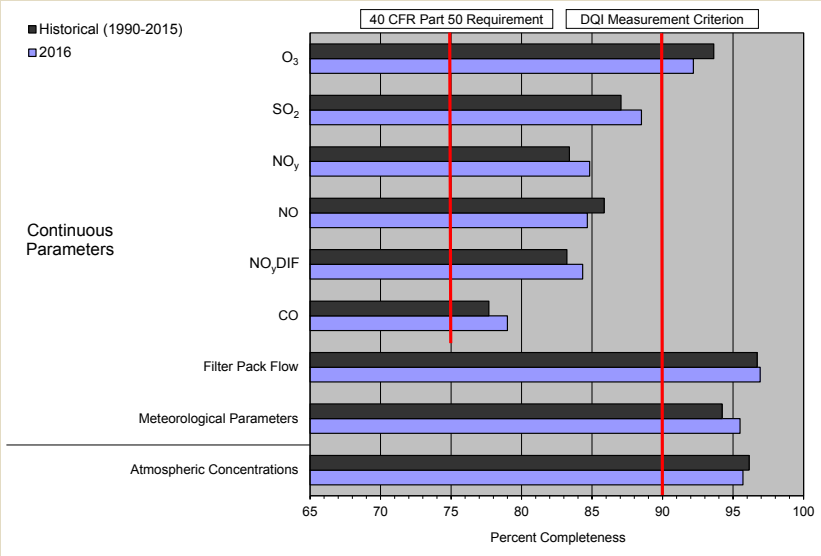

Figure 3-4 Annual Mean NH_4^+ Concentrations for 2016

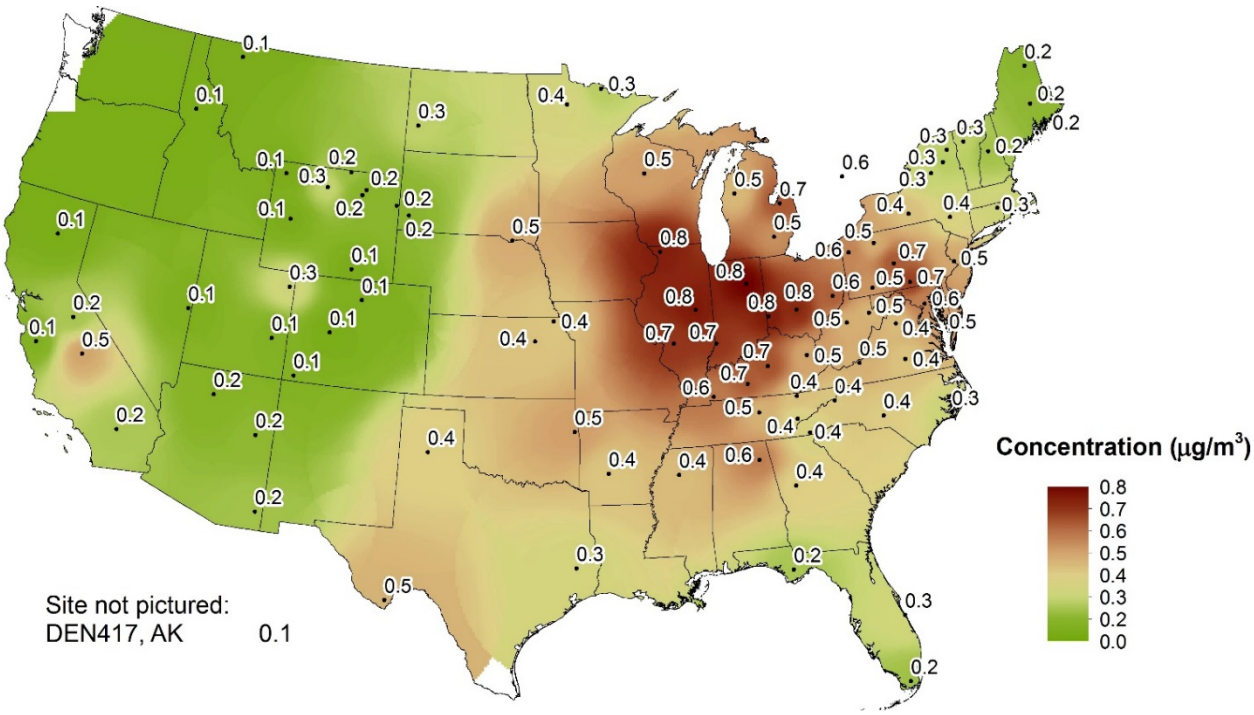

Figure 3-5 Trends in Annual Mean NH_4^+ Concentrations

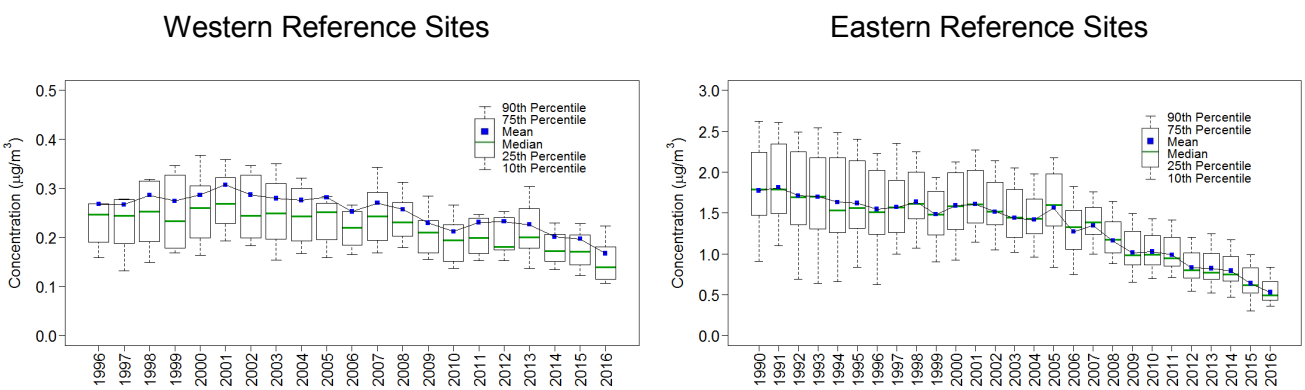

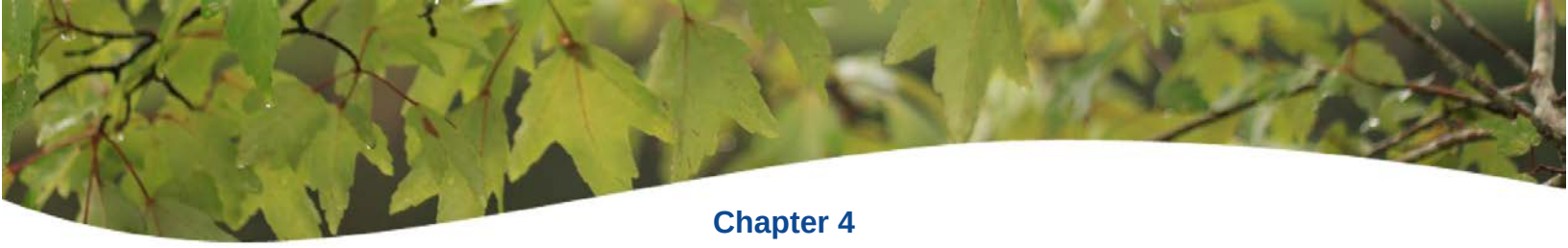

Chapter 4

Update on the Ammonia Monitoring Network

The Ammonia Monitoring Network (AMoN) operates passive ammonia samplers at 103 locations, 69 of which are located at CASTNET sites. AMoN is managed by the National Atmospheric Deposition Program. The network has been in operation since 2007 and provides information on 2-week integrated ammonia concentrations. Like other NADP networks, the goal of AMoN is to operate a long-term (i.e., for several decades), spatially diverse network with consistent measurements, covering all sensitive ecoregions of the continental United States.

Reduced nitrogen [ammonia (NH_3) + NH_4^+] is an important component to total nitrogen deposition. Wet deposition of NH_4^+ measured by NTN has been increasing in many areas of the United States over the past 10 years; however, until 2007, gaseous NH_3 concentrations were not routinely measured. Ammonia is the most prevalent alkaline gas in the atmosphere and is released into the air from a variety of agricultural sources (animal waste, fertilizer application, and agricultural burning), biological sources, gas and oil production and processing, and combustion. Agriculture is by far the largest source, producing approximately 80 percent of gaseous NH_3 emissions (EPA National Emissions Inventory, 2014). Although NH_3 is beneficial when used as NH_3-based fertilizer, it can have a negative effect on the environment when it reacts with acidic ions such as SO_4^{2-} and NO_3^- to form $PM_{2.5}$, which contributes to negative impacts on human health and visibility degradation. Atmospheric deposition of reduced nitrogen also contributes to eutrophication of sensitive ecosystems, decreases in species diversity, and increases in invasive species.

Average annual NH_3 concentrations for 2016 for the sites that met completeness requirements are mapped in Figure 4-1 and show a wide range of concentrations from a low of 0.2 µg/m^3 in New Hampshire (NH02) to a high of 15.9 µg/m^3 in northern Utah (UT01). The Utah monitoring site is located on a Utah State University research farm and small quantities of livestock are often present (Martin and Baasandorj, 2016). The farm is situated in the Cache Valley, an area with frequent stagnant weather. The next highest concentrations ranged from 3.4 to 4.3 µg/m^3 at eight sites west of the Mississippi River. The highest concentration east of the Mississippi was observed at Cranberry, NC (NC02) with a measured concentration of 5.2 µg/m^3. High NH_3 concentrations can be attributed to local emissions from hog and cattle feeding and waste and crop fertilization and production.

Figure 4-1 Annual Mean NH_3 Concentrations at AMoN sites for 2016

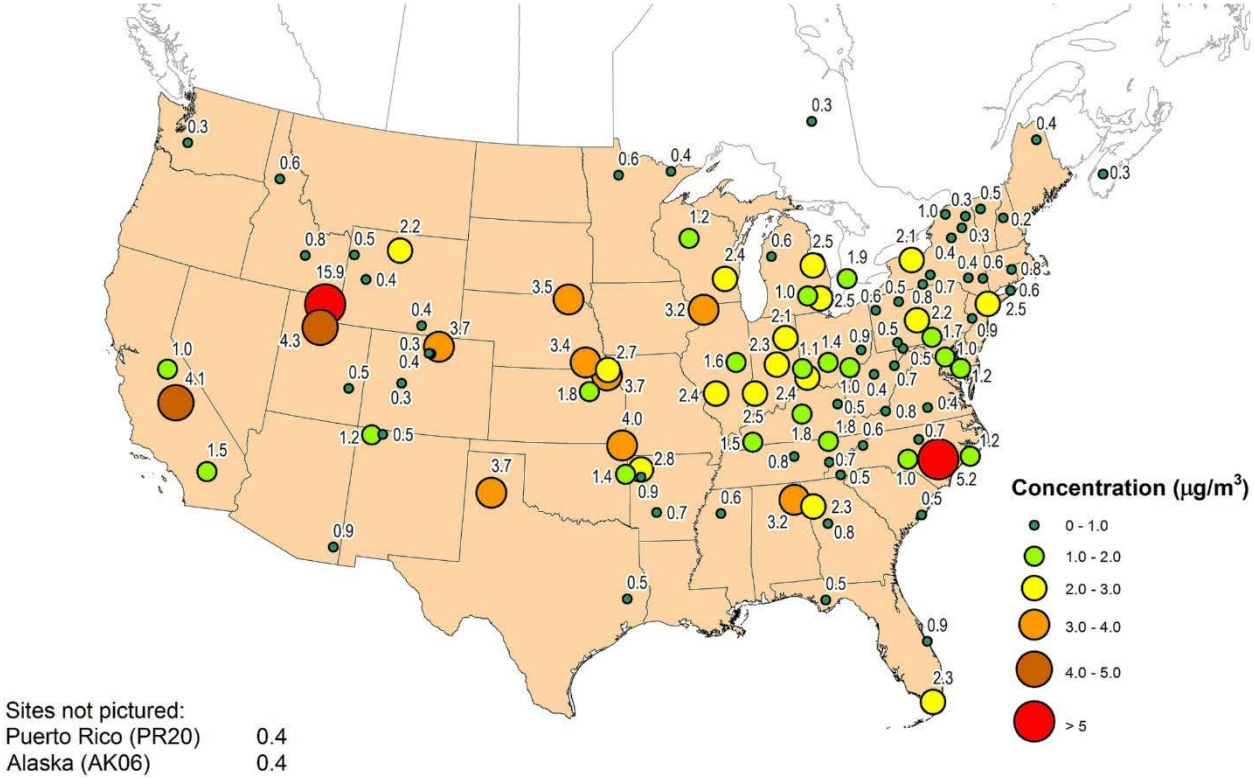

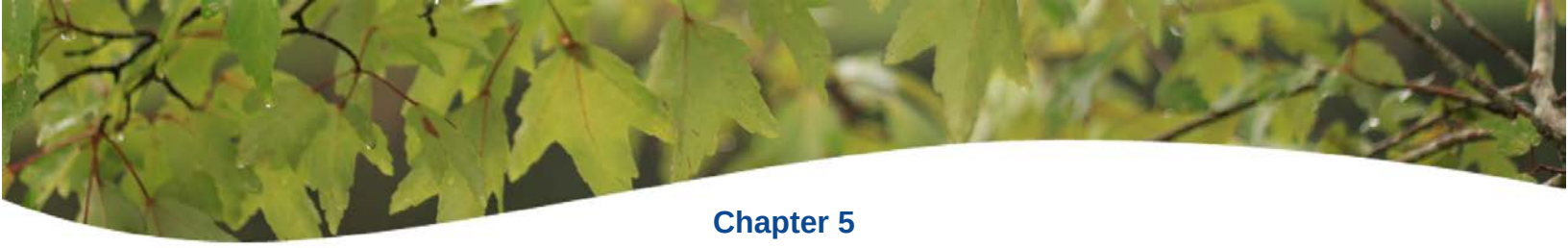

Chapter 5

Sulfur Pollutant Concentrations

During 2016, weekly average concentrations of sulfur dioxide and particulate sulfate were measured using 3-stage filter packs at 95 CASTNET monitoring stations. Maps of 2016 annual mean concentrations show the geographic distribution of the two pollutants across the United States. Annual sulfur dioxide and sulfate concentrations were aggregated over 34 eastern and 16 western reference sites in order to estimate trends, which are depicted using box plots. The sulfur dioxide pollutants measured at the eastern reference sites declined by 86 percent over the 27-year period from 1990 through 2016. Particulate sulfate concentrations were reduced by 70 percent. Measured concentrations of sulfur dioxide and sulfate have decreased steadily since 2005. Sulfur dioxide and sulfate concentrations measured at the 16 western reference sites have decreased by 46 and 31 percent, respectively, over the 21-year period 1996 through 2016.

Annual mean concentrations of SO_2 and SO_4^{2-} for 2016 are presented in this chapter. Additional maps of 2016 quarterly mean concentrations are provided in CASTNET quarterly data reports (Wood, 2016a; 2016b; 2017a; 2017b). Trends in annual mean concentrations over the 27-year period, 1990 through 2016, were derived from measurements from the 34 CASTNET eastern reference sites and for the 21-year period, 1996 through 2016, from data measured at the 16 CASTNET western reference sites. See Appendix A for descriptions of the designated reference sites.

Sulfur Dioxide Concentrations

Annual mean SO_2 concentrations are shown in Figure 5-1 for 2016. Annual mean concentrations were highest in the Midwest and East near and downwind of the Ohio River. Box plots of annual mean SO_2 concentrations aggregated over the 34 eastern reference sites from 1990 through 2016 (right side) and the 16 western reference sites from 1996 through 2016 (left side) are depicted in Figure 5-2. The y-axes on the western and eastern plots have different scales because concentrations measured at the western CASTNET sites were much lower than those measured at the eastern sites. Three-year mean concentrations for the CASTNET eastern reference sites for 1990–1992 and 2014–2016 were 8.8 $\mu g/m^3$ and 1.2 $\mu g/m^3$, respectively. This change constitutes an 86 percent reduction in 3-year mean SO_2 concentrations between the two periods. The 2016 mean level of 0.8 $\mu g/m^3$ was the lowest concentration measured by the eastern reference sites in the history of the network and represents a significant decline from the 2005 mean concentration of 6.0 $\mu g/m^3$.

The box plots for the western reference sites indicate a decline in annual mean SO_2 concentrations aggregated over the 16 sites. Three-year mean SO_2 concentrations for 1996–1998 and 2014–2016 were 0.6 $\mu g/m^3$ and 0.3 $\mu g/m^3$, respectively. This change constitutes a 46 percent reduction in 3-year mean SO_2 concentrations at the CASTNET western reference sites over the 21 years.

Figure 5-1 Annual Mean SO_2 Concentrations for 2016

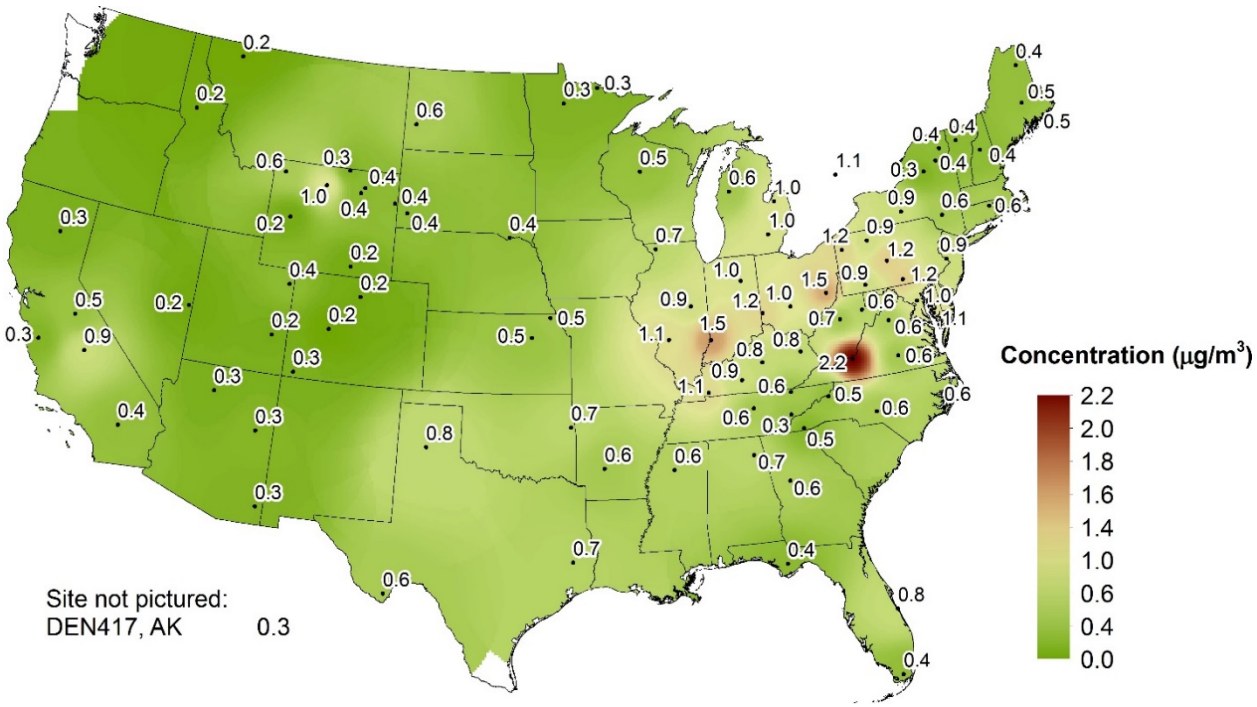

The 2016 average sulfur dioxide concentration for the eastern reference sites was 0.8 µg/m^3. The eastern sulfur dioxide data show a substantive decline since 1997. The reduction (86 percent) in sulfur dioxide concentrations over the period 1990 through 2016 is consistent with the reduction (94 percent) in sulfur dioxide emissions from EGUs operating in the eastern United States.

Figure 5-2 Trends in Annual Mean SO_2 Concentrations

Western Reference Sites

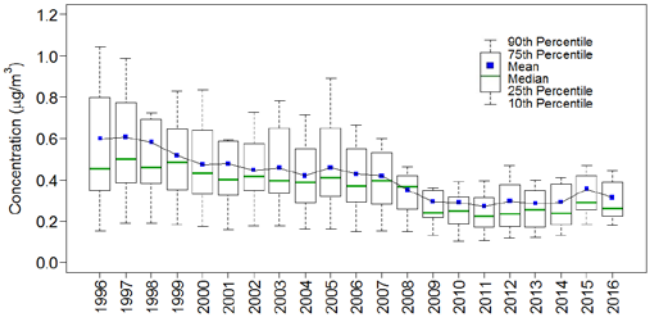

Eastern Reference Sites

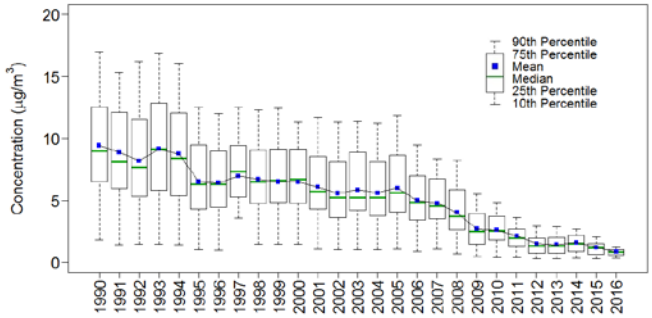

Figure 5-3 Trend in Annual Composite SO_2 Emissions from Regulated EGUs Operating in the Eastern United States

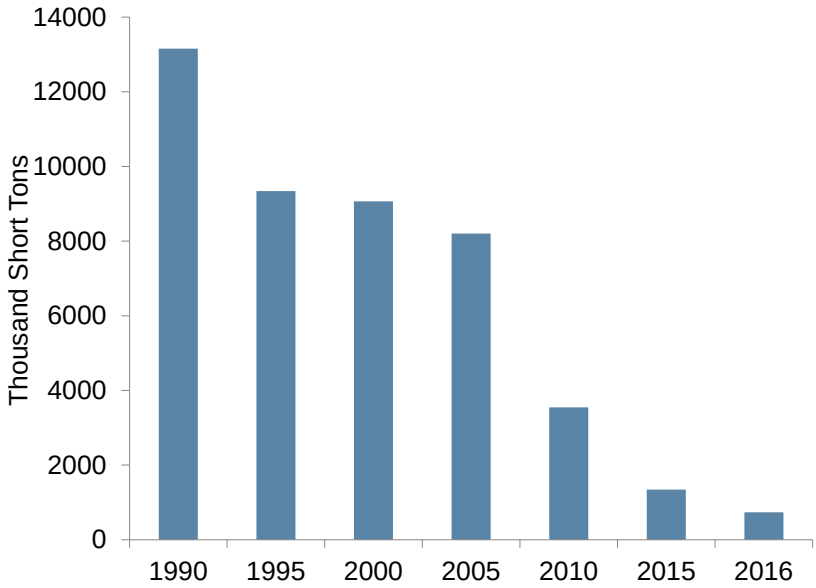

Source: EPA (2017)

Figure 5-3 illustrates the trend in SO_2 emissions from regulated EGUs from 1990 through 2016 aggregated over the eastern United States. The 27-year decline in aggregated emissions was 94 percent, which is consistent with the 86 percent reduction (Figure 5-2) in annual mean SO_2 concentrations aggregated over the CASTNET eastern reference sites.

Particulate Sulfate Concentrations

Figure 5-4 shows a map of 2016 annual mean particulate SO_4^{2-} concentrations. Figure 5-5 provides box plots of annual mean SO_4^{2-} concentrations from the 34 eastern reference sites (right side) and 16 western reference sites. The figure shows a substantial decline in SO_4^{2-} over the 27 years for the eastern CASTNET reference sites. Of particular interest, concentrations declined rapidly from 2005 through 2016. The difference between 3-year means from 1990–1992 to 2014–2016 depicts a 70 percent reduction in SO_4^{2-} from 5.4 µg/m^3 to 1.6 µg/m^3. The 2016 mean SO_4^{2-} level of 1.2 µg/m^3 for the eastern reference sites was the lowest in the history of the network. The box plots for the western reference sites are provided on the left side of Figure 5-5. The data show a 31 percent reduction in annual mean SO_4^{2-} concentrations aggregated over the 16 sites with 1996–1998 and 2014–2016 concentrations of 0.8 µg/m^3 and 0.5 µg/m^3, respectively.

Figure 5-4 Annual Mean SO_4^{2-} Concentrations for 2016

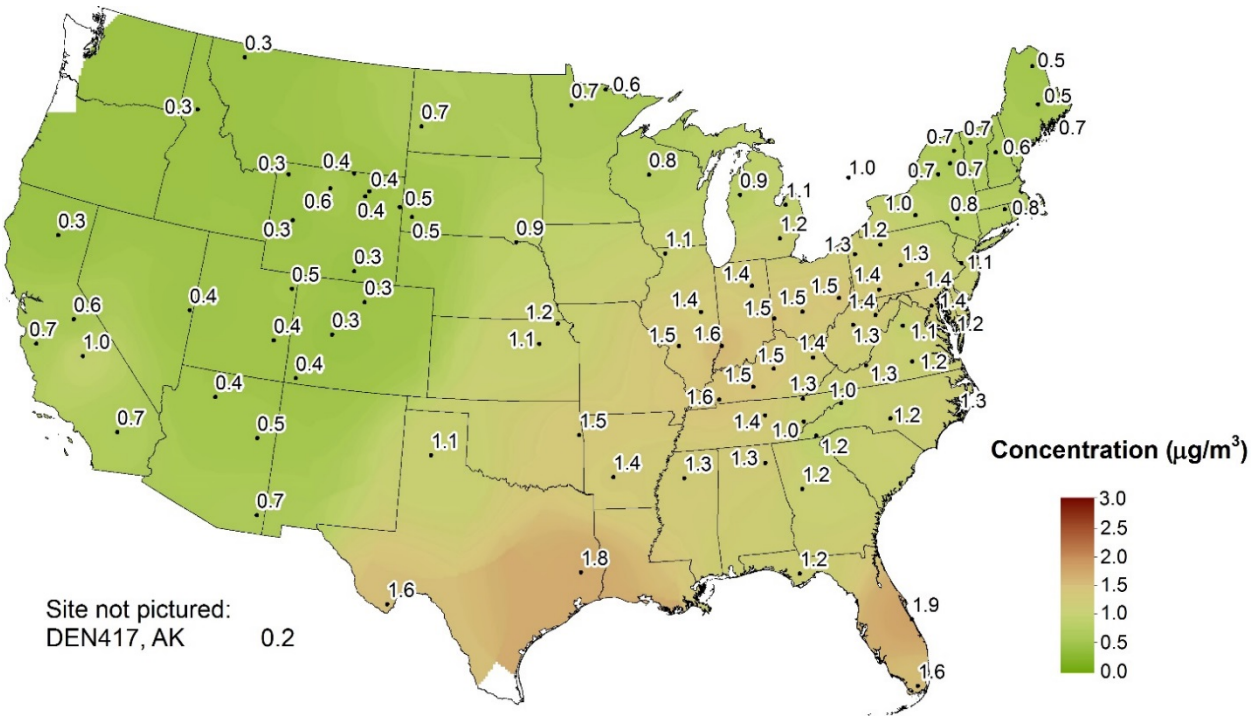

The 2016 average sulfate concentration for the eastern reference sites was 1.2 µg/m^3, the lowest level in the history of the network. The eastern sulfate data show a substantive decline since 2005. Sulfate concentrations declined more slowly than sulfur dioxide concentrations at the eastern reference sites. Western sulfate concentrations were lower and decreased at a slower rate than concentrations measured at the eastern sites.

Figure 5-5 Trends in Annual Mean SO_4^{2-} Concentrations

Western Reference Sites

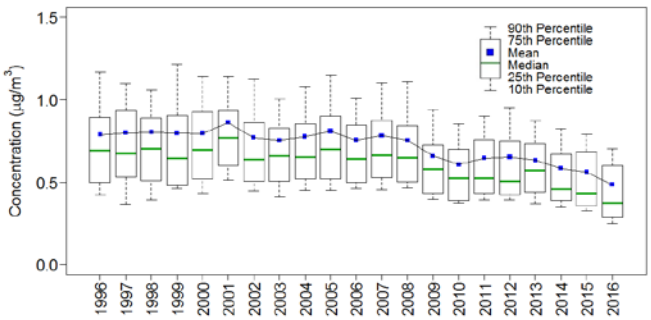

Eastern Reference Sites

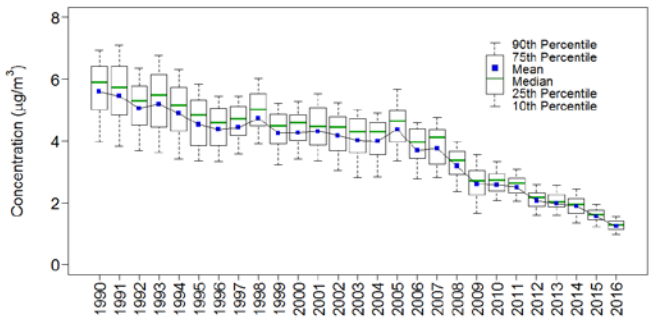

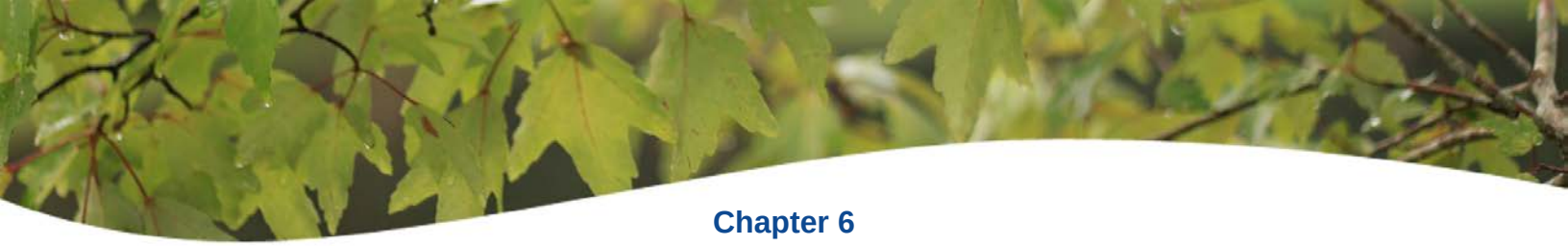

Chapter 6

Continuous Trace-level Gas Concentrations

Trace-level, gaseous, air quality monitors were operated continuously at eight CASTNET sites during 2016. EPA operated six monitors and NPS operated two. The measurements at these sites were performed to (1) provide data for regional model input and evaluation, (2) generate data to elucidate atmospheric processes such as ozone and fine particulate matter formation, and (3) support EPA NCore monitoring. Total reactive oxides of nitrogen were measured at all eight sites, sulfur dioxide at four sites, and carbon monoxide at two sites. Total reactive oxides of nitrogen concentrations were highest at the suburban Beltsville, MD site and lowest at the high-elevation, mountainous sites.

Trace-level gas analyzers were deployed at six EPA and two NPS CASTNET sites during 2016. Other federal, tribal, and state agencies also measured NO/NO_y at CASTNET or nearby sites in Maine, North Dakota, Oklahoma, and South Dakota. Table 6-1 lists the site locations, start dates, and the trace-level gas parameters measured at each CASTNET site. These data were sampled continuously and archived as 1-hour values.

Table 6-1 Continuous, Trace-level Gas Monitoring Stations Operated at CASTNET Sites during 2016

Site Location	Start Dates	Measurements
Beltsville, MD (BEL116)	March 2005	NO/NO_y and SO_2
Mammoth Cave National Park, KY (MAC426)*	May 2009	NO/NO_y, SO_2, and CO
Bondville, IL (BVL130)	July 2012	NO/NO_y, SO_2, and CO
Huntington Wildlife Forest, NY (HWF187)	November 2012	NO/NO_y
Pinedale, WY (PND165)	May 2013	NO/NO_y
Cranberry, NC (PNF126)	October 2013	NO/NO_y
Rocky Mountain National Park, CO (ROM206)	October 2013	NO/NO_y
Great Smoky Mountains National Park (GRS420)*	November 2014	NO/NO_y and SO_2

Note: *Operated by NPS

NO_y is defined as NO_x [NO + nitrogen dioxide (NO_2)] plus NO_z [HNO_3, nitrous acid (HONO), peroxyacetyl nitrate, peroxyproyl nitrate, other organic nitrates, and nitrite]. It consists of reactive gases that are considered precursors of O_3 and $PM_{2.5}$. Measurement of NO_y begins with conversion to NO using a thermal catalytic converter and measurement of the NO by chemiluminescence. Continuous SO_2 is measured using ultraviolet fluorescence, and CO is measured by gas filter correlation.

Figure 6-1 provides a map of the CASTNET continuous trace-level gas monitoring locations. All EPA sites were operated according to the CASTNET QAPP Appendix 11, “Procuring, Installing, and Operating NCore Air Monitoring Equipment at CASTNET Sites” (Wood, 2015). NPS sites were operated according to the NPS QAPP (Air Resource Specialists, 2015).

Figure 6-1 CASTNET NO_y Monitoring Network in 2016

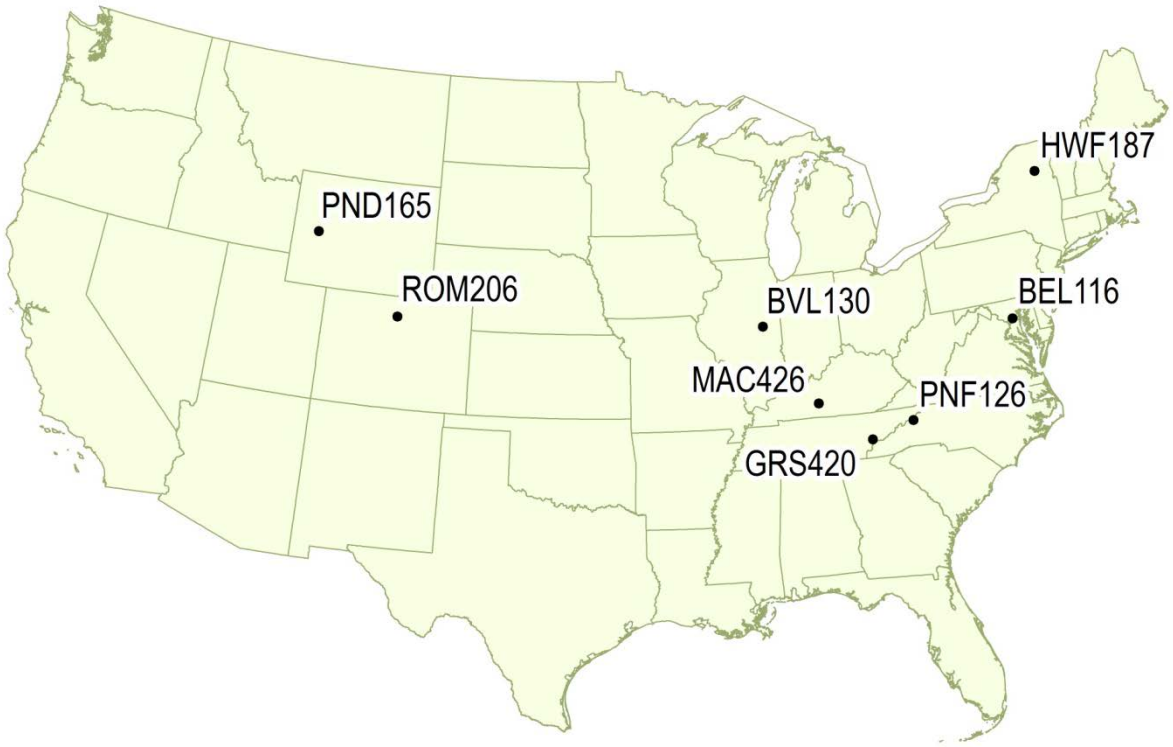

Figures 6-2 through 6-4 and Figure 6-6 present 2016 annual average hourly composite diurnal profiles of SO_2, NO_y, and O_3 for BEL116, BVL130, MAC426, and GRS420, respectively. Figures 6-5 and 6-7 through 6-9 show the 2016 annual average hourly composite diurnal profiles of NO_y and O_3 for HWF187, PNF126, PND165, and ROM206. The profiles in Figures 6-2 through 6-9 were constructed by averaging all values from the same hour for 2016. Sulfur dioxide and NO_y are plotted against the left y-axis, and O_3 is plotted against the right y-axis in the eight diagrams. The figures illustrate that differences in geography, terrain, and elevation affect concentrations of photochemically reactive pollutants in the boundary layer.

Figure 6-2 BEL116, MD 1-hour Mean Concentrations of SO_2, NO_y, and O_3 for 2016

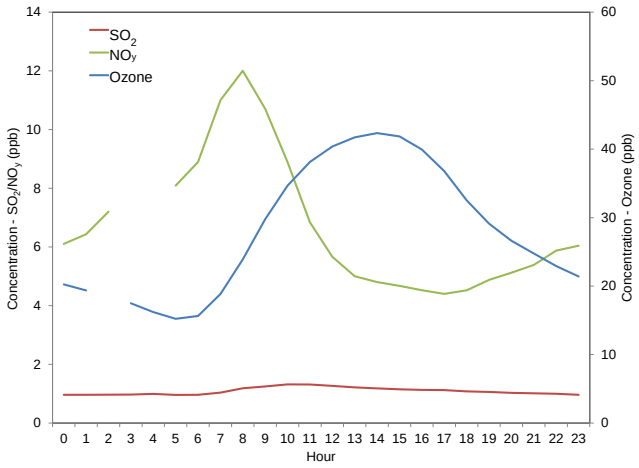

Figure 6-3 BVL130, IL 1-hour Mean Concentrations of SO_2, NO_y, and O_3 for 2016

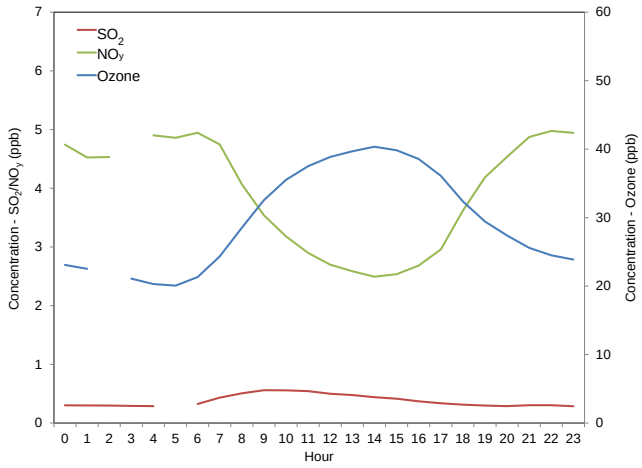

Figure 6-4 MAC426, KY 1-hour Mean Concentrations of SO_2, NO_y, and O_3 for 2016

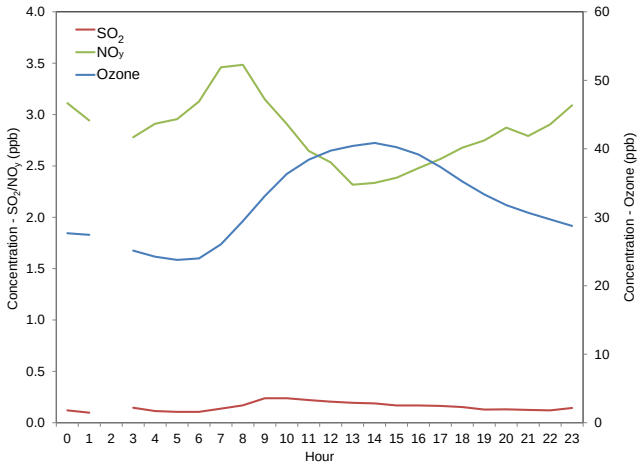

Figure 6-5 HWF187, NY 1-hour Mean Concentrations of NO_y and O_3 for 2016

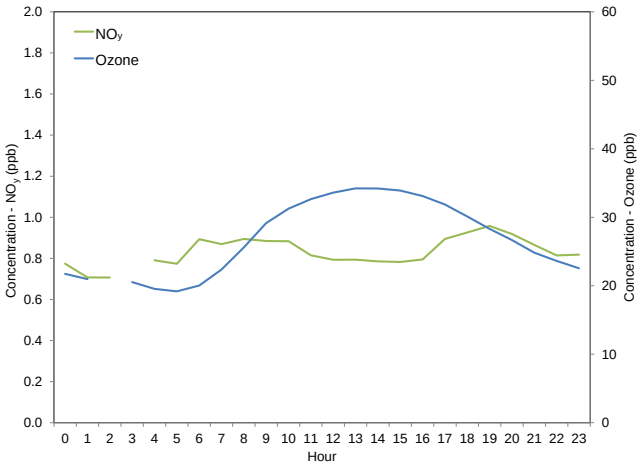

Figure 6-6 GRS420, TN 1-hour Mean Concentrations of SO_2, NO_y, and O_3 for 2016

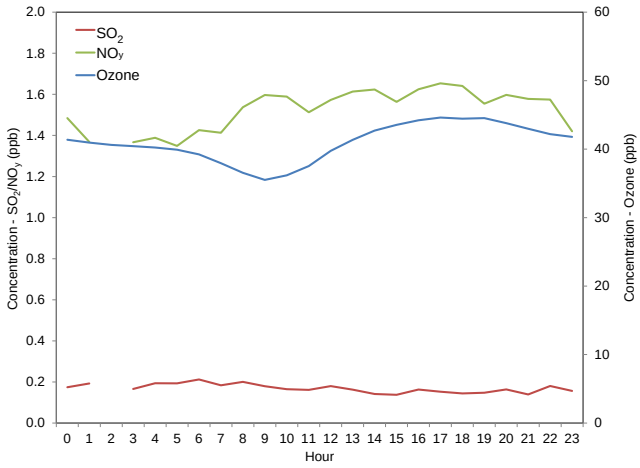

Figure 6-7 PNF126, NC 1-hour Mean Concentrations of NO_y and O_3 for 2016

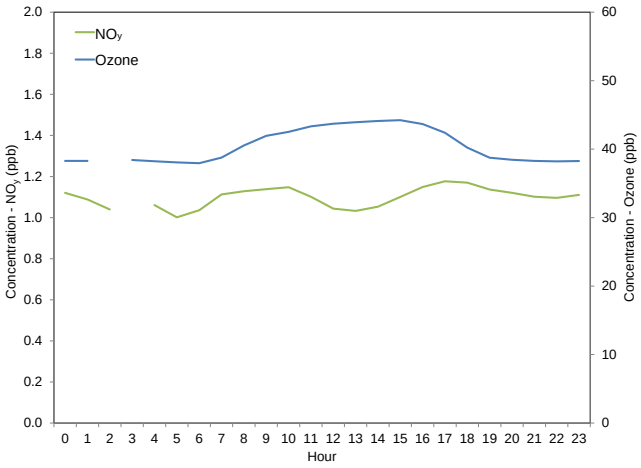

Figure 6-8 PND165, WY 1-hour Mean Concentrations of NO_y and O_3 for 2016

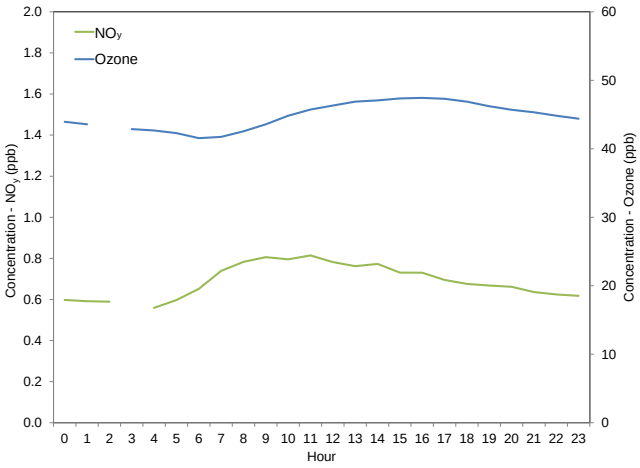

Figure 6-9 ROM206, CO 1-hour Mean Concentrations of NO_y and O_3 for 2016

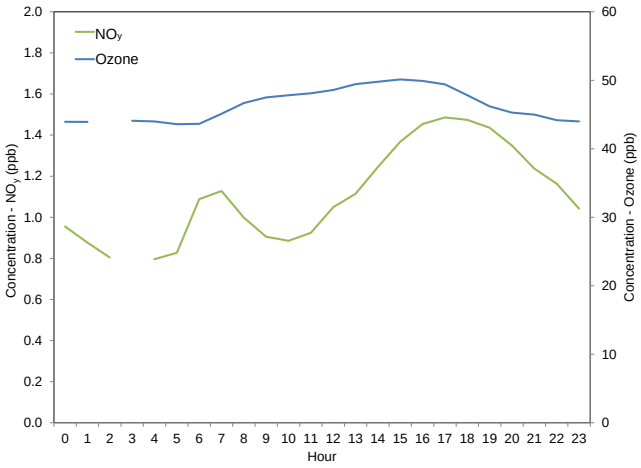

Table 6-2 Summary of 2016 Minimum and Maximum Values from Diurnal Charts

Site Location	Site Elevation (meters)	NO_y (ppb)		O_3 (ppb)	
		Minimum	Maximum	Minimum	Maximum
BEL116, MD	47	4.4	12.0	15	42
BVL130, IL	213	2.5	5.0	20	40
MAC426, KY	243	2.3	3.5	24	41
HWF187, NY	497	0.7	1.0	19	34
GRS420, TN	793	1.3	1.7	36	45
PNF126, NC	1,216	1.0	1.2	38	44
PND165, WY	2,386	0.6	0.8	42	47
ROM206, CO	2,742	0.8	1.5	44	50

Continuous Trace-level NO_y and Ozone

The minimum and maximum mean composite NO_y and O_3 concentrations shown in Figures 6-2 through 6-9 are summarized in Table 6-2. The sites are listed in order of elevation. The highest NO_y concentrations were measured at BEL116, which is situated in an area with numerous mobile-source NO_x emissions. Low NO_y values (less than 2.0 ppb) were recorded at the five rural sites in New York, Tennessee, North Carolina, Wyoming, and Colorado. The eight profiles in Figures 6-2 through 6-9 illustrate the loss of O_3 during the late afternoon and nighttime hours and its production during daylight hours. The diurnal change was less pronounced at the six rural sites. The BEL116 site observed the largest nighttime loss and subsequent highest daytime production, an average difference of about 27 ppb of O_3 for 2016. The BVL130 data illustrate a typical diurnal relationship between NO_y and O_3 concentrations with high NO_y concentrations associated with vehicular NO_x emissions in the morning and evening and elevated O_3 concentrations in the afternoon. The data from the rural MAC426 site also show a diurnal evolution with the highest NO_y concentrations in the morning and the evening and highest O_3 concentrations in the afternoon. The MAC426 data appear similar to measurements made at an urban site.

Ozone concentrations were also measured at the eight sites listed in Table 6-2 during 2016. The highest O_3 concentration (50 ppb) was recorded at ROM206. The concentrations measured at the four sites with the highest elevations show less 24-hour variation than the other four sites because of the dearth of nighttime O_3 loss/depletion mechanisms near the high-elevation monitors (Talbot *et al.*, 2005). In particular, nighttime dry deposition is small because fresh nitric oxide is not available to react with O_3 and sparse vegetation produces little scavenging. The ROM206 data suggest a production or transport of NO_y around sunset. There are no significant NO_x sources in the immediate area. The increase in NO_y is likely a result of the transformation of polluted air masses from the Front Range Urban Corridor and the frequent late afternoon upslope flow from the east (Baumann *et al.*, 1997).

Continuous Trace-level NO_y and Filter Pack Total Nitrate Concentrations

Nitric acid and particulate NO_3^- are measured on CASTNET filter packs, and the sum is reported as total NO_3^-. Because HNO_3 and particulate NO_3^- are measured as components of NO_y, NO_y concentrations should always be higher than total NO_3^- levels (i.e., the ratio of NO_y to total NO_3^- should always be greater than 1.0). A comparison of weekly mean continuous NO_y concentrations with filter pack total NO_3^- levels at BVL130, PNF126, and PND165 for 2016 was used to evaluate the measurements (Figures 6-10 through 6-12). The NO_y concentrations were consistently higher than the total NO_3^- levels, as expected. The results are similar for the other five sites. The weekly total NO_3^- concentrations, the average weekly NO_y levels, and their ratios are listed in Table 6-3. These were calculated as the average of all valid weekly filter pack concentrations, the average of mean NO_y values matching the run time of the weekly filter packs, and the average of the ratios calculated for each week. Weekly NO_y levels were higher than the weekly total NO_3^- concentrations with ratios of NO_y to total NO_3^- varying from 2.46 at PNF126 to 10.87 at BEL116. The highest concentration (0.98 ppb) of total NO_3^- was measured at BVL130.

Huntington Wildlife Forest, NY (HWF187)

Figure 6-10 Comparison of BVL130, IL Weekly Mean Continuous Trace-level NO_y and Filter Pack Total NO_3^- Concentrations

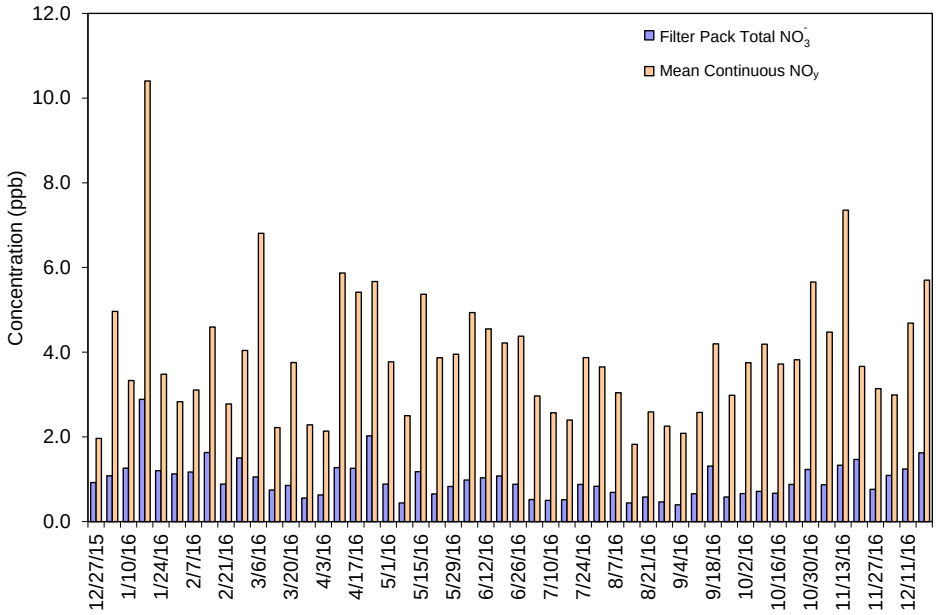

Figure 6-11 Comparison of PNF126, NC Weekly Mean Continuous Trace-level NO_y and Filter Pack Total NO_3^- Concentrations

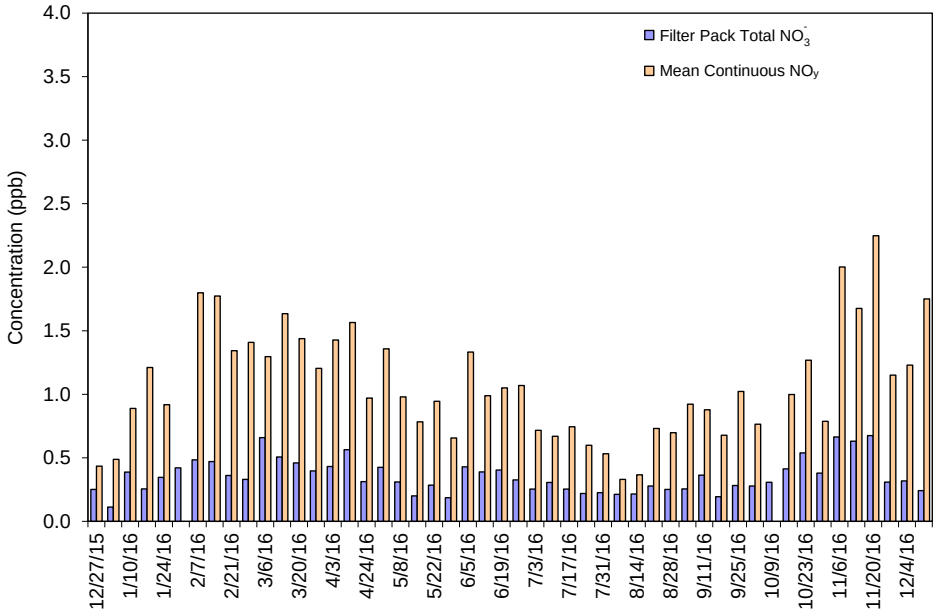

Figure 6-12 Comparison of PND165, WY Weekly Mean Continuous Trace-level NO_y and Filter Pack Total NO_3^- Concentrations

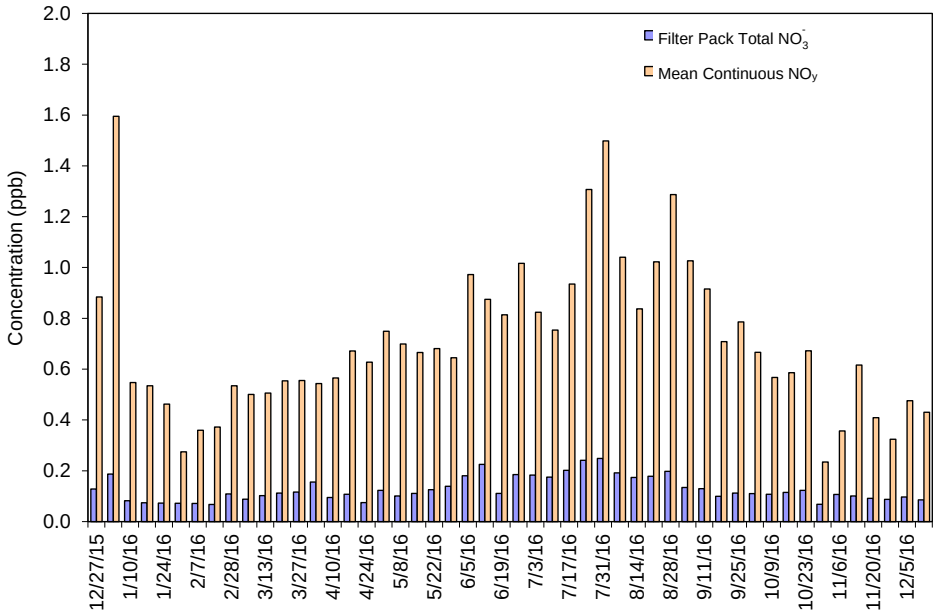

Table 6-3 Summary of Total NO_3^- and NO_y Measurements for 2016

Site Location	Total NO_3^- (ppb)	NO_y (ppb)	Ratio
BEL116, MD	0.76	8.01	10.87
BVL130, IL	0.98	4.39	5.03
MAC426, KY	0.70	2.79	4.30
HWF187, NY	0.21	0.94	3.58
GRS420, TN	0.45	1.97	4.93
PNF126, NC	0.33	0.81	2.46
PND165, WY	0.14	0.75	5.27
ROM206, CO	0.20	1.20	5.86

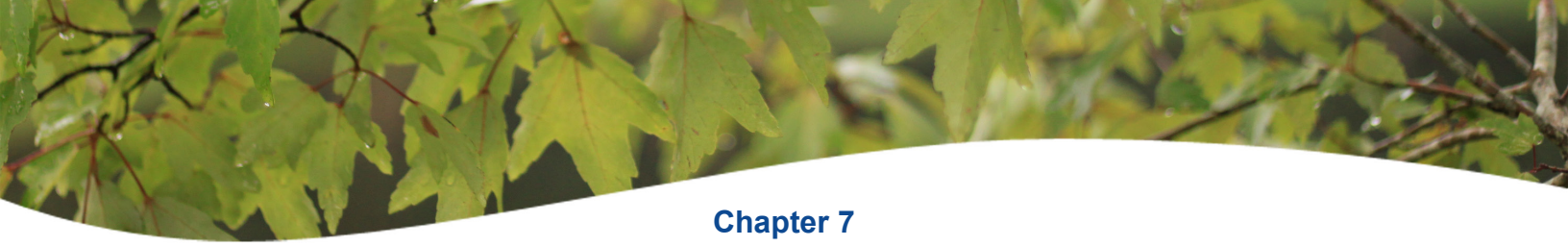

Chapter 7

Effects of Wildfires on Air Quality

Wildfires produce large amounts of smoke, fine particulate matter, nitrogen oxides, and other trace-level gases. In particular, in the western United States, wildfires and prescribed agricultural and forest management burns are large sources of aerosols and trace gases. The 2016 western wildfire season was extensive, especially following the winter of 2015–2016 drought. The Maple Fire at the western edge of Yellowstone National Park burned over 45,000 acres in August 2016. Fine particulate matter concentrations measured at IMPROVE sites in and near the park showed elevated concentrations. The Jack Fire in Arizona started on May 29, 2016 and continued to burn until July 1. During that period, it burned 33,850 acres in the Coconino National Forest, which is located about 24 kilometers south of Flagstaff.

Wildfires occur naturally in the United States. In the West, wildfires and prescribed agricultural and forest management burns are a large global source of aerosols and trace-level gases from burning vegetation, buildings, and other materials. Smoke from wildfires is a significant source of air pollution and can pose potential risks to health, visibility, and safety. According to Liu *et al*. (2016), open fires contributed significantly (about 37 percent) to $PM_{2.5}$ emitted in the contiguous United States and produced substantial amounts of O_3 precursors. Wildfires usually consume more biomass fuel per unit area burned than prescribed fires. Land use changes, wildfire management strategies, and climate change have increased wildfire size and frequency and the length of the fire season in the western United States. The 2016 western wildfire season was extensive in both area burned and length of the season, especially following the drought during the winter of 2015–2016.

Liu *et al*. (2016) analyzed aircraft air pollutant measurements in three plumes from wildfires in the western United States in 2013. The study reported an extensive set of emission factors for about 80 gases and five components of submicron particulate matter (PM_1) from these wildfires. The measured emission factors were used to estimate the annual wildfire emissions of CO, NO_x, total non-methane organic compounds, and PM_1 from 11 western states. The wildfires emitted high amounts of PM_1 with organic aerosol dominating the mass. The results from Liu *et al*. (2016) indicate that PM_1 emissions from wildfires are substantially higher than those from prescribed burns and that prescribed burning may be an effective method to reduce overall fine particle emissions.

Measurements from CASTNET, IMPROVE, the EPA Chemical Speciation Network (CSN), and other federal and state networks provide information to characterize the impacts of wildfires on air quality and visibility near critical resources such as national parks. In 2016, fires extended from the northern tier states to Arizona, New Mexico, and Texas. Figure 7-1 gives box plots of third quarter mean O_3 measurements aggregated over the CASTNET western reference sites (Appendix A). The O_3 box plots were constructed by averaging all valid hourly O_3 concentrations within third quarter by site and

then averaging those averages for all western reference sites. The figure shows increased aggregated mean concentrations for 2016.

Figure 7-1 Trends in Third Quarter Mean O_3 Concentrations at CASTNET Western Reference Sites

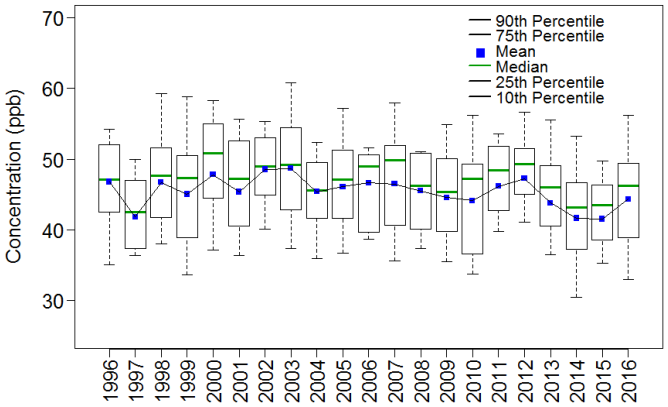

During the 2016 fire season, 22 fires burned in Yellowstone National Park, WY (YEL408). The park is required to protect human life as well as the approximately 2 percent of Yellowstone's 2.2 million acres that are considered developed (e.g., roads, buildings, and other infrastructure) from the threat of fire, while at the same time letting fire play its ecological role in the landscape as much as possible. 2016 was the most active fire year since 1988 with 62,000 acres burned. Seven wildfires were the result of human activity such as a campfire, vehicle operation, or cigarettes. The remainder of the 2016 wildfires resulted from natural causes (i.e., lightning). Eleven fires were suppressed because infrastructure was threatened. Many fires were managed to allow them to perform their natural role in the ecosystem. The largest of these fires, the Maple Fire, burned over 45,000 acres.

Figure 7-2 is a photograph of the Maple Fire in Wyoming, August 21, 2016, taken by the Visible Infrared Imaging Radiometer Suite (VIIRS) instrument aboard the National Oceanic and Atmospheric Administration (NOAA)/National Aeronautics and Space Administration (NASA) Suomi National Polar-orbiting Partnership satellite. The Maple Fire was detected the evening of August 8, 2016 by an aircraft passing over Yellowstone. The fire was located 6 kilometers (km) east of the park's west boundary, 8 km northeast of the community of West Yellowstone, MT, and 4.5 km from Madison Junction. Rain accompanied by cool weather at the end of August slowed the spread of the Maple Fire that had come within 5 km of West Yellowstone.

Figure 7-2 Satellite Photo of Wyoming Maple Fire August 21, 2016

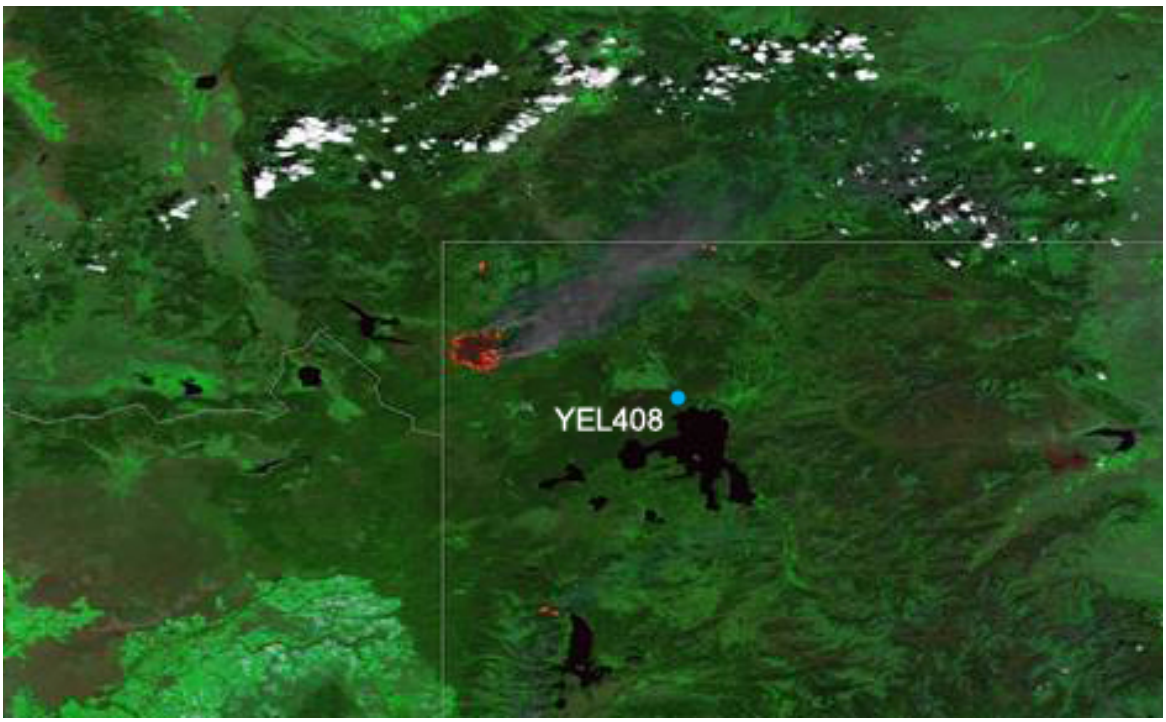

Source: NOAA Environmental Visualization Laboratory/NASA (2016)

Hourly and DM8A O_3 concentrations measured at three Wyoming CASTNET sites [Basin (BAS601), Pinedale (PND165), and YEL408] over the period of August 11, 2016 through September 6, 2016 are plotted in Figure 7-3. Time series of $PM_{2.5}$ concentrations measured over the period July 8, 2016 through October 6, 2016 at IMPROVE sites in Wyoming [Boulder Lake (BOLA1), Bridger Wilderness (BRID1), North Absaroka (NOAB1), and Yellowstone (YELL2)] are shown in Figure 7-4. Comparatively high $PM_{2.5}$ concentrations were measured at YELL2 and NOAB1 after the fire started. For example, $PM_{2.5}$ concentrations were 2.92 times higher at NOAB1 and 2.59 times higher at YELL2 during the period of the Maple Fire than they were during the remainder of July through August. Concentrations were reduced by the end of the month.

Lightning started the Jack Fire in Arizona on May 29, 2016, and it continued to burn until July 1. During that period, it burned 33,850 acres in the Coconino National Forest, which is located about 24 km south of Flagstaff, 113 km south-southeast of the CASTNET site at Grand Canyon National Park (GRC474), and 145 km west of the CASTNET site at Petrified National Forest (PET427). Figure 7-5 shows smoke from the Jack Fire streaming eastward. Weekly average O_3 concentrations shown in Figure 7-6 for three CASTNET sites in Arizona [GRC474, PET427, and Chiricahua National Monument (CHA467)] and one in Colorado [Mesa Verde National Park (MEV405)] showed no significant change after the beginning of the Jack Fire. Time series of $PM_{2.5}$ concentrations measured over the period April 30, 2016 through July 29, 2016 at nearby IMPROVE sites Grand Canyon (GRCA2), Petrified National Forest (PEFO1), Chiricahua (CHIR1), and Mesa Verde National Park

(MEVE1) are shown in Figure 7-7. Fine particulate matter concentrations measured at PEFO1 and CHIR1 were elevated during the fire except for relative minima for two samples on June 14 and June 17, 2016. Synoptic weather data (NOAA National Centers for Environmental Prediction, 2018) suggest the wind direction shifted southeast during those two sampling periods, transporting the fire plume away from the samplers at PEFO1 and CHIR1. $PM_{2.5}$ concentrations were 1.5 times higher at CHIR1 and 2.25 times higher at PEFO1 during the period of the Jack Fire than during the remainder of April through July.

Figure 7-3 Time Series of Wyoming CASTNET O_3 Data

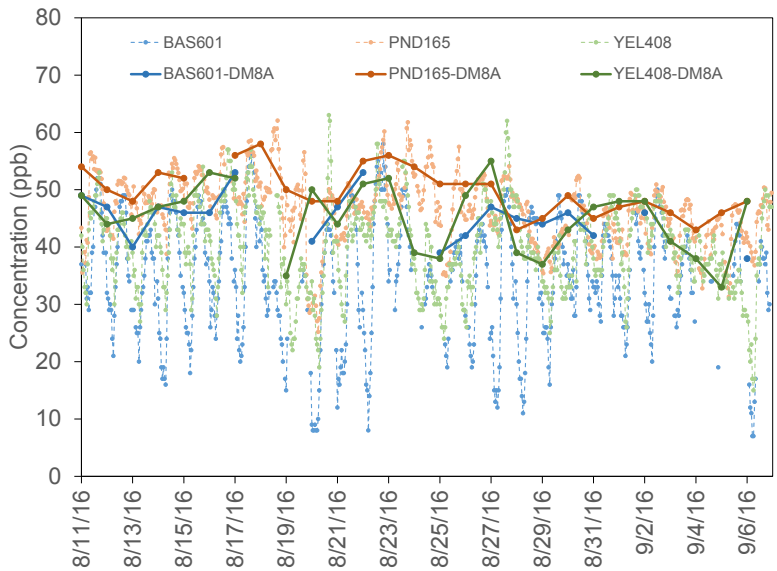

Figure 7-4 Time Series of Wyoming IMPROVE $PM_{2.5}$ Data

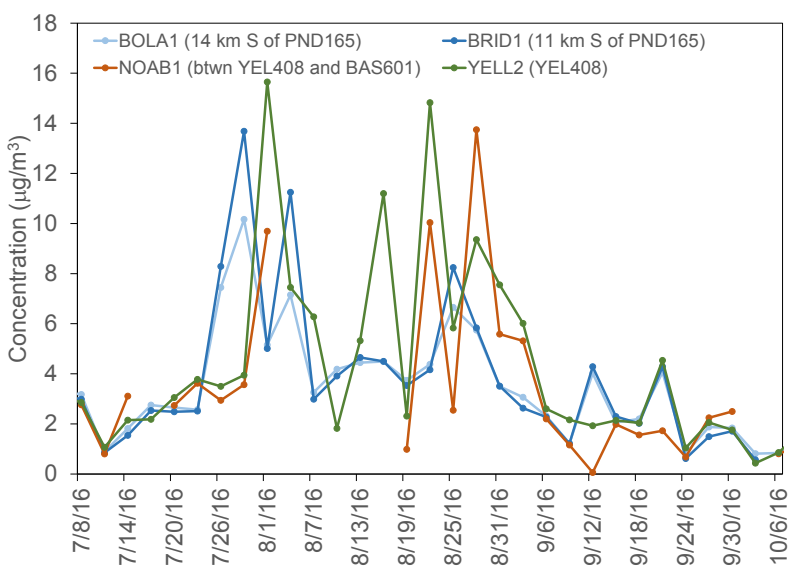

Note: Corresponding CASTNET site with the location of the IMPROVE site in relation to the CASTNET site listed in parentheses.

Figure 7-5 Satellite photo of Arizona Jack Fire June 9, 2016

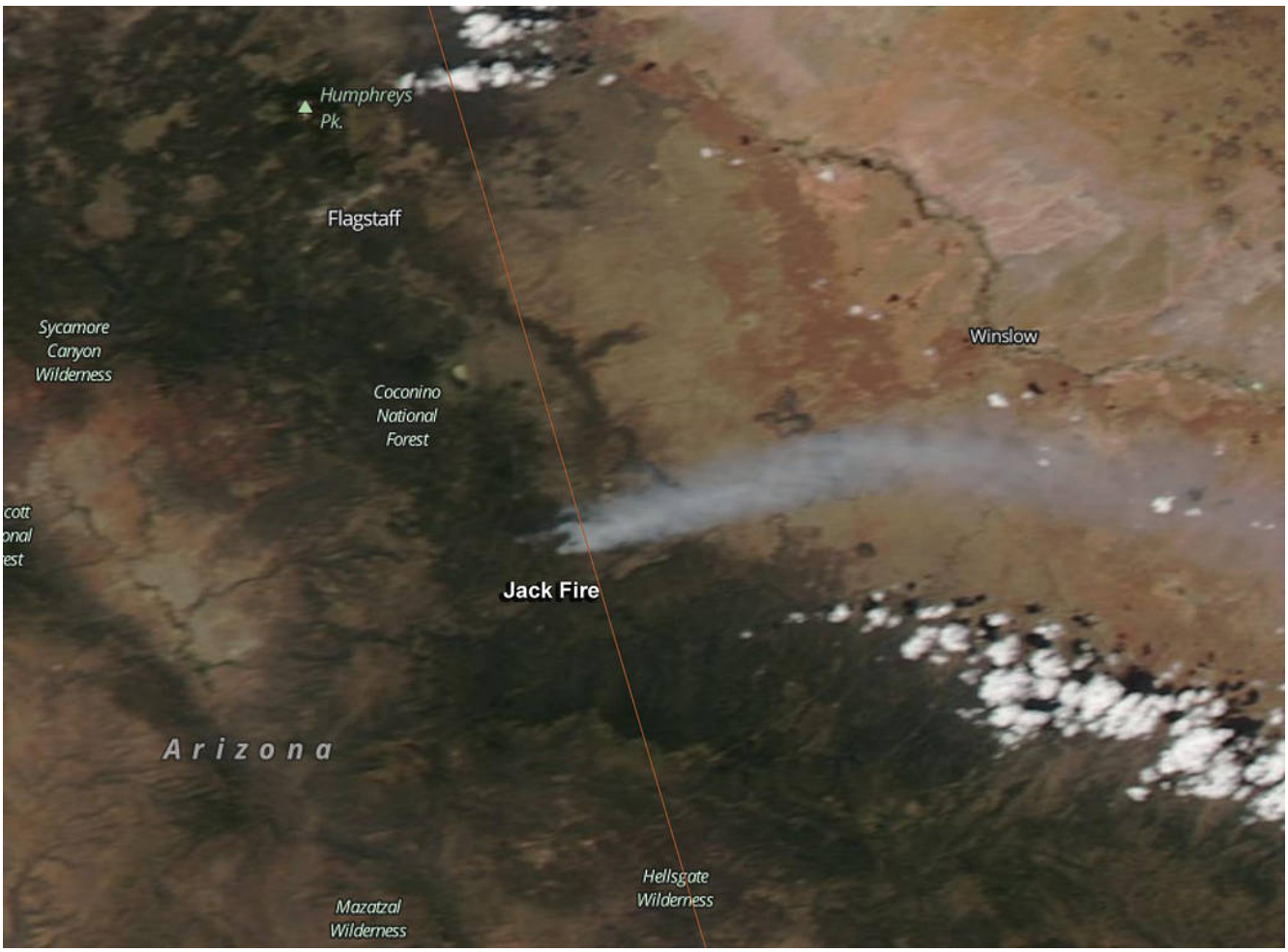

Source: NASA (2016), LANCE/EOSDIS MODIS Rapid Response Team, GSFC

Figure 7-6 Time Series of CASTNET O_3 Data for Sites in Arizona (PET427 GRC474, CHA467) and Colorado (MEV405)

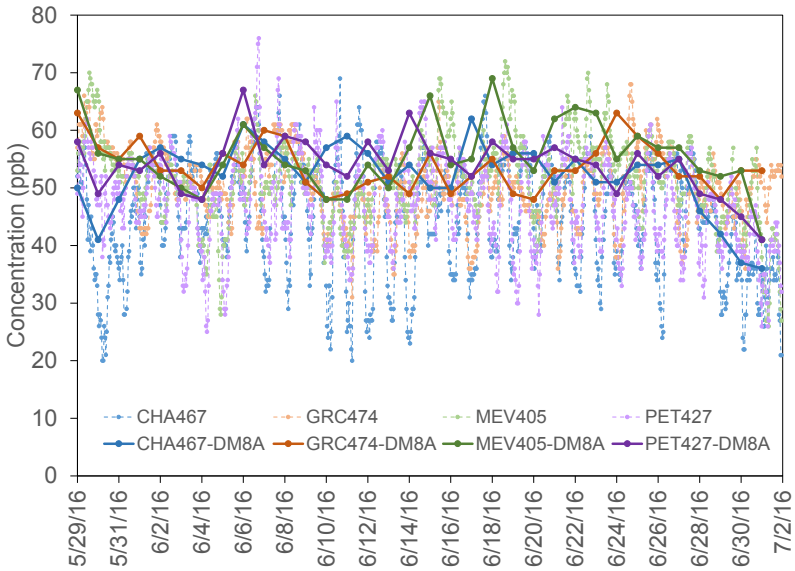

Figure 7-7 Time Series of IMPROVE $PM_{2.5}$ Data for Sites in Arizona (PEF01, GRCA2, CHIR1) and Colorado (MEVE1)

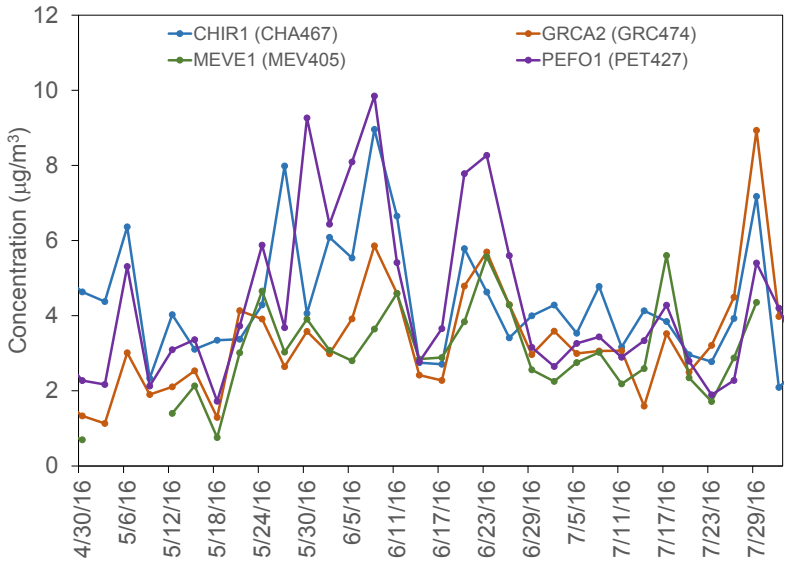

Note: IMPROVE sites are approximately co-located with the corresponding CASTNET site listed in parentheses.

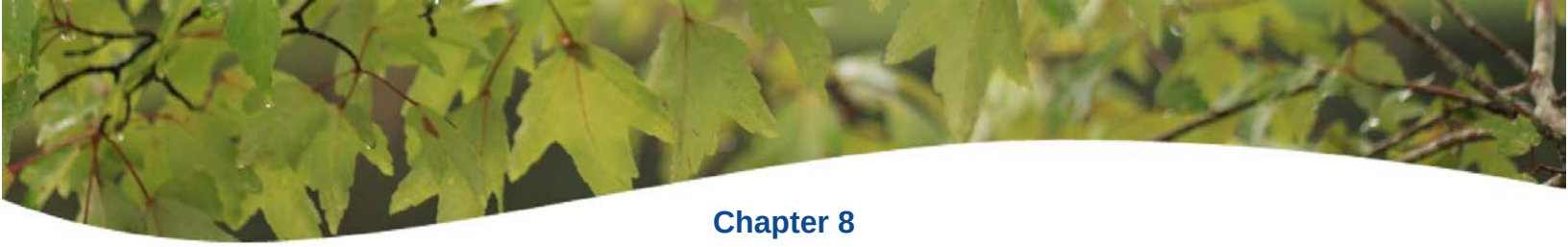

Chapter 8

Atmospheric Deposition of Nitrogen

CASTNET was designed to provide estimates of the dry deposition of nitrogen and sulfur pollutants across the United States. To assess the status of dry and total deposition for 2016, EPA used NADP's Total Deposition Science Committee Hybrid Method. The hybrid method combines measured pollutant concentrations with output from the CMAQ modeling system. Total deposition was calculated as the sum of estimated dry and wet deposition.

Gaseous and particulate nitrogen pollutants are deposited to the environment through dry and wet atmospheric processes. A primary goal of CASTNET is to estimate the dry deposition of pollutants from the atmosphere to sensitive ecosystems. The NADP Total Deposition Science Committee (TDep) Hybrid Method (EPA, 2015d; Schwede and Lear, 2014) combines CASTNET monitoring data with output from the CMAQ modeling system (Byun and Schere, 2006) to estimate dry deposition. The TDep method gives priority to using measurement data from air quality monitoring sites when available and to CMAQ output in areas where monitoring data are not available. In addition, CMAQ provides modeled data for species that are not routinely measured. The TDep method and its recent updates are discussed on the TDep web page (http://nadp.slh.wisc.edu/committees/tdep/). See also the NADP Fact Sheet, "Hybrid Approach to Mapping Total Deposition," (http://nadp.slh.wisc.edu/lib/brochures/tdepsheet.pdf).

The TDep method estimates wet deposition using PRISM to develop a continuous grid of precipitation data. PRISM uses terrain elevation, slope, and aspect and climatic measurements to estimate precipitation. Pollutant concentrations in precipitation, which were estimated for the PRISM grid, were provided by NADP/NTN. The concentration and precipitation grids were merged in order to estimate pollutant wet deposition rates. Dry and wet deposition fluxes were added to obtain estimates of total deposition, which are presented on the maps in this chapter as kilograms per hectare per year (kg ha^{-1} yr^{-1}).

Figure 8-1 illustrates TDep method estimates of dry fluxes of nitrogen (N) for 2016. The magnitude of the deposition fluxes is illustrated by the shading in the figure legend. A map of total deposition of N for 2016 is given in Figure 8-2. The percentage of total deposition of N due to dry deposition is shown in Figure 8-3. A map of TDep method estimates of total deposition of reduced N species for 2016 is given in Figure 8-4. Figure 8-5 gives the percentage of reduced N species from dry deposition. Dry deposition of N species that are not routinely measured but are estimated by the TDep method is shown in the map in Figure 8-6. The percentage of total deposition of N that is not measured directly but is calculated by the TDep method is shown in Figure 8-7. Annual gross dry deposition of NH_3 for 2016 is shown in Figure 8-8, and the net dry deposition of NH_3 is given in Figure 8-9.

Figure 8-1 TDep Dry Deposition Estimates of N (kg ha^{-1} yr^{-1}) for 2016

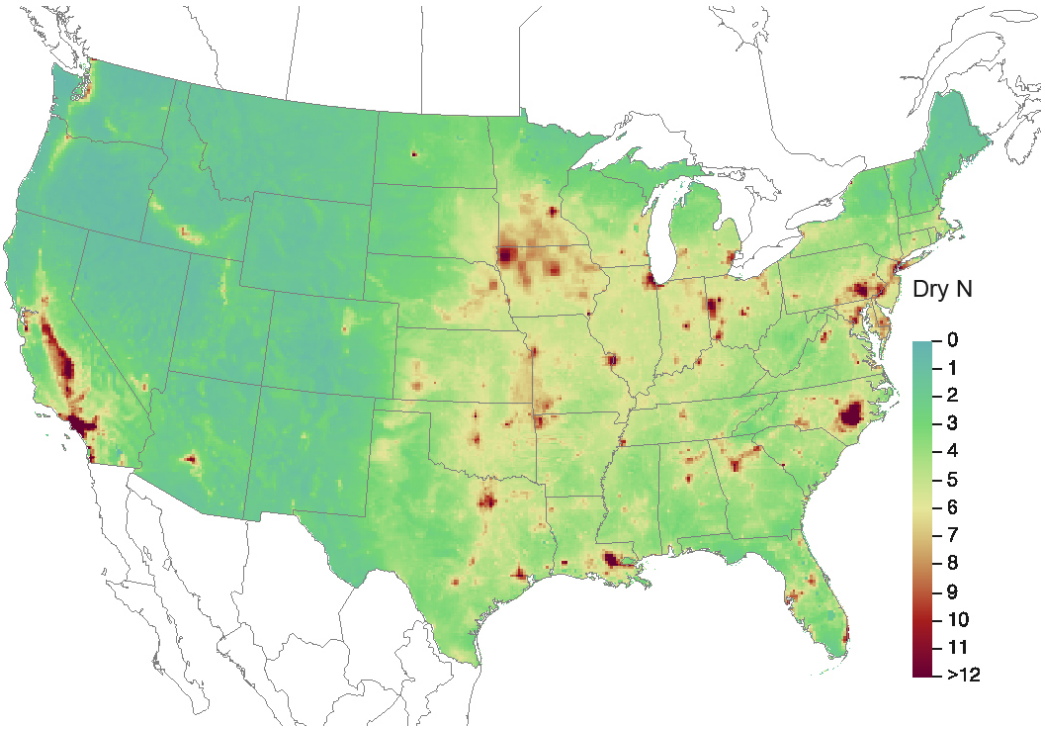

Source: CASTNET|CMAQ|NADP/NTN

Figure 8-2 TDep Total Deposition Estimates of N (kg ha^{-1} yr^{-1}) for 2016

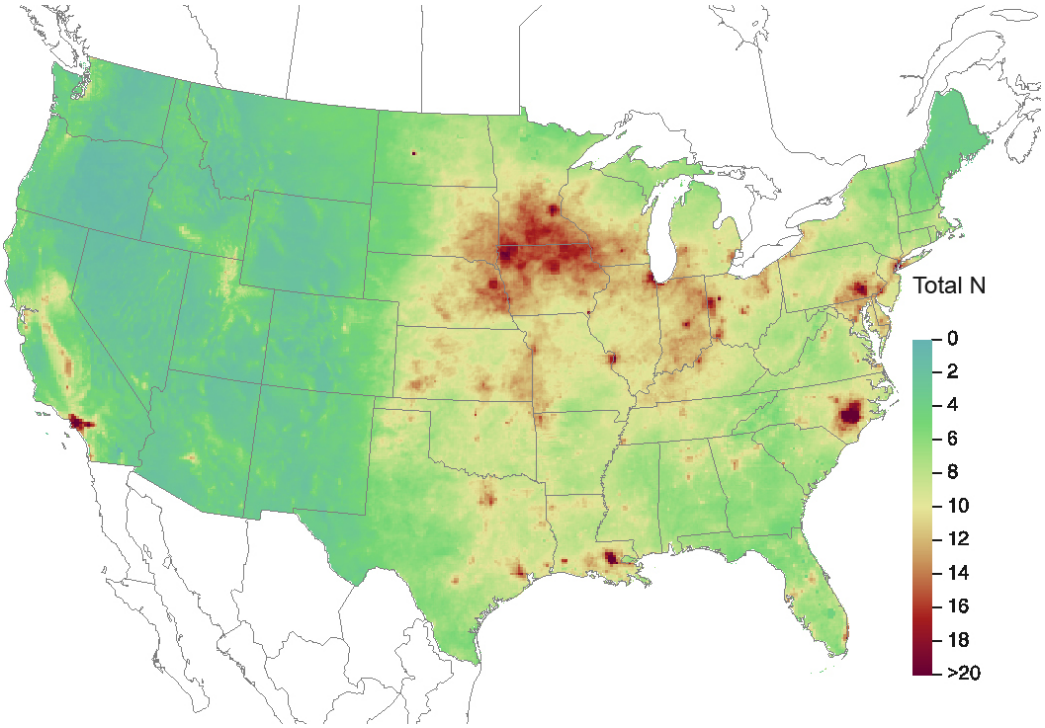

Source: CASTNET|CMAQ|NADP/NTN

Figure 8-3 TDep Percent of Total Deposition of N from Dry Deposition for 2016

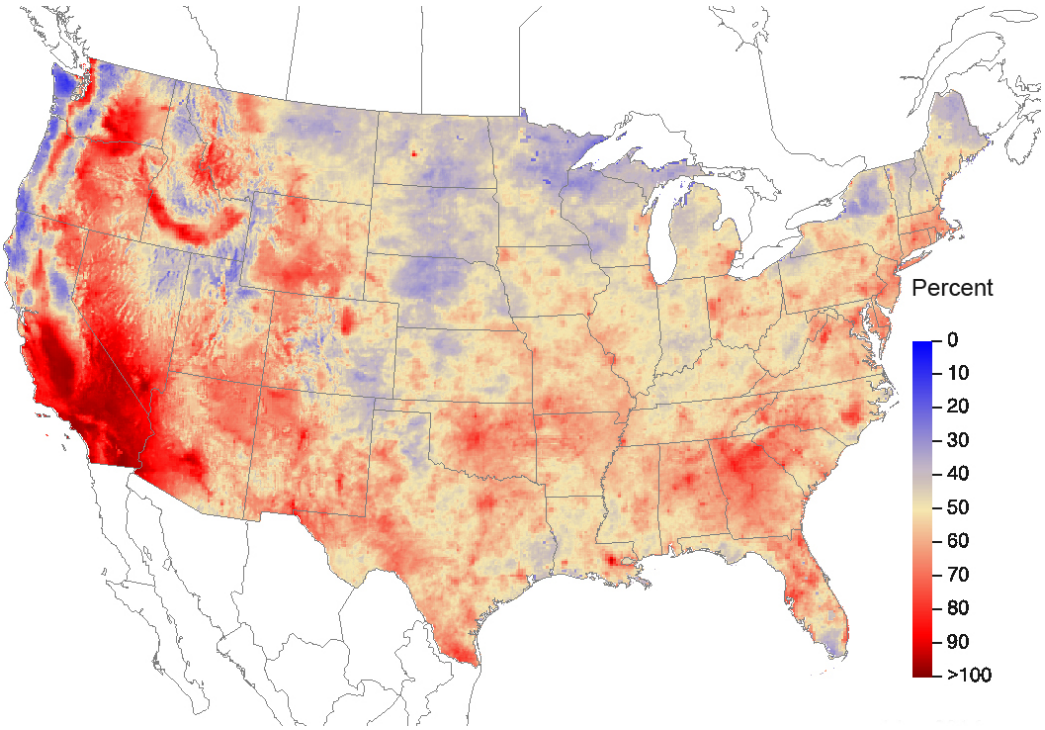

Source: CASTNET|CMAQ|NADP/NTN

Figure 8-4 TDep Total Deposition Estimates of Reduced N Species (kg ha^{-1} yr^{-1}) for 2016

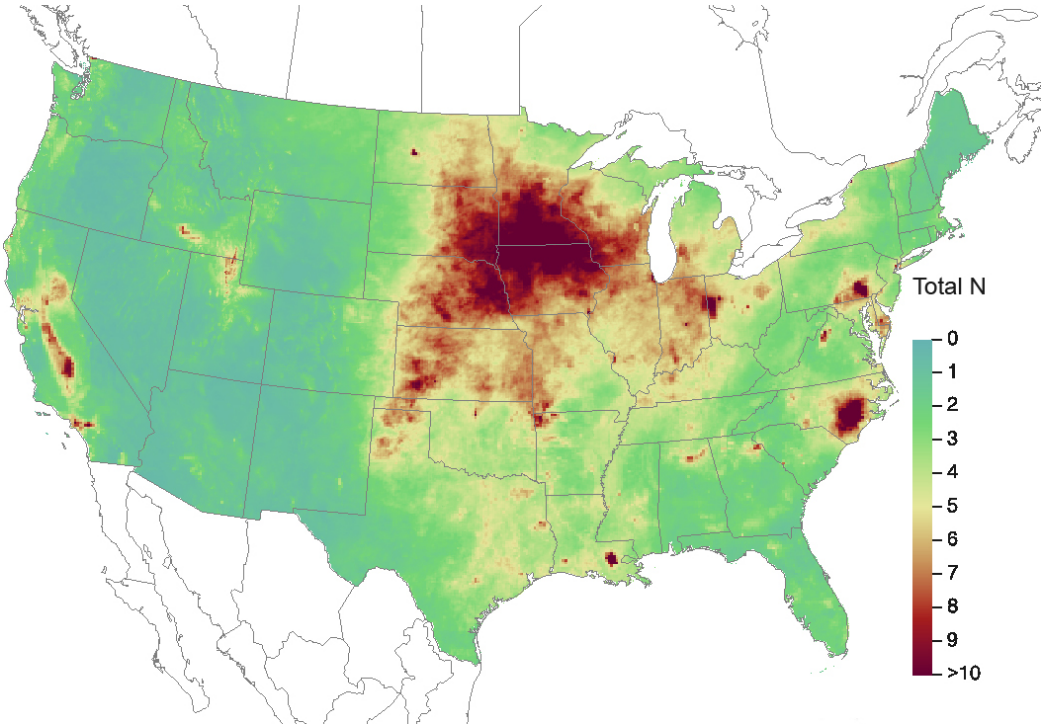

Source: CASTNET|CMAQ|NADP/NTN

Figure 8-5 TDep Percent of Total Deposition of Reduced N Species from Dry Deposition for 2016

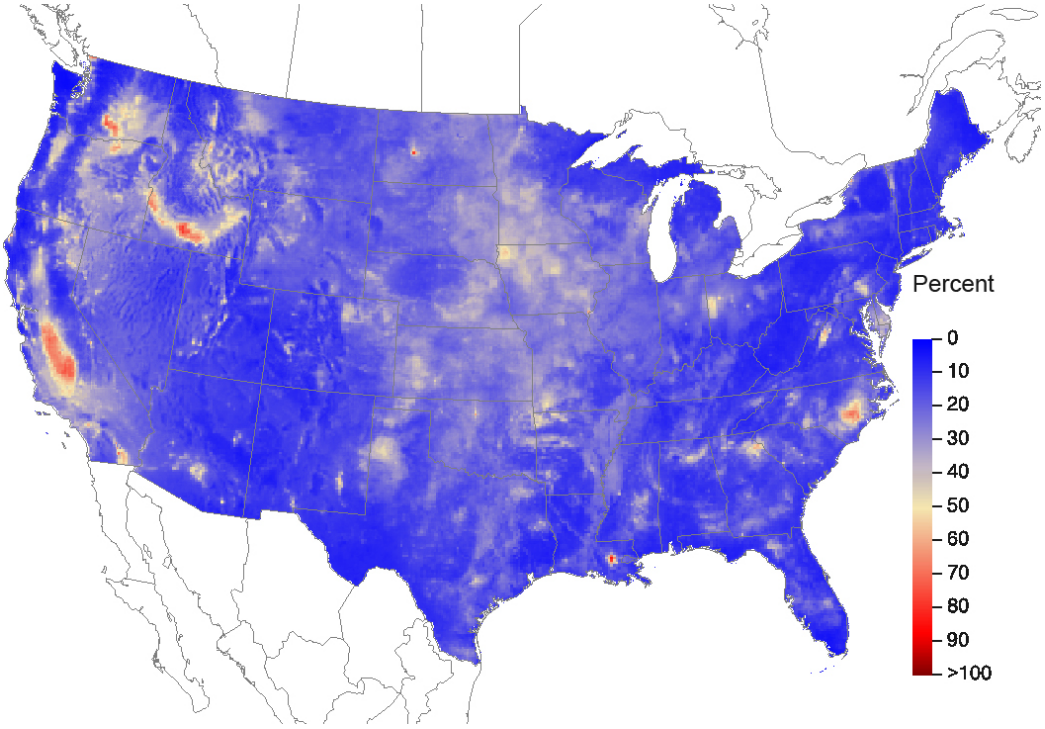

Source: CASTNET|CMAQ|NADP/NTN

Figure 8-6 TDep Dry Deposition Estimates of Unmonitored N Species (kg ha^{-1} yr^{-1}) for 2016

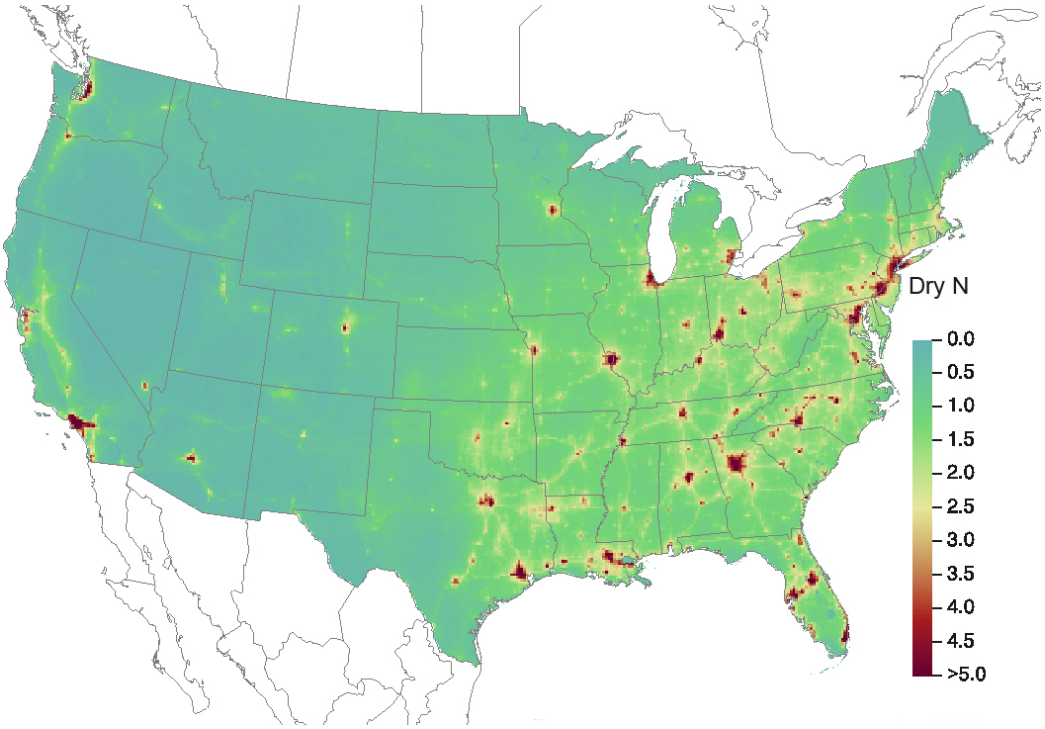

Source: CASTNET|CMAQ|NADP/NTN

Figure 8-7 TDep Percent of Total Deposition of N from Dry Deposition of Unmonitored Species for 2016

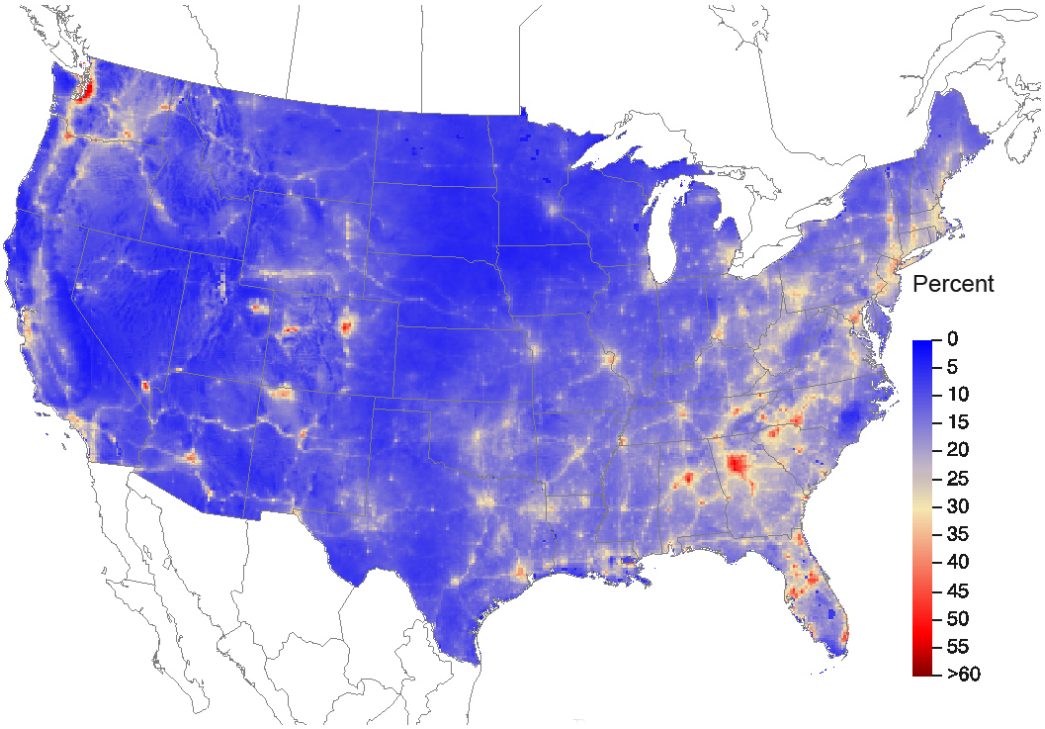

Source: CASTNET|CMAQ|NADP/NTN

Figure 8-8 TDep Gross Dry Deposition of NH_3 as N (kg ha^{-1} yr^{-1}) for 2016

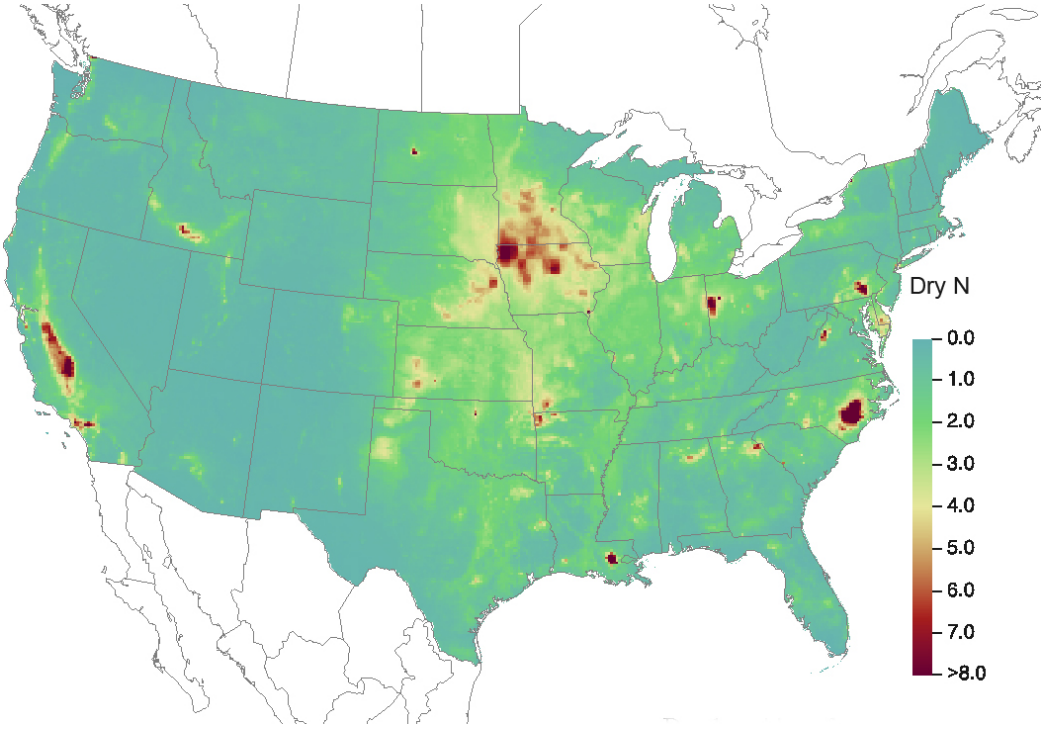

Source: CASTNET|CMAQ|NADP/NTN

Figure 8-9 TDep Net Dry Deposition of NH_3 as N (kg ha^{-1} yr^{-1}) for 2016

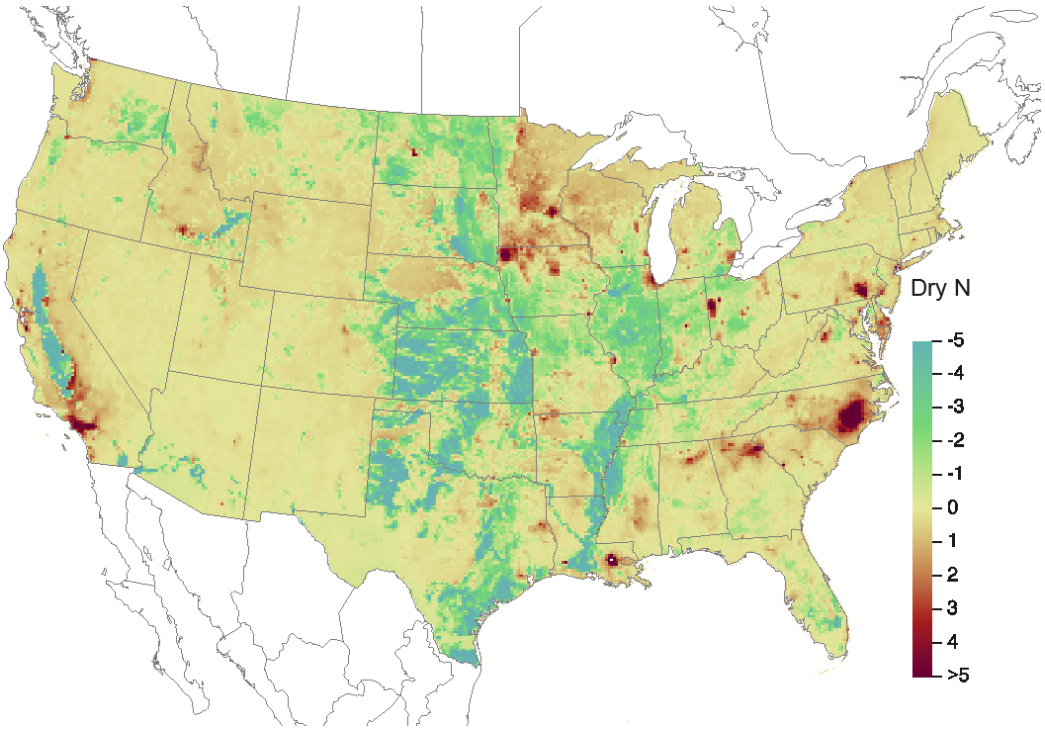

Source: CASTNET|CMAQ|NADP/NTN

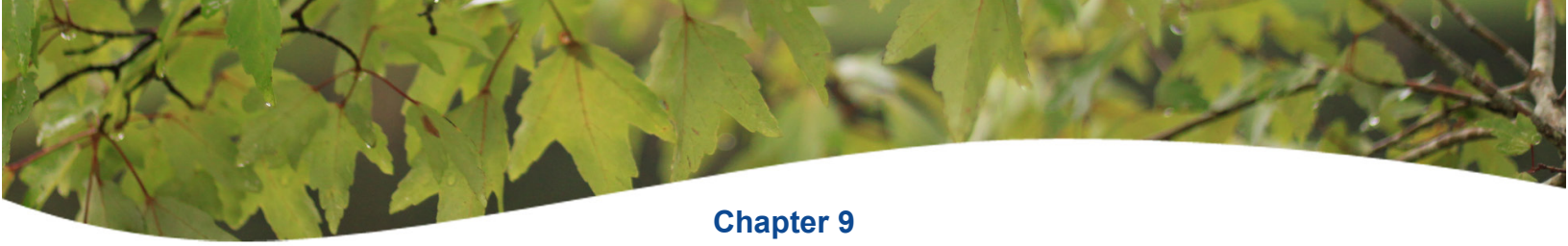

Chapter 9

Monitoring on Whiteface Mountain during 2015 and 2016

Continuous, trace-level, gaseous air quality monitors and filter pack samplers were run at two CASTNET sites on Whiteface Mountain during 2015 and 2016. The measurements at these sites were performed to (1) analyze differences in air quality resulting from variance in elevation and exposure and to (2) provide data to understand atmospheric processes such as ozone formation.

Whiteface Mountain in the Adirondack Mountains in upstate New York has been the site of many research studies over the decades and has a long history of atmospheric chemistry measurements. A CASTNET small footprint filter pack site (WFM105) was installed near an NTN precipitation collector in 2012. This location is also known as the Marble Mountain Lodge site and sits on the eastern shoulder of the Whiteface massif at an elevation of 604 meters. A seasonal CASTNET small footprint site, WFM007, was installed at the Summit Observatory location in 2015 and usually operates from May or June through September or October, as conditions allow. The Summit Observatory is at the peak of the mountain at 1,483 meters. Continuous O_3, NO_2, NO, and SO_2 have been measured at both locations since the late 1980s. The continuous data used in this chapter were provided by the Atmospheric Sciences Research Center (ASRC) of the State University of New York and the New York State Energy Research and Development Authority (NYSERDA).

Weekly filter pack concentrations of SO_4^{2-}, SO_2, NO_3^-, NH_4^+, HNO_3^-, and Ca^{2+} from WFM105 and WFM007, the lodge and summit sites, respectively, were compared for 2015 and 2016 during the warm season from the onset of sampling at the summit location in the spring until the site was closed for the season in the fall. Additionally, continuous SO_2 and filter pack SO_2 data from both locations were analyzed during the period of operation for the summit location. Continuous O_3, NO, and NO_2 data, which are available year-round from both sites, were compared for 2015 and 2016 (ASRC, 2017).

Figures 9-1 and 9-2 depict seasonal average filter pack concentrations of SO_4^{2-}, SO_2, NO_3^-, NH_4^+, HNO_3^-, and Ca^{2+} for 2015 and 2016 at both WFM105 and WFM007. Sulfate, SO_2, and NH_4^+ seasonal concentrations were higher at WFM105 than WFM007 for both years, with the 2015 concentrations being higher than the 2016 concentrations. The WFM007 summit site had higher concentrations of NO_3^-, HNO_3^-, and Ca^{2+} than WFM105 in 2015. Comparisons were similar in 2016 with the exception that HNO_3^- concentrations were higher at WFM105.

Concentrations were higher in 2015 than 2016 at WFM105 with the exceptions of HNO_3^- and Ca^{2+}, which had similar concentrations (0.5 µg/m^3 versus 0.512 µg/m^3 for HNO_3^- and 0.119 µg/m^3 versus 0.12 µg/m^3 for Ca^{2+}) for both years. The 2015 concentrations were greater than 2016 concentrations at WFM007 for all analytes.

Figure 9-1 Warm Season Filter Pack Concentrations for WFM105 and WFM007 for 2015

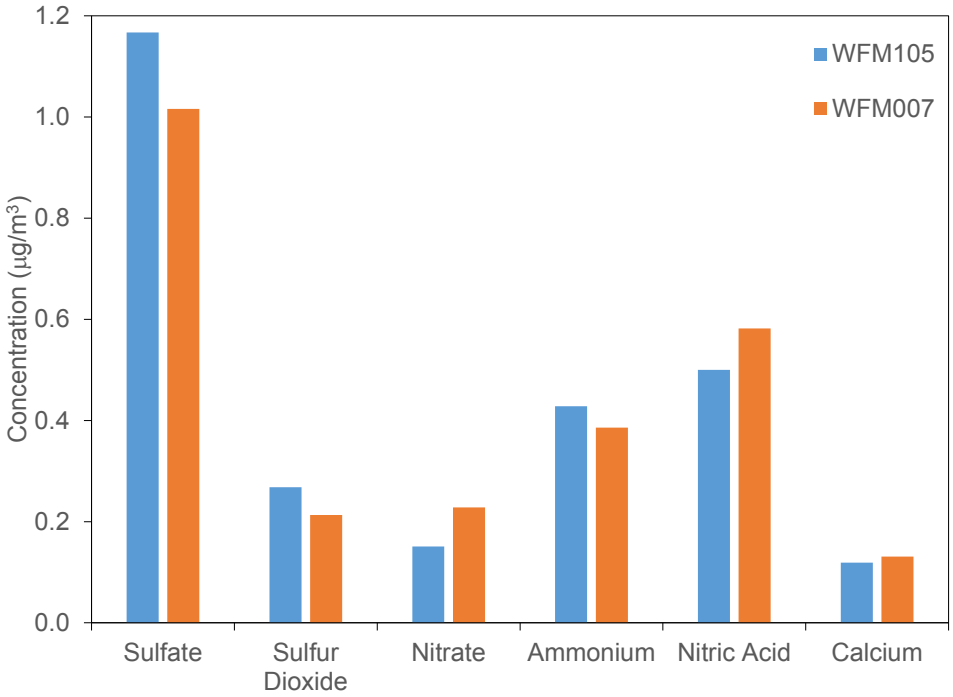

Figure 9-2 Warm Season Filter Pack Concentrations for WFM105 and WFM007 for 2016

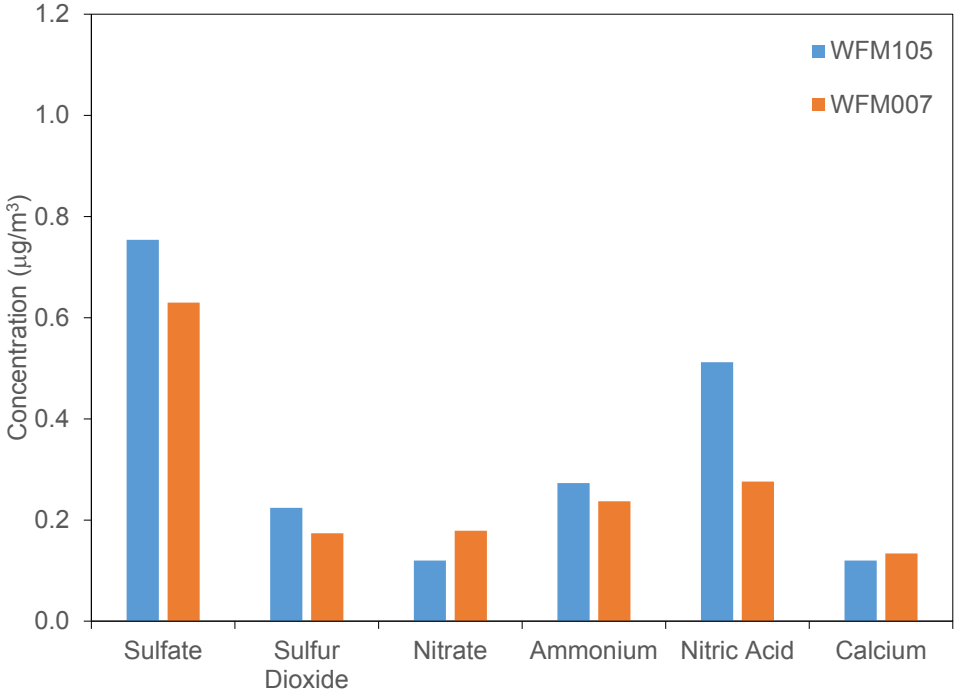

Sulfur dioxide and SO_4^{2-} are both produced by SO_2 emissions. The ratio of SO_4^{2-} to SO_2 is a measure of the age of the polluted air mass. Higher SO_4^{2-} concentrations relative to SO_2 levels measured at both sites suggest that air pollution measured at Whiteface Mountain was produced during transport from distant pollutant sources.

Figure 9-3 shows seasonal filter pack and continuous SO_2 concentrations from both locations for 2015 and 2016. The filter pack SO_2 concentrations were higher than the continuous concentrations at both sites during both years. The 2015 seasonal concentrations for filter pack and continuous SO_2 were higher than the 2016 seasonal concentrations.

Figure 9-3 Warm Season Filter Pack and Continuous SO_2 Concentrations at WFM105 and WFM007 for 2015 and 2016

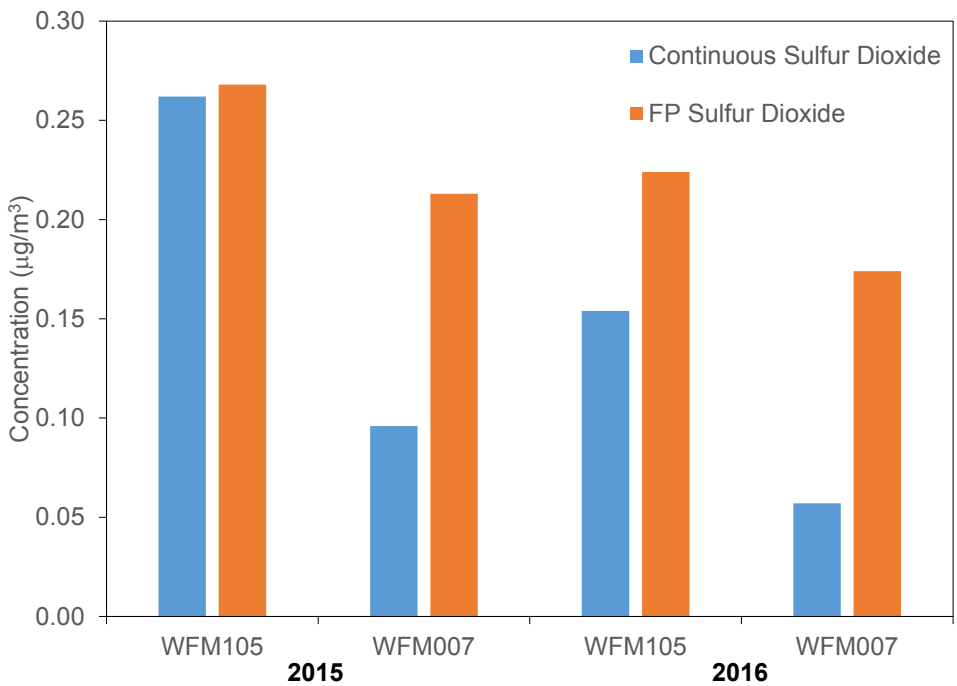

Quarterly averages of O_3 for both years and both sites are presented in Figure 9-4. WFM007 generally had higher quarterly averages than WFM105 with exception of third quarter 2015. Quarterly O_3 averages were greater in 2016 than 2015 at both sites with the exception of the first quarter for WFM007. Ozone values were not available for fourth quarter 2015 for WFM105.

Figure 9-4 Quarterly Average O_3 Concentrations for WFM105 and WFM007 for 2015 and 2016

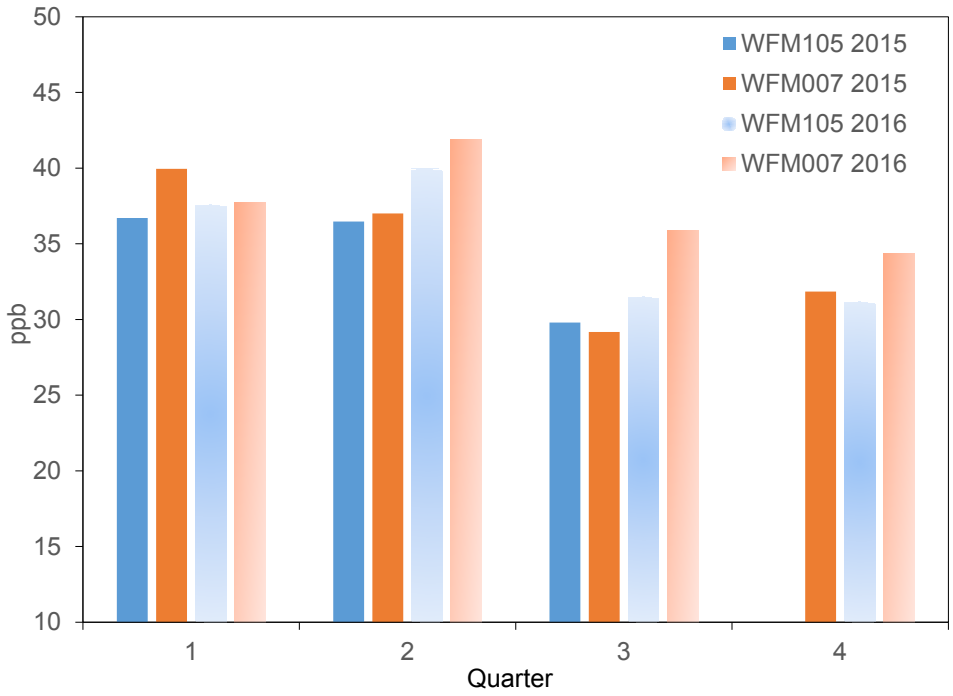

Continuous NO and NO_2 quarterly average concentrations for both sites for 2015 and 2016 are plotted in Figure 9-5. WFM105 measured higher quarterly averages of NO and NO_2 than WFM007 for both years. Data were not available for fourth quarter 2015 from WFM105.

Nitrogen dioxide concentration values for 2015 at WFM105 were greater with respect to the 2016 values. However, the 2015 NO concentration values at WFM105 were lower than 2016 for the first and second quarters and equal for the third quarter. Concentrations of both analytes were greater at WFM007 in 2015 than 2016.

Figure 9-5 NO and NO_2 Continuous Data for WFM105 and WFM007 for 2015 and 2016

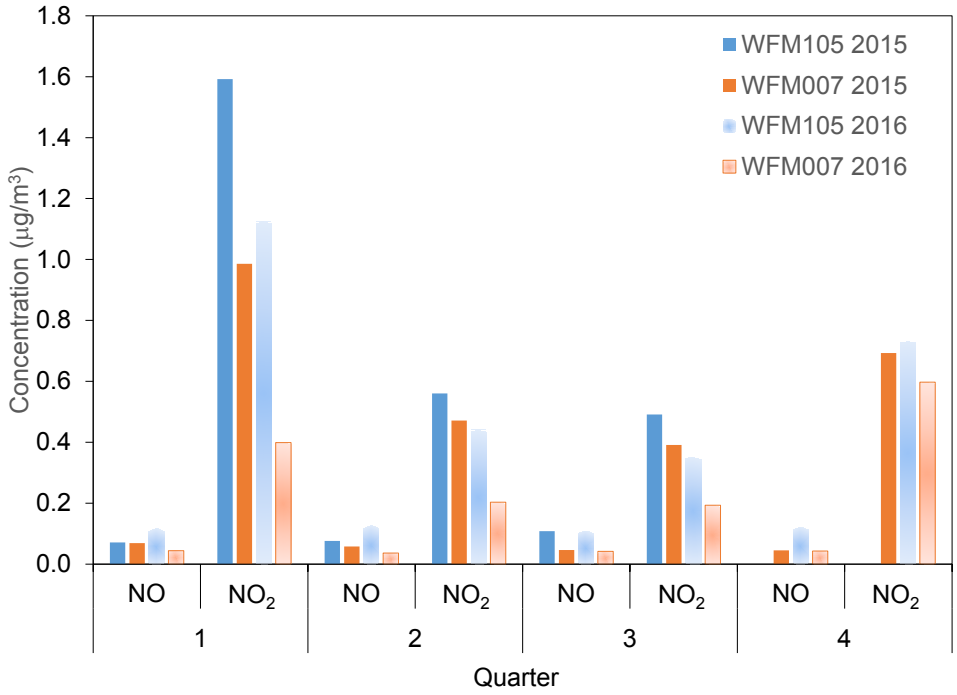

Diurnal plots of O_3, NO, and NO_2 for both locations for the 2007 and 2016 warm seasons are shown in Figures 9-6 through 9-9. Data from 2007 were selected to illustrate the changes in air quality over a 10-year period. The O_3 and NO_2 concentrations were higher at WFM007 in 2007 than at WFM105. While NO values were about equivalent at the two sites, WFM105 had a higher diurnal peak. There was no discernible diurnal pattern for O_3 in 2007 at WFM007, but both locations showed a midday minimum for NO_2 due to conversion to O_3 by daytime photochemical processes.

Ozone values were again greater at WFM007 than WFM105 in 2016. However, the NO_2 values were lower at WFM007 with respect to the WFM105 site. The NO concentrations were also lower at the WFM007 site. The 2016 NO_2 concentrations at WFM105 again showed a midday peak for ozone and a dip for NO_2; WFM007 showed a slight midday decline for both parameters.

Figure 9-6 WFM105 O_3, NO, and NO_2 Concentrations for Warm Season 2007

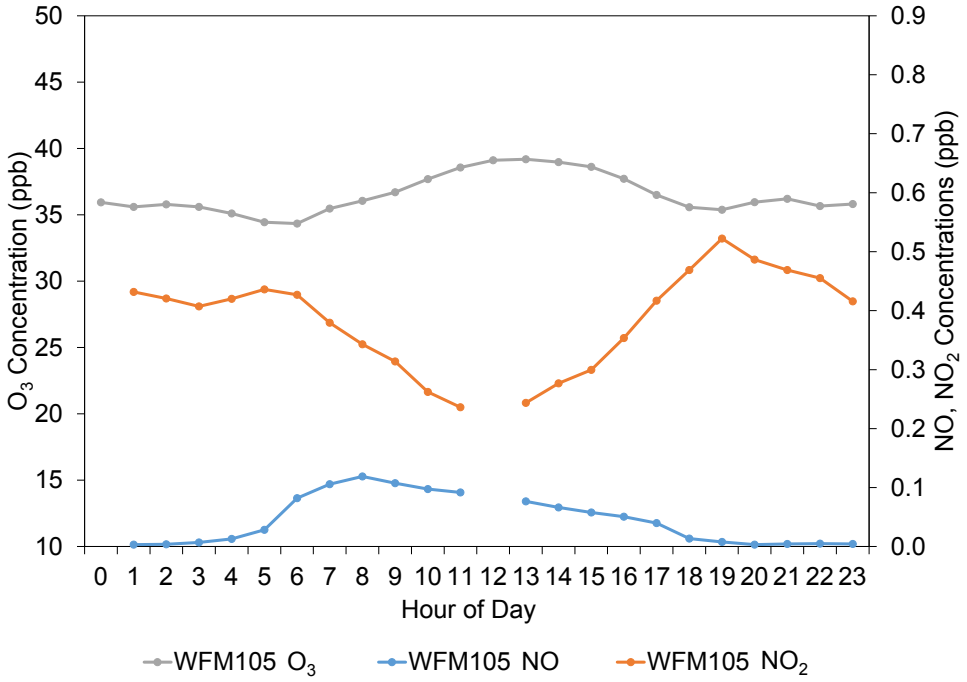

Figure 9-7 WFM007 O_3, NO, and NO_2 Concentrations for Warm Season 2007

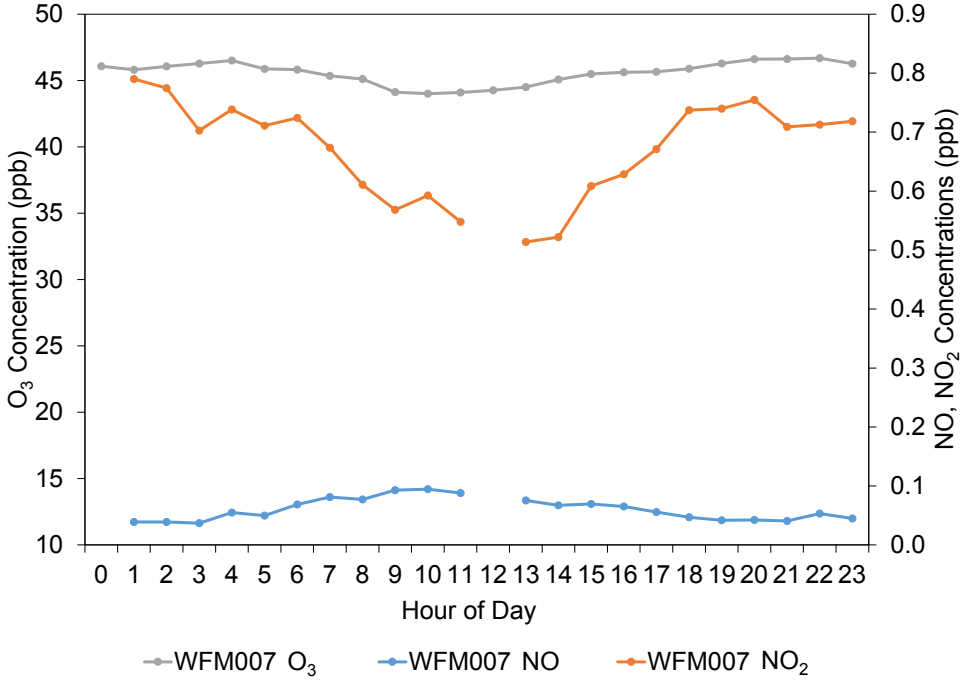

Figure 9-8 WFM105 O_3, NO, NO_2 Concentrations for Warm Season 2016

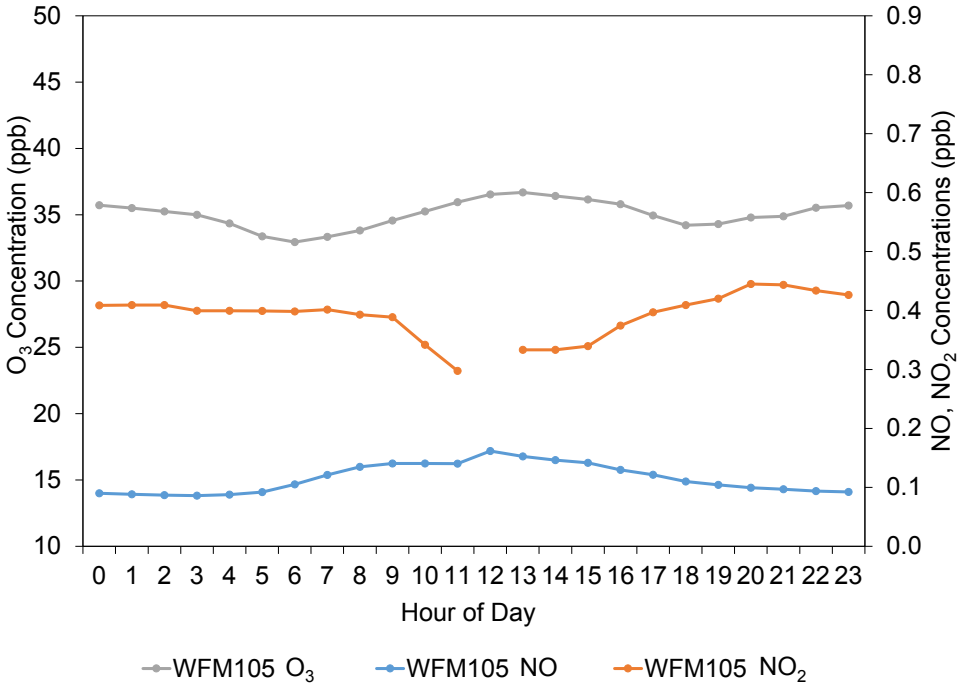

Figure 9-9 WFM007 O_3, NO, and NO_2 Concentrations for Warm Season 2016

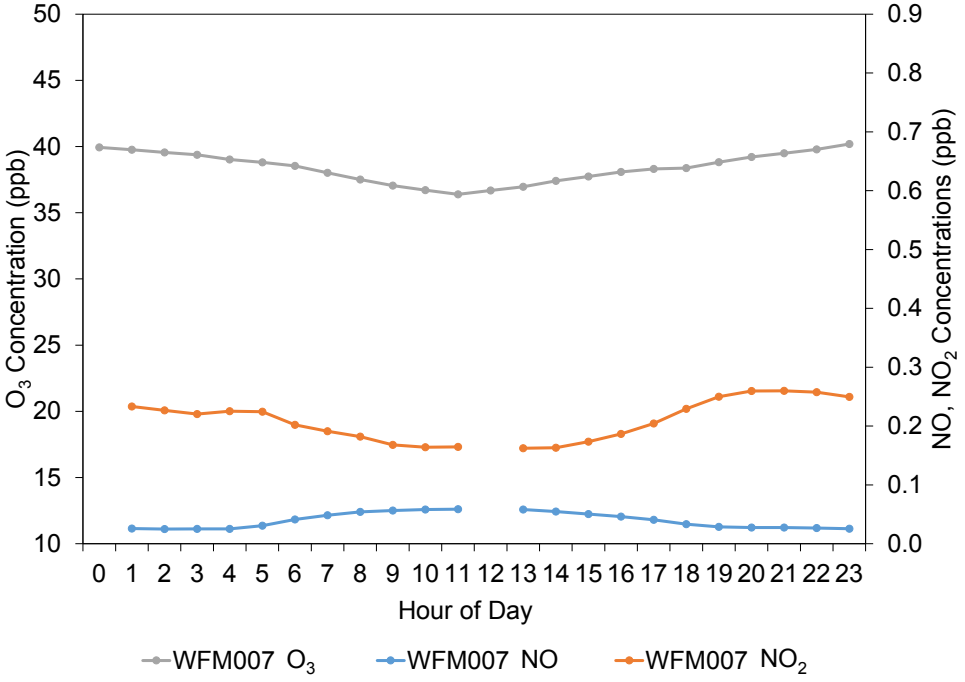

The 2016 average warm season NO and NO_2 concentrations were higher than the 2007 warm season averages at WFM105, while the 2016 O_3 average was slightly lower (37 ppb in 2007 versus 35 ppb in 2016). This pattern was reversed at the summit, WFM007, where the 2016 warm season averages of all three analytes were lower than the 2007 averages.

Figures 9-10 and 9-11 show O_3 concentrations for both Whiteface Mountain locations for 2015 and 2016 and for the nearby, lower elevation CASTNET site at Huntington Wildlife Forest, NY (HWF187) to provide a more detailed analysis of the diurnal pattern for O_3 and to illustrate the significant diurnal change of O_3 at lower elevations.

Figure 9-10 Ozone Concentrations for Warm Season 2015

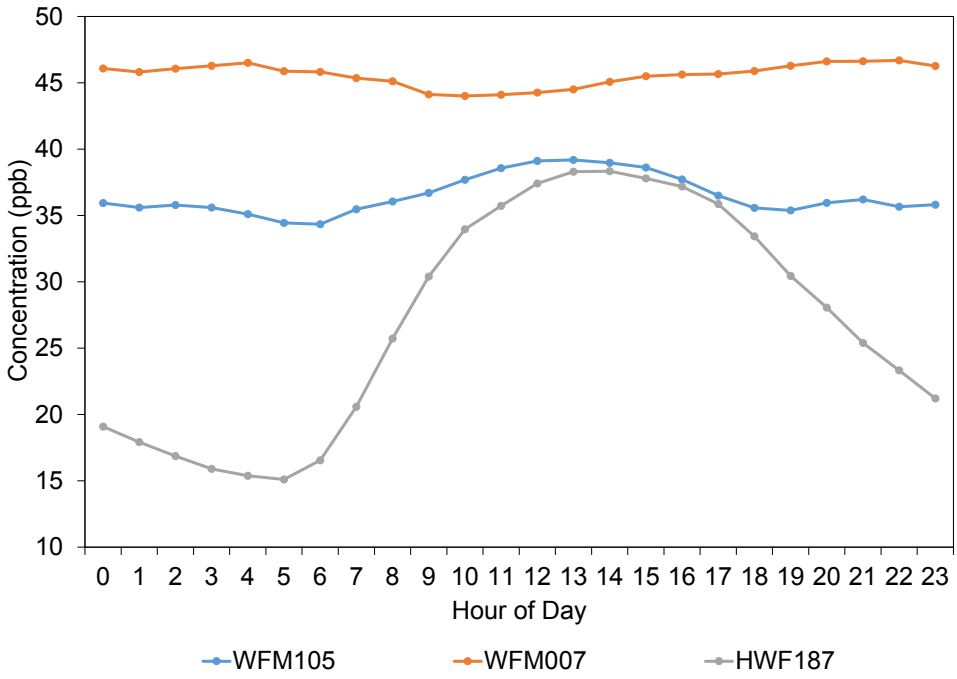

Figure 9-11 Ozone Concentrations for Warm Season 2016

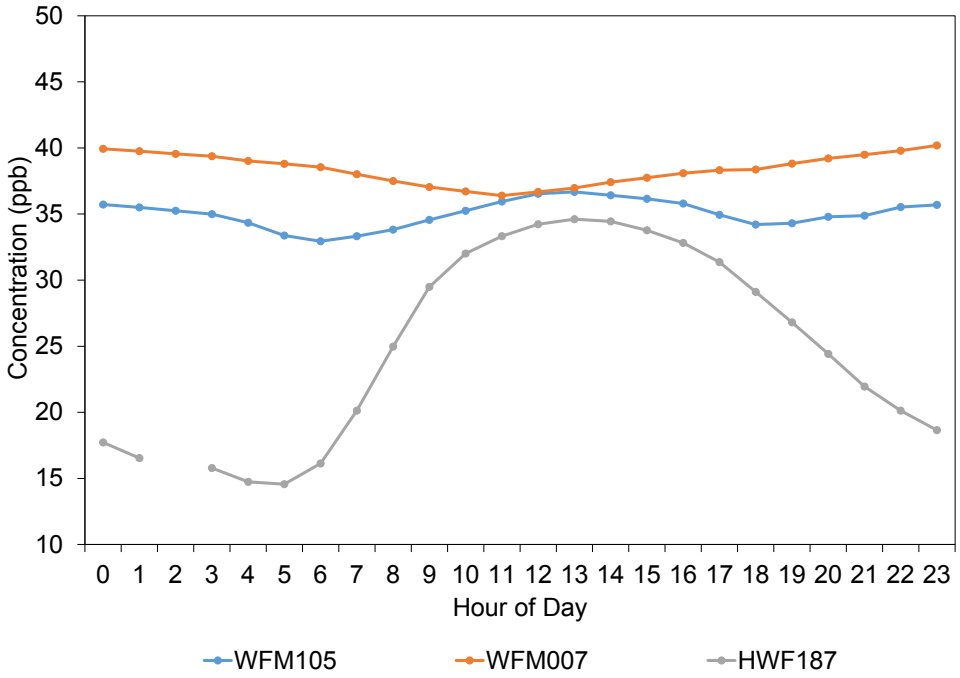

Ozone levels were are highest at WFM007, the summit, and showed little diurnal variation, most likely due to a lack of depletion mechanisms, e.g., little vegetation to produce dry deposition and no fresh NO to scavenge O_3. WFM105 ozone values were greater than those at HWF187. A slight diurnal pattern was discernible at WFM105, but it was not as pronounced as the diurnal patterns seen at HWF187, which exhibited a diurnal change of around 20 ppb daily.

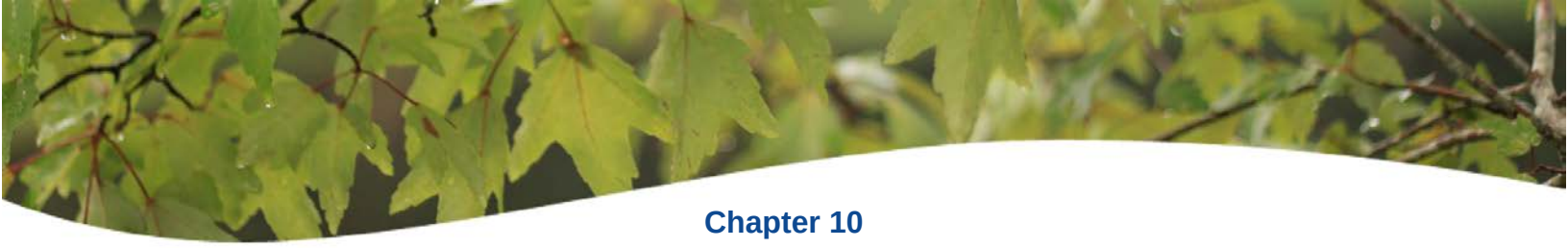

Chapter 10

Atmospheric Deposition of Sulfur, Base Cations, and Chloride

CASTNET was designed to provide estimates of the dry deposition of nitrogen and sulfur pollutants, base cations, and chloride across the United States. EPA used the NADP TDep method to assess the status of dry and wet deposition for 2016. Total deposition was calculated as the sum of estimated dry and wet deposition.

Gaseous and particulate sulfur pollutants, base cations, and chloride are deposited to the environment through dry and wet atmospheric processes. A principal goal of CASTNET is to estimate the rate of dry deposition of these compounds from the atmosphere to sensitive ecosystems. The NADP TDep method (EPA, 2015d; Schwede and Lear, 2014) was used to estimate dry and wet deposition. Dry and wet deposition rates were summed to obtain total deposition across the United States.

Sulfur Deposition

Figure 10-1 shows a map of TDep method estimates of dry deposition rates of sulfur (S) for 2016. Estimated rates of total deposition of sulfur for 2016 are given in Figure 10-2. The magnitude of the deposition fluxes is illustrated by the shading in the figure legends. The percentage of total deposition of S due to dry deposition is shown in Figure 10-3.

Deposition of Base Cations and Chloride

A map of 2016 estimated total deposition of base cations (Ca^{2+}, K^{+}, Mg^{2+}, and Na^{+}) is given in Figure 10-4. Figure 10-5 provides estimated rates for 2016 for total deposition of Cl^{-}.

Scenic View from PNF126, NC

Figure 10-1 TDep Dry Deposition Estimates of S (kg ha^{-1} yr^{-1}) for 2016

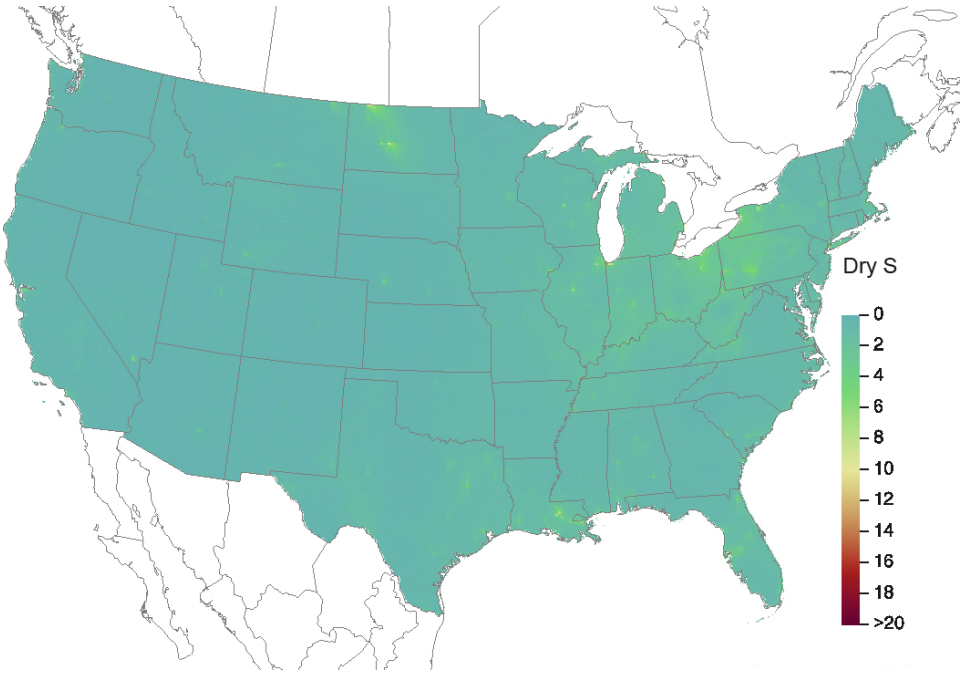

Source: CASTNET|CMAQ|NADP/NTN

Figure 10-2 TDep Total Deposition Estimates of S (kg ha^{-1} yr^{-1}) for 2016

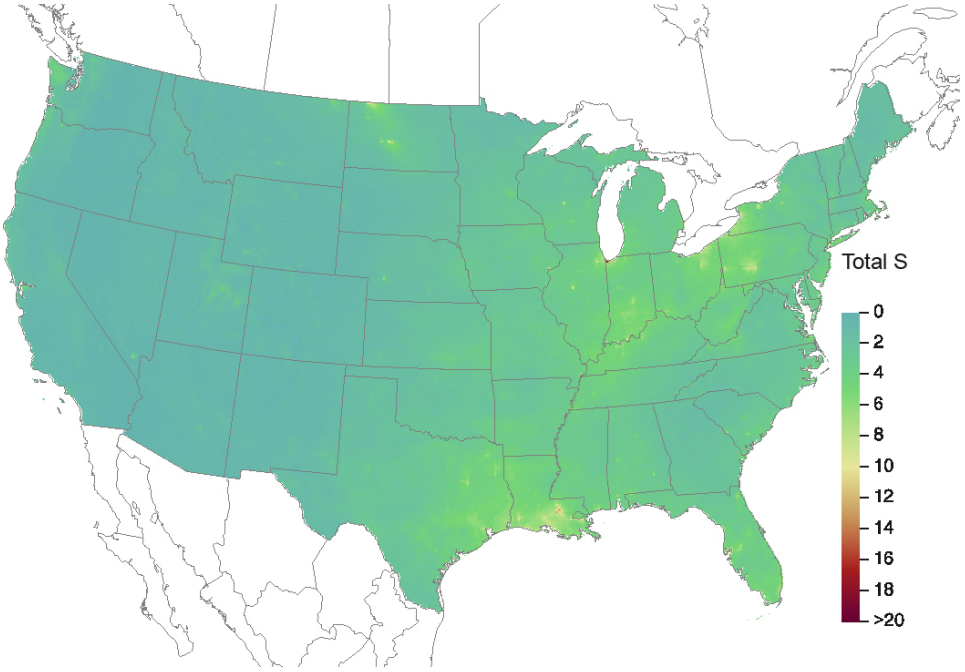

Source: CASTNET|CMAQ|NADP/NTN

Figure 10-3 TDep Percent of Total Deposition of S from Dry Deposition for 2016

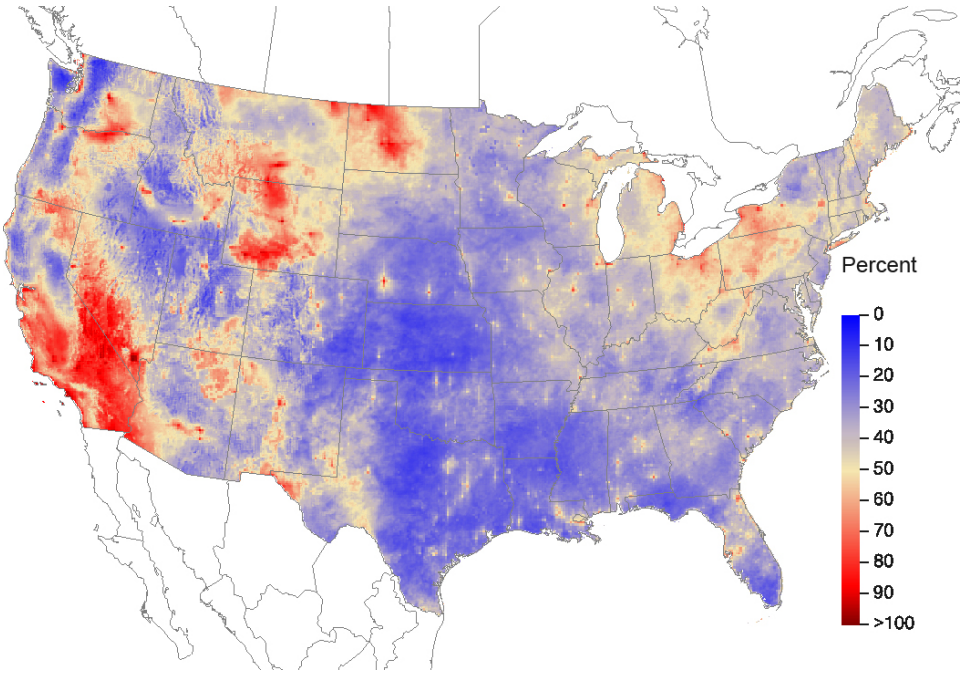

Source: CASTNET|CMAQ|NADP/NTN

Figure 10-4 TDep Total Deposition Estimates of the Base Cations Ca^{2+}, K^{+}, Mg^{2+}, Na^{+} (kiloequivalents per hectare per year) for 2016

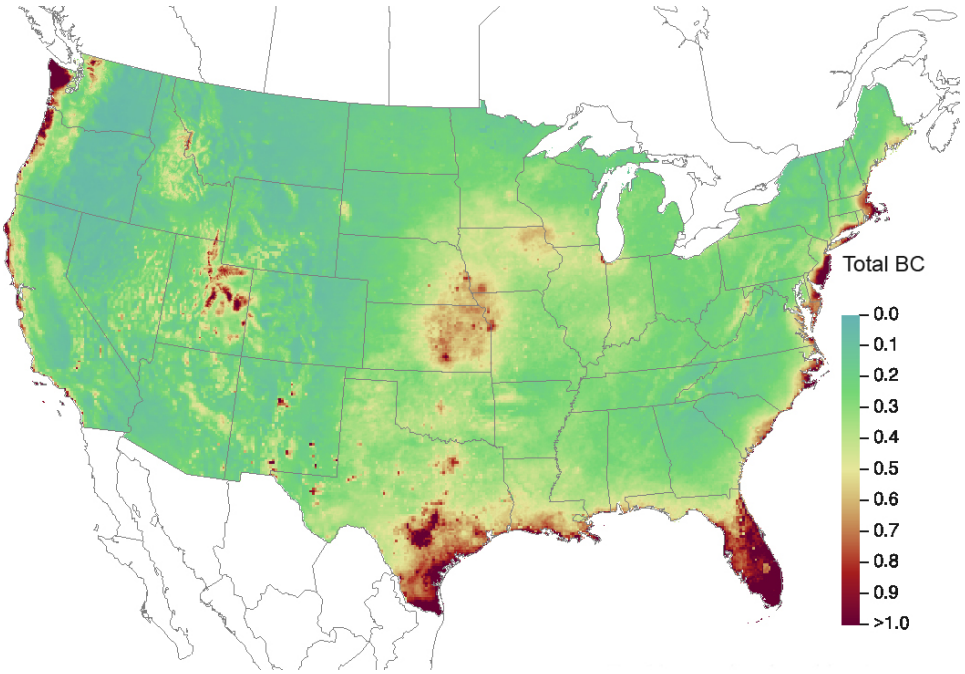

Source: CASTNET|CMAQ|NADP/NTN

Figure 10-5 TDep Total Deposition Estimates of Total Cl^- (kg ha^{-1} yr^{-1}) for 2016

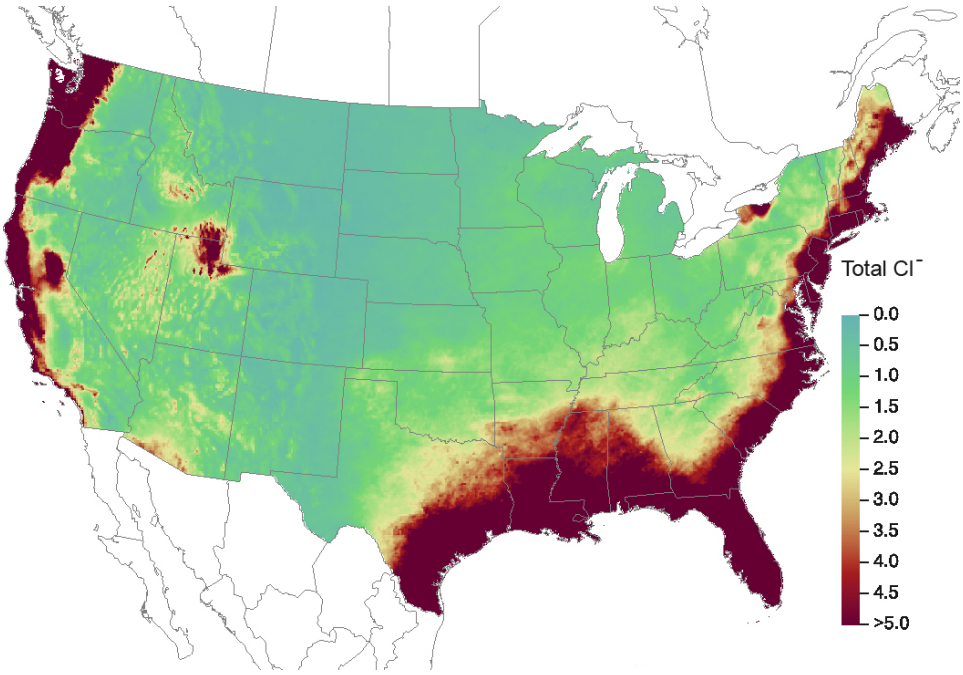

Source: CASTNET|CMAQ|NADP/NTN

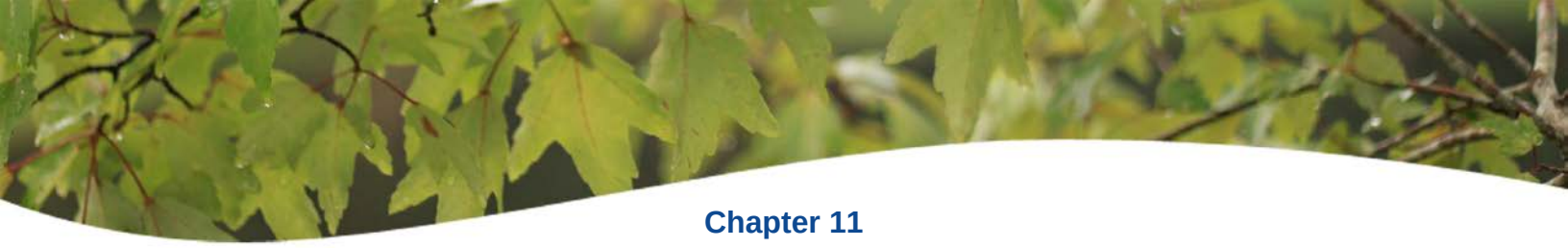

Chapter 11

Critical Loads for Open and Closed Canopy Herbaceous Ecosystems

Critical loads were estimated for biodiverse open and closed canopy herbaceous ecosystems based on TDep estimates of wet and dry deposition of nitrogen across the United States. Three-year averages for 2013–2015 were compared for the open and closed ecosystems. Open canopy systems had more extensive critical load exceedance rates than the closed systems. The analysis suggests that, for the majority of regions where data were available, the loss of herbaceous biodiversity due to air pollutant deposition is unlikely. However, areas in Minnesota and North Carolina are likely experiencing loss of herbaceous biodiversity because of elevated levels of nitrogen deposition.

Critical loads describe the threshold at which a natural system is impacted by deposition of nitrogen (N) and/or sulfur (S) air pollutants. Critical loads provide tools that allow the evaluation of the sensitivity and the potential impact of air pollution on terrestrial and aquatic ecosystems. This chapter focuses on critical loads for herbaceous biodiversity and their potential exceedances. A critical load exceedance is the case when deposition is greater than the critical load (e.g., total deposition of N > critical load). Critical load exceedances indicate (1) a risk of negative impacts to natural resources as a result of air pollutant deposition, (2) whether pollutant deposition might be impacting natural systems, and (3) where impacts to the landscape might be occurring. For ecosystems impacted by deposition of pollutants, changes in critical load exceedances provide information to indicate if deposition has improved enough to allow ecosystem recovery, to judge the effectiveness of emission reduction policies and strategies, and to inform land management decisions.

The critical loads for herbaceous biodiversity were determined by Simkin *et al*. (2016) and were based on total deposition of N (wet and dry). The critical loads describe the level of deposition of N above which decreases in herbaceous plant species richness (i.e., total number of unique species per plot of land) were observed. They are expressed in terms of kg ha^{-1} yr^{-1} of N deposition. The analysis by Simkin *et al*. (2016) used a nationwide statistical analysis of 15,136 forest, woodland, shrubland, and grassland sites assembled from 12 distinct data sets.

The critical loads from Simkin *et al*. (2016) were calculated separately for open canopy and closed canopy systems based on Level 1 of the U. S. National Vegetation Classification (USNVC, 2016). A total of 11,819 plots were located in closed canopy systems while 3,317 were in open canopy systems. An open system includes grasslands, shrublands, and woodlands. A closed system includes those herbaceous species growing in the forest understories. This distinction was made because reduced sunlight limits the growth, reproduction, and other biological factors that in turn reduce the richness of the herbaceous community growing in the understory of forests (Neufeld and Young, 2014).

Critical loads were derived statistically using multiple regression models relating the species richness of a plot to environmental factors that included deposition of N, temperature, precipitation, soil pH, and others. A critical load was then estimated using a two-step process whereby the partial derivative of the best statistical model was selected, which yielded an equation for the critical load based on temperature, precipitation, and soil pH. Using that equation, the critical load was calculated at a given plot using local environmental data.

Critical load exceedances were evaluated using total N deposition values derived from TDep simulations (Chapter 8). A three-year average from 2013–2015 was compared to each plot for both open and closed systems. The range of the critical loads for closed canopy forest was 7.3 to 19.6 kg ha^{-1} yr^{-1} of N deposition, while open canopy environments were lower with a range of 7.4 to 9.0 kg ha^{-1} yr^{-1} of N deposition (Figure 11-1). Open canopy sites are designated as triangles while closed canopy systems are noted as circles. Figure 11-2 shows the spatial extent of critical load exceedances where data were available. Green triangles/circles show sites where the critical load was not exceeded while red triangles/circles indicate deposition greater than the critical load. Yellow triangles/circles show the sites where deposition of N was within 1 kg ha^{-1} yr^{-1} of the critical load. The open canopy systems had a higher exceedance rate (red triangles) of 22.7 percent than the closed canopy systems of 1.6 percent (red circles). The regions with the higher exceedances are in Minnesota and North Carolina. There were also many examples where deposition was near (i.e., within 1 kg ha^{-1} yr^{-1}) the critical load (yellow circles/triangles) for closed and open systems. Sites that did not exceed the critical load were far more common. Open canopy sites did not exceed their critical load 69 percent of the time (green triangles) while forested systems did not exceed their critical load at 94 percent of the sites (green circles). This analysis suggests that, for the majority of regions where data were available, the loss of herbaceous biodiversity due to air pollution is unlikely. However, areas in Minnesota and North Carolina are likely experiencing loss of herbaceous biodiversity because of the deposition of elevated levels of N to these systems.

Figure 11-1 Critical Loads of Nitrogen Deposition for Herbaceous Biodiverse Ecosystems Determined by Simkin *et al*. (2016)

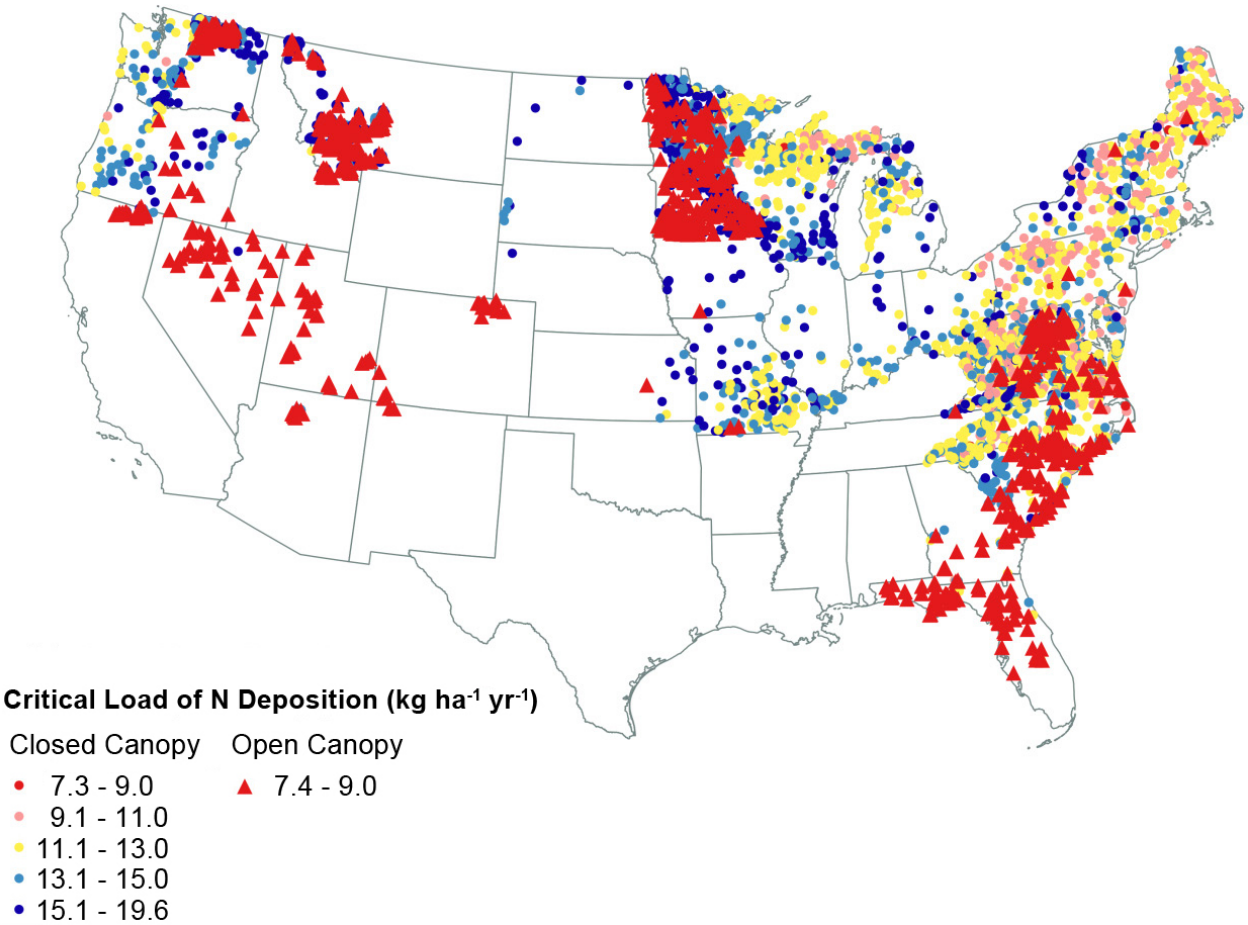

Figure 11-2 Critical Loads Exceedance for Herbaceous Biodiverse Ecosystems from TDep Deposition Estimates

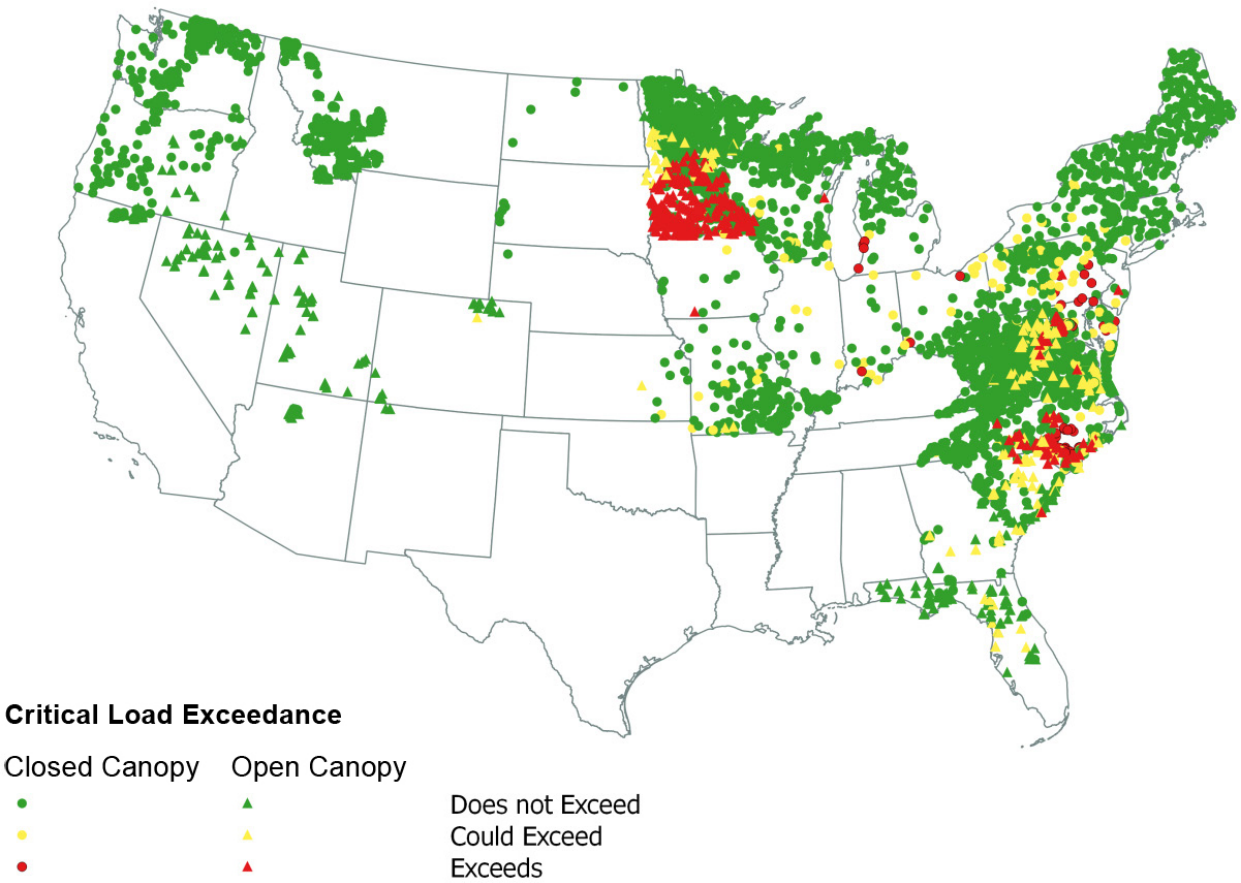

References

Air Resource Specialists (ARS). 2015. *Gaseous Pollutant Monitoring Program Quality Assurance Project Plan (QAPP)* Revision 3. Prepared for the National Park Service, Air Resources Division, Denver, CO. https://www.nature.nps.gov/air/Monitoring/docs/2010510_NPS_ARD_GPMP_QAPP.pdf Accessed May 2018.

Atmospheric Sciences Research Center (ASRC). 2017. Air Quality Monitoring. http://pireds.asrc.cestm.albany.edu:3000/. Accessed June 2018.

Baumann, K., Williams, E. J., Olson, J. A., Harder, J. W., and Fehsenfeld F. C. 1997. Meteorological Characteristics and Spatial Extent of Upslope Events during the 1993 Tropospheric OH Photochemistry Experiment. *J. Geophys. Res*., 102(D5), 6199–6213, doi: 10.1029/96JD03251.

Byun, D. and Schere, K. L. 2006. Review of the Governing Equations, Computational Algorithms, and Other Components of the Models-3 Community Multiscale Air Quality (CMAQ) Modeling System. *Applied Mechanics Reviews*, 59: 51-77. doi: 10.1115/1.2128636.

International Organization for Standardization (ISO). 2005. Statistical Methods for the Use in Proficiency Testing by Interlaboratory Comparisons, Annex C, Robust Analysis, Section C.1: Algorithm A. Standard 13528. ISO 13528:2005(E).

Lefohn, A. S. and Runeckles, V. C. 1987. Establishing a Standard to Protect Vegetation - Ozone Exposure/Dose Considerations. *Atmos. Environ*., 21:561-568.

Liu, X., Huey, L. G., Yokelson, R. J., Selimovic, V., Simpson, I. J., Muller, M., Jimenez, J. L., Campuzano-Jost, P., Beyersdorf, A. J., Blake, D. R., Butterfield, Z., Choi, Y., Crounse, J. D., Day, D. A., Diskin, G. S., Dubey, M. K., Fortner, E., Hanisco, T. F., Hu, W., King, L. E., Kleinman, L., Meinardi, S., Mikoviny, T. Onasch, T. B., Palm, B. B., Peischl, J., Pollack, I. B., Ryerson, T. B., Sasche, G. W., Sedlacek, A. J., Shilling, J. E., Springston, S., St. Clair, J. M., Tanner, D. J., Teng, A. P., Wennberg, P. O., Wisthaler, A., and Wolfe, G. M. 2017. Airborne Measurements of Western U.S. Wildfire Emissions: Comparison with Prescribed Burning and Air Quality Implications. *J. Geophys. Res. Atmos*., 122, 6108–6129, doi: 10.1002/2016JD026315.

References (continued)

Lyman, S., Mansfield, M., Tran, H., and Tran, T. 2016. *Annual Report. Uintah Basin Air Quality Research Project.* Utah State University. Prepared for Utah Legislature, Document Number: BRC_161116A.

Martin, R. S. and Baasandorj, M. 2016. *A Comparison of AMoN Measurements with Localized, Arrayed Passive NH_3 Samplers in Northern Utah*. National Atmospheric Deposition Program (NADP), 2016 Fall Meeting, Santa Fe, NM, Oct. 31–Nov. 4.

National Aeronautic and Space Administration (NASA). 2016. *NASA Satellite Sees Smoke Streaming from Arizona's Jack Fire*. Land Atmosphere Near Real-time Capability (LANCE)/Earth Observing System Data and Information System (EOSDIS) Moderate Resolution Imaging Spectroradiometer (MODIS) Rapid Response Team, Goddard Space Flight Center (GSFC) https://www.nasa.gov/image-feature/goddard/2016/nasa-satellite-sees-smoke-streaming-from-arizonas-jack-fire. Accessed November 2017.

National Oceanic and Atmospheric Administration (NOAA)/National Aeronautic and Space Administration (NASA). 2016. *Maple Fire Threatens Western Edge of Yellowstone National Park*. Environmental Visualization Laboratory. https://www.nasa.gov/image-feature/goddard/2016/maple-fire-threatens-western-edge-of-yellowstone-national-park. Accessed November 2017.

National Oceanic and Atmospheric Administration (NOAA) National Centers for Environmental Prediction (NCEP), Weather Prediction Center. 2016. Daily Weather Map, June 14 and June 17, 2016. https://www.wpc.ncep.noaa.gov/dailywxmap/index_20160614.html and https://www.wpc.ncep.noaa.gov/dailywxmap/index_20160617.html. Accessed August 2018.

Neeman, E. M., Crosman, E. T., Horel, J. D., and Avey, L. 2015. Simulations of Cold-Air Pool Associated with Elevated Wintertime Ozone in the Uintah Basin, Utah. 2015. *Atmos. Chem. Phys*., 15, 135-151, 2015.

Neufeld, H., and Young. D. R. 2014. “Ecophysiology of the Herbaceous Layer in Temperate Deciduous Forests.” In *Ecophysiology of the Herbaceous Layer in Forests of Eastern North America*, edited by F. Gilliam, pp. 34–95. Oxford University Press, New York. doi: 10.1093/acprof:osobl/9780199837656.001.0001

Schwede, D. B. and Lear, G. G. 2014. A Novel Hybrid Approach for Estimating Total Deposition in the United States. *Atmos. Environ*., 92:207-220. doi: 10.1016/j.atmosenv.2014.04.008.

References (continued)

Simkin, S. M., Allen, E. B., Bowman, W. D., Clark, C. M., Belnap, J., Brooks, M. L., Cade, B. S., Collins, S. L., Geiser, L. H., Gilliam, F. S., Jovan, S. E., Pardo, L. H., Schulz, B. K., Stevens, C. J. Suding, K. N., Throopo, H. L., and Waller, D. M. 2016. Conditional Vulnerability of Plant Diversity to Atmospheric Nitrogen Deposition across the United States. *Proceedings of the National Academy of Sciences* 113:4086-4091. doi: 10.1073/pnas.1515241113.

Talbot, R., Mao, H., and Sive, B. 2005. Diurnal Characteristics of Surface Level O_3 and other Important Trace Gases in New England, *J. Geophys. Res.*, 110, D09307, doi:10.1029/2004JD005449.

U.S. Environmental Protection Agency (EPA). 2017. Air Markets Program Data. https://ampd.epa.gov/ampd/ Accessed June 2018.

U.S. Environmental Protection Agency (EPA). 2016. *Treatment of Air Quality Data Influenced by Exceptional Events*. https://www.epa.gov/air-quality-analysis/treatment-air-quality-data-influenced-exceptional-events. June 2018.

U.S. Environmental Protection Agency (EPA). 2015a. *Clean Air Status and Trends Network Factsheet-2015*. https://www3.epa.gov/castnet/docs/CASTNET-Factsheet-2015.pdf. Accessed May 2018.

U.S. Environmental Protection Agency (EPA). 2015b. Interpretation of the Primary and Secondary National Ambient Air Quality Standards for Ozone. Title 40 *Code of Federal Regulations* (CFR) Appendix U to Part 50. https://www.ecfr.gov/cgi-bin/text-idx?SID=9b5c394e6ac7be772c8f605a6554e08b&mc=true&node=pt40.2.50&rgn=div5#ap40.2.50_119.u. Accessed June 2018.

U.S. Environmental Protection Agency (EPA). 2015c. Title 40 *Code of Federal Regulations* (CFR) Part 50, Primary and Secondary National Ambient Air Quality Standards. https://www.ecfr.gov/cgi-bin/text-idx?SID=b67492f51b28e27bf9b4226033416c93&mc=true&node=pt40.2.50&rgn=div5. Accessed June 2018.

U.S. Environmental Protection Agency (EPA). 2015d. *Total Deposition Estimates Using a Hybrid Approach.* ftp://ftp.epa.gov/castnet/tdep/Total_Deposition_Documentation_current.pdf. Accessed June 2018.

References (continued)

U.S. Environmental Protection Agency (EPA). 2014. National Emissions Inventory (NEI) Data. https://www.epa.gov/air-emissions-inventories/2014-national-emissions-inventory-nei-data Accessed March 27, 2017.

U.S. Environmental Protection Agency (EPA). 2008. National Ambient Air Quality Standards for Ozone; Final Rule. *Federal Register* 73, No. 60 (March). EPA-HQ-OAR-2005-0172.

U.S. National Vegetation Classification (USNVC). 2016. *United States National Vegetation Classification Database*, V2.0. Federal Geographic Data Committee, Vegetation Subcommittee, Washington DC. usnvc.org.

Ute Indian Tribe. 2016. *Ozone NAAQS Exceedances Occurring June 8 and 9, 2015, Uinta Basin of Utah*. Submitted to U.S. Environmental Protection Agency (EPA), Region 8, August 30, 2016.

Wood Environment & Infrastructure Solutions, Inc. (Wood)*. 2017a. Clean Air Status and Trends Network (CASTNET) Fourth Quarter 2016 Data Report. Prepared for U.S. Environmental Protection Agency (EPA), Office of Air and Radiation, Clean Air Markets Division, Washington, DC. Contract No. EP-W-15-003. Gainesville, FL.

Wood Environment & Infrastructure Solutions, Inc. (Wood)*. 2017b. Clean Air Status and Trends Network (CASTNET) Third Quarter 2016 Data Report. Prepared for U.S. Environmental Protection Agency (EPA), Office of Air and Radiation, Clean Air Markets Division, Washington, DC. Contract No. EP-W-15-003. Gainesville, FL.

Wood Environment & Infrastructure Solutions, Inc. (Wood)*. 2016a. Clean Air Status and Trends Network (CASTNET) First Quarter 2016 Data Report. Prepared for U.S. Environmental Protection Agency (EPA), Office of Air and Radiation, Clean Air Markets Division, Washington, DC. Contract No. EP-W-15-003. Gainesville, FL.

Wood Environment & Infrastructure Solutions, Inc. (Wood)*. 2016b. Clean Air Status and Trends Network (CASTNET) Second Quarter 2016 Data Report. Prepared for U.S. Environmental Protection Agency (EPA), Office of Air and Radiation, Clean Air Markets Division, Washington, DC. Contract No. EP-W-15-003. Gainesville, FL.

* Formerly known as Amec Foster Wheeler Environment & Infrastructure, Inc.

References (continued)

Wood Environment & Infrastructure Solutions, Inc. (Wood)*. 2015. Clean Air Status and Trends Network (CASTNET) Quality Assurance Project Plan (QAPP) Revision 8.3. Prepared for U.S. Environmental Protection Agency (EPA), Office of Air and Radiation, Clean Air Markets Division, Washington, DC. Contract No. EP-W-09-028. Gainesville, FL. http://java.epa.gov/castnet/documents.do.

Wood Environment & Infrastructure Solutions, Inc. (Wood)*. 2012. Clean Air Status and Trends Network (CASTNET) 2010 Annual Report. Prepared for U.S. Environmental Protection Agency (EPA), Office of Air and Radiation, Clean Air Markets Division, Washington, DC. Contract No. EP-W-09-028. Gainesville, FL.

Youden, W.J. (Ku, H.H., ed). 1969. *Precision Measurement and Calibration*. NBS Special Publication 300-Volume 1. U.S. Government Printing Office, Washington, DC.

* Formerly known as Amec Foster Wheeler Environment & Infrastructure, Inc.

Appendix A
Locational and Operational Characteristics of CASTNET Sites

Table A-1 Locational and Operational Characteristics of CASTNET Sites (1 of 3)

Site ID	Site Name	Start date	Latitude	Longitude	Elevation	Nearby NADP	Land Use	Terrain	Agency	Reference
ABT147, CT	Abington	12/28/1993	41.8405	-72.0104	202	CT15	Urban/Agric	Rolling	EPA	
ACA416, ME	Acadia NP	12/1/1998	44.3771	-68.2608	158	ME98	Forest	Rolling	NPS	
ALC188, TX	Alabama-Coushatta	4/6/2004	30.7016	-94.674	105	TX10	Prairie	Rolling	EPA	
ALH157, IL	Alhambra	6/28/1988	38.869	-89.6228	164	IL46	Agric	Flat	EPA	E
ANA115, MI	Ann Arbor	6/28/1988	42.4166	-83.9022	266	MI52	Forest	Flat	EPA	E
ARE128, PA	Arendtsville	6/28/1988	39.9232	-77.3079	266	PA00	Agric	Rolling	EPA	E
ASH135, ME	Ashland	12/20/1988	46.6038	-68.4132	231	ME00	Agric	Flat	EPA	E
BAS601, WY	Basin	11/6/2012	44.28	-108.0411	1242	MT00	Prairie	Rolling	BLM	
BBE401, TX	Big Bend NP	7/18/1995	29.3027	-103.1778	1052	TX04	Forest	Complex	NPS	W
BEL116, MD	Beltsville	11/1/1988	39.0282	-76.8171	47	MD99	Range	Flat	EPA	E
BFT142, NC	Beaufort	12/28/1993	34.8847	-76.6207	5	NC06	Agric	Flat	EPA	
BUF603, WY	Buffalo	11/6/2012	44.1442	-106.1089	1324	WY99	Prairie	Rolling	BLM	
BVL130, IL	Bondville	2/9/1988	40.052	-88.3725	213	IL11	Agric	Flat	EPA	E
BWR139, MD	Blackwater NWR	7/4/1995	38.445	-76.1113	1	MD15	Forest/ Marsh	Coastal	EPA	
CAD150, AR	Caddo Valley	10/4/1988	34.1793	-93.0988	78	AR03	Forest	Complex	EPA	E
CAN407, UT	Canyonlands NP	1/24/1995	38.4583	-109.8213	1809	UT09	Desert	Complex	NPS	W
CAT175, NY	Claryville	5/10/1994	41.9423	-74.552	754	NY68	Forest	Complex	EPA	
CDR119, WV	Cedar Creek	11/10/1987	38.8795	-80.8477	240	WV05	Forest	Complex	EPA	E
CDZ171, KY	Cadiz	1/5/1999	36.7841	-87.8502	190	KY99	Agric	Rolling	EPA	
CHA467, AZ	Chiricahua NM	4/25/1989	32.0094	-109.3891	1570	AZ98	Range	Complex	NPS	W
CHE185, OK	Cherokee Nation	4/2/2002	35.7508	-94.6698	305	AR27	Agric	Rolling	EPA	
CKT136, KY	Crockett	8/24/1993	37.9215	-83.0663	376	KY35	Agric	Rolling	EPA	
CND125, NC	Candor	9/25/1990	35.2633	-79.8375	172	NC36	Forest	Rolling	EPA	E
CNT169, WY	Centennial	5/9/1989	41.3645	-106.24	3175	WY95	Forest	Complex	EPA	W
COW005, NC	Coweeta Screwdriver Knob	11/18/2014	35.0469	-83.4531	960	NC25	Forest	Complex	EPA	
COW137, NC	Coweeta	11/4/1987	35.0605	-83.4303	683	NC25	Forest	Complex	EPA	E
CTH110, NY	Connecticut Hill	9/29/1987	42.4009	-76.6535	511	NY67	Forest	Rolling	EPA	E
CVL151, MS	Coffeeville	12/27/1988	34.0027	-89.7992	138	MS30	Forest	Rolling	EPA	
DCP114, OH	Deer Creek	9/28/1988	39.6359	-83.2606	264	OH54	Agric	Rolling	EPA	E
DEN417, AK	Denali NP	10/6/1998	63.7232	-148.9676	661	AK03	Forest	Complex	NPS	
DIN431, UT	Dinosaur NM	11/20/2013	40.4373	-109.3046	1463	CO15	Desert	Complex	NPS	
EGB181, ON	Egbert	12/27/1994	44.2311	-79.7831	227	NY10	Agric	Rolling	EPA	
ESP127, TN	Edgar Evins	3/22/1988	36.0389	-85.7331	302	KY10	Forest	Rolling	EPA	E
EVE419, FL	Everglades NP	10/6/1998	25.3912	-80.6808	2	FL11	Forest/ Marsh	Flat	NPS	
FOR605, WY	Fortification Creek	5/21/2013	44.3395	-105.9198	1408	WY99	Prairie	Rolling	BLM	
GAS153, GA	Georgia Station	6/28/1988	33.1812	-84.4101	265	GA41	Agric	Rolling	EPA	E
GLR468, MT	Glacier NP	12/27/1988	48.5103	-113.9968	976	MT05	Forest	Complex	NPS	W
GRB411, NV	Great Basin NP	5/16/1995	39.0051	-114.2159	2060	NV05	Forest	Complex	NPS	W
GRC474, AZ	Grand Canyon NP	5/16/1989	36.0586	-112.1836	2073	AZ03	Forest	Rolling	NPS	W
GRS420, TN	Great Smoky NP- Look Rock	10/16/1998	35.6335	-83.9416	793	TN11	Forest	Complex	NPS	

Table A-1 Locational and Operational Characteristics of CASTNET Sites (2 of 3)

Site ID	Site Name	Start date	Latitude	Longitude	Elevation	Nearby NADP	Land Use	Terrain	Agency	Reference
GTH161, CO	Gothic	5/16/1989	38.9563	-106.9859	2915	CO10	Range	Complex	EPA	W
HOW191, ME	Howland Ameriflux	9/27/2011	45.204	-68.74	68	ME09	Forest	Rolling	EPA	
HOX148, MI	Hoxeyville	10/31/2000	44.1809	-85.739	297	MI53	Forest	Flat	EPA	
HWF187, NY	Huntington Wildlife Forest	5/28/2002	43.973	-74.2233	497	NY20	Forest	Complex	EPA	
IRL141, FL	Indian River Lagoon	7/9/2001	27.8492	-80.4556	2	FL99	Coastal/ Marsh	Flat/ Water	EPA	
JOT403, CA	Joshua Tree NP	2/16/1995	34.0696	-116.3889	1244	CA67	Desert	Complex	NPS	W
KEF112, PA	Kane Experimental Forest	1/3/1989	41.5981	-78.7679	618	PA29	Forest	Rolling	EPA	E
KIC003, KS	Kickapoo Tribe	2/18/2014	39.8539	-95.6578	367	KS97	Prairie	Rolling	EPA	
KNZ184, KS	Konza Prairie	3/26/2002	39.1022	-96.6096	346	KS31	Prairie	Flat	EPA	
LAV410, CA	Lassen Volcanic NP	7/25/1995	40.54	-121.5765	1756	CA96	Forest	Complex	NPS	W
LRL117, PA	Laurel Hill	12/15/1987	39.9883	-79.2516	609	PA83	Forest	Complex	EPA	E
MAC426, KY	Mammoth Cave NP	7/24/2002	37.1314	-86.1481	243	KY10	Agric	Rolling	NPS	
MCK131, KY	Mackville	7/31/1990	37.7047	-85.0487	293	KY03	Agric	Rolling	EPA	E
MCK231, KY	Mackville Co-located	12/29/1992	37.7047	-85.0487	293	KY03	Agric	Rolling	EPA	
MEV405, CO	Mesa Verde NP	1/10/1995	37.1984	-108.4905	2165	CO99	Forest	Complex	NPS	W
MKG113, PA	M.K. Goddard	1/12/1988	41.4268	-80.1452	377	NY10	Forest	Rolling	EPA	E
NEC602, WY	Newcastle	11/7/2012	43.873	-104.1919	1468	WY99	Prairie	Rolling	BLM	
NIC001, NY	Nicks Lake	11/20/2012	43.6805	-74.9891	525	NY29	Forest	Rolling	NYSDEC	
NPT006, ID	Nez Perce Tribe	12/15/2015	46.2756	-116.0216	945		Forest	Rolling	EPA	
OXF122, OH	Oxford	8/18/1987	39.5311	-84.7235	284	OH09	Agric	Rolling	EPA	E
PAL190, TX	Palo Duro SP	4/24/2007	34.8806	-101.6647	1053	TX02	Prairie	Complex	EPA	
PAR107, WV	Parsons	1/19/1988	39.0904	-79.6617	510	WV18	Forest	Complex	EPA	E
PED108, VA	Prince Edward	11/3/1987	37.1652	-78.3071	149	VA24	Forest	Rolling	EPA	E
PET427, AZ	Petrified Forest	9/12/2002	34.8225	-109.8925	1723	AZ97	Desert	Flat	NPS	
PIN414, CA	Pinnacles NM	5/16/1995	36.4832	-121.1569	335	CA66	Forest	Complex	NPS	W
PND165, WY	Pinedale	12/27/1988	42.929	-109.7878	2386	WY06	Forest	Rolling	EPA	W
PNF126, NC	Cranberry	12/27/1988	36.1054	-82.045	1216	NC45	Forest	Mountain-top	EPA	E
PRK134, WI	Perkinstown	9/27/1988	45.2065	-90.5972	462	WI35	Agric	Rolling	EPA	E
PSU106, PA	Penn State	1/6/1987	40.7209	-77.9318	364	PA42	Agric	Rolling	EPA	E
QAK172, OH	Quaker City	1/5/1999	39.9427	-81.3379	371	OH49	Agric	Rolling	EPA	
RED004, MN	Red Lake Nation	8/26/2014	47.8638	-94.8352	372	MN16	Forest	Flat	EPA	
ROM206, CO	Rocky Mountain NP Co-located	7/3/2001	40.2781	-105.5456	2742	CO19	Forest	Complex	EPA	
ROM406, CO	Rocky Mountain NP	12/20/1994	40.2781	-105.5456	2743	CO19	Forest	Complex	NPS	W
SAL133, IN	Salamonie Reservoir	6/28/1988	40.816	-85.6614	250	IN20	Agric	Flat	EPA	E
SAN189, NE	Santee Sioux	7/5/2006	42.8292	-97.8541	434	SD99	Range	Rolling	EPA	
SEK430, CA	Sequoia & Kings Canyon NP - Ash Mountain	4/7/2005	36.4895	-118.8292	510	CA75	Forest	Mountain-top	NPS	

Table A-1 Locational and Operational Characteristics of CASTNET Sites (3 of 3)

Site ID	Site Name	Start date	Latitude	Longitude	Elevation	Nearby NADP	Land Use	Terrain	Agency	Reference
SHE604, WY	Sheridan	11/6/2012	44.93	-106.85	1115	MT00	Prairie	Rolling	BLM	
SHN418, VA	Shenandoah NP - Big Meadows	6/28/1988	38.5231	-78.4347	1073	VA28	Forest	Mountain-top	NPS	E
SND152, AL	Sand Mountain	12/27/1988	34.289	-85.9701	349	AL99	Agric	Rolling	EPA	E
SPD111, TN	Speedwell	6/12/1989	36.4698	-83.8265	361	TN04	Agric	Rolling	EPA	E
STK138, IL	Stockton	12/28/1993	42.2872	-90	281	IL18	Agric	Rolling	EPA	
SUM156, FL	Sumatra	12/27/1988	30.1102	-84.9904	16	FL23	Forest	Flat	EPA	E
THR422, ND	Theodore Roosevelt NP	10/6/1998	46.8948	-103.3777	850	ND00	Forest	Rolling	NPS	
UND002, VT	Underhill	11/13/2012	44.5283	-72.8688	399	VT99	Forest	Complex	EPA	
UVL124, MI	Unionville	6/28/1988	43.6136	-83.3599	202	MI51	Agric	Flat	EPA	E
VIN140, IN	Vincennes	8/4/1987	38.7408	-87.4849	136	IN22	Agric	Rolling	EPA	E
VOY413, MN	Voyageurs NP	6/13/1996	48.4125	-92.8292	429	MN32	Forest	Rolling	NPS	
VPI120, VA	Horton Station	6/2/1987	37.3298	-80.5575	920	VA13	Agric	Mountain-top	EPA	E
WFM007, NY	Whiteface Mountain Summit	6/4/2015	44.36608	-73.90312	1415	NY98	Forest	Complex	EPA	
WFM105, NY	Whiteface Mountain	11/20/2012	44.39	-73.86	570	NY98	Forest	Complex	NYSDEC	
WNC429, SD	Wind Cave NP	11/20/2003	43.5576	-103.4839	1292	SD04	Prairie	Rolling	NPS	
WSP144, NJ	Washington Crossing	12/27/1988	40.3123	-74.8727	59	NJ99	Range	Rolling	EPA	E
WST109, NH	Woodstock	12/27/1988	43.9445	-71.7008	255	NH02	Forest	Complex	EPA	E
YEL408, WY	Yellowstone NP	6/26/1996	44.5654	-110.4003	2400	WY08	Agric	Rolling	NPS	W
YOS404, CA	Yosemite NP - Turtleback Dome	9/25/1995	37.7133	-119.7062	1605	CA99	Forest	Complex	NPS	W

Note: NM = National Monument
NP = National Park
NWR = National Wildlife Reserve
SP = State Park
E = eastern reference site
W = western reference site

Appendix B
Acronyms and Abbreviations

List of Acronyms and Abbreviations

A2LA	American Association for Laboratory Accreditation
AMNet	Atmospheric Mercury Network
AMoN	Ammonia Monitoring Network
AQS	EPA's Air Quality System
ARP	Acid Rain Program
ASRC	Atmospheric Sciences Research Center
BLM	Bureau of Land Management
BOLA1	IMPROVE site at Boulder Lake, WY
BRID1	IMPROVE site at Bridger Wilderness, WY
Ca^{2+}	particulate calcium
CAPMoN	Canadian Air and Precipitation Monitoring Network
CASTNET	Clean Air Status and Trends Network
CFR	Code of Federal Regulations
CHIR1	IMPROVE site at Chiricahua National Monument, AZ
Cl^-	particulate chloride
CMAQ	Community Multiscale Air Quality Modeling System
CO	carbon monoxide
CSN	Chemical Speciation Network
DM8A	daily maximum 8-hour average
DQI	data quality indicator
ECAN	Environment Canada
EGUs	electric generating units
EPA	U. S. Environmental Protection Agency
GRCA2	IMPROVE site at Grand Canyon National Park
HNO_3	nitric acid
HONO	nitrous acid
IEC	International Electrotechnical Commission
IMPROVE	Interagency Monitoring of Protected Visual Environments
ISO	International Organization for Standardization
K^+	particulate potassium
kg ha^{-1} yr^{-1}	kilograms per hectare per year
km	kilometer
m	meter
MARPD	mean absolute relative percent difference
MDN	Mercury Deposition Network
MEVE1	IMPROVE site at Mesa Verde National Park
Mg^{2+}	particulate magnesium
N	nitrogen
Na^+	particulate sodium

List of Acronyms and Abbreviations (continued)

NAAQS	National Ambient Air Quality Standards
NADP	National Atmospheric Deposition Program
NASA	National Aeronautics and Space Administration
NCore	EPA's National Core Monitoring
NH_3	ammonia
NH_4^+	particulate ammonium
NM	National Monument
NO	nitrogen oxide
NO_2	nitrogen dioxide
NO_3^-	particulate nitrate
NO_x	nitrogen oxides (NO + NO_2)
NO_y	total reactive oxides of nitrogen
NO_z	HNO_3, nitrous oxide, peroxyacetyl nitrate, peroxyproyl nitrate, other organic nitrates, and nitrite
NOAA	National Oceanic and Atmospheric Administration
NOAB1	IMPROVE site at North Absaroka, WY
NPS	National Park Service
NTN	National Trends Network
NYSDEC	New York State Department of Environmental Conservation
NYSERDA	New York State Energy Research and Development Authority
O_3	ozone
PEFO1	IMPROVE site at Petrified Forest National Park, AZ
PM_1	submicron particulate matter
$PM_{2.5}$	fine particulate matter
ppb	parts per billion
ppm	parts per million
PRISM	Parameter-elevation Regressions on Independent Slopes Model
PT	proficiency testing
QA	quality assurance
QAPP	Quality Assurance Project Plan
S	sulfur
SO_2	sulfur dioxide
SO_4^{2-}	particulate sulfate
TDEP	NADP Total Deposition Science Committee
total NO_3^-	gaseous HNO_3 + particulate NO_3^-
$\mu g/m^3$	micrograms per cubic meter
UDAQ	Utah Department of Air Quality
USNVC	United States National Vegetation Classification
VIIRS	Visible Infrared Imaging Radiometer Suite

List of Acronyms and Abbreviations (continued)

VOC	volatile organic compounds
WARMS	Wyoming Air Resources Monitoring System
YELL2	IMPROVE site at Yellowstone National Park